

PHOTOPHYSICAL AND THEORETICAL STUDIES ON SOME
FLUOROPHORES WITH INTRAMOLECULAR CHARGE
TRANSFER EXCITED STATES

A Thesis
Submitted for the Degree of
DOCTOR OF PHILOSOPHY

By
T. Soujanya



School of Chemistry
University of Hyderabad
Hyderabad 500 046
India

May, 1996

to my daughter
Srujana

CONTENTS

	Page No.
STATEMENT	i
CERTIFICATE	ii
ACKNOWLEDGEMENT	iii
CHAPTER INTRODUCTION	
1.1 Charge separation in donor-acceptor molecules	1
1.2 Motivation of the present work	3
1.3 Layout of the Thesis	7
1.4 References	7
CHAPTER 2 TICT PHENOMENON: AN OVERVIEW	
2.1 The TICT concept	12
2.1.1 Alternative mechanisms	15
2.1.2 Supporting data	16
2.2 Properties of the TICT state	16
2.3 Factors influencing the TICT process	17
2.3.1 Nature of the substituent	17
2.3.2 Ground state twist angle	20
2.3.3 Effect of solvent polarity	20
2.3.4 Effect of viscosity	22
2.3.5 Effect of temperature	23
2.3.6 Effect of pressure	24
2.4 Theoretical approaches to the TICT phenomenon	25
2.5 Variety of TICT systems	26
2.6 References	29
CHAPTER 3 EXPERIMENTAL AND THEORETICAL DETAILS	
3.1 Experimental	37
3.1.1 Materials preparation and purification	37
3.1.2 Solution preparation procedure for spectral measurements	42
3.1.3 Measurements of fluorescence quantum yields	43

3.1.4	Measurements of dipole moment changes on excitation	43
3.1.5	Calculation of radiate and nonradiative lifetimes	47
3.1.6	Instrumentation	48
3.2	Theoretical	52
3.2.1	Semi-empirical calculations	52
3.2.2	Calculation of solvation energies	54
3.3	References	56
CHAPTER 4	A STUDY OF THE TICT PHENOMENON IN AMINOBENZONITRILES BY AMI METHOD	
4.1	Introduction	58
4.2	Ground state properties	61
4.3	Excited state properties	68
4.3.1	Dipole moments	68
4.3.2	Excited state energies and barrier to twisting	71
4.3.3	Absorption spectra	73
4.3.4	Fluorescence spectra	75
4.4	Limitations of the method	76
4.5	References	77
CHAPTER 5	PHOTOPHYSICAL STUDIES ON AMINO-PHTHALI MIDES	
5.1	Photophysical behaviour of AP and DAP in homogeneous media	81
5.1.1	Spectral data	82
5.1.2	Dipole moment change on excitation	93
5.1.3	Fluorescence quantum yields, lifetimes, radiative and nonradiative rate constants	96
5.1.4	Theoretical calculations	101
5.1.5	An interpretation of the photophysical properties in terms of TICT mechanism.	113
5.1.6	Effect of viscosity	118
5.2	Photophysical studies in microheterogeneous environments	121
5.2.1	Absorption spectra	122
5.2.2	Fluorescence spectra and enhancement	126
5.2.3	The binding constants	136

	5.2.4	Fluorescence decay curves	140
	5.2.5	Nature of the Complex	143
	5.2.6	Aminophthalimides in micellar environment	149
	5.3	References	152
CHAPTER 6		EXCITED STATE DIPOLE MOMENTS FROM SOLVATOCHROMIC DATA	
	6.1	Studies on NBD derivatives	157
	6.1.1	Selection of Onsager cavity radius	157
	6.1.2	Nature of the emitting state and rotary decay mechanisms: A theoretical analysis.	162
	6.2	Studies on coumarin derivatives	168
	6.3	References	179
CHAPTER 7		SUMMARY	
	7.1	Results	182
	7.2	Scope of further work	187

Statement

I hereby declare that the matter embodied in this Thesis is the result of investigation carried out by me in the School of Chemistry, University of Hyderabad, India under the supervision of **Dr. Anunay Samanta**.

In keeping with the general practice of reporting scientific observations due acknowledgements have been made wherever the work described is based on the findings of other investigators.


T. Soujanya

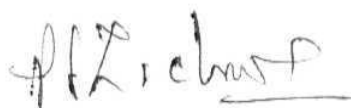
Certificate

Certified that the work contained in the Thesis entitled *Photophysical and Theoretical Studies on Some Fluorophores with Intramolecular Charge Transfer Excited States* has been earned out by T. Soujanya under my supervision and that the same has not been submitted elsewhere for a degree.



Dr. Anunay Samanta

Thesis Supervisor



Dean

School of Chemistry

ACKNOWLEDGEMENTS

It is great occasion for me to express my deep sense of gratitude and heartfelt thanks to Dr. Anunay Samanta, for his inspiring guidance, kind co-operation and encouragement throughout the course of this work. Working with him is an experience and worth remembering. My association with him has played a major role in shaping my attitudes on academic as well as non-academic issues.

I am very thankful to Dr. T.P. Radhakrishnan, and Dr. M. Durga Prasad for their timely help in computational work. I thank all the faculty members of the School of Chemistry for their co-operation.

I thank Dr. A. Chattopadhyay and S. Mukherjee of CCMB for their co-operation in measurement of some fluorescence lifetimes.

I wish to express my gratitude to my husband, Y. Balaji Rao, for his constant support and encouragement throughout the course of my academic career. His timely understanding is gratefully acknowledged.

I wholeheartedly thank my labmates G. Saroja, B. Ramachandram and S. Murthy, for their support in writing of this thesis. Their pleasant association and generous co-operation is highly acknowledged.

I thank my colleagues in the School of Chemistry', past and present, for rendering their help whenever I approached. I would like a special mention of P.S. Chandrakala, H. Aneetha, M. Vijjulatha, T. Anita and A. Manjula for their help in many ways.

I specially thank Dr. K.V. Reddy of C.I.L. for good co-operation and Ms. Nirmalanda for recording fluorescence spectra. I thank Mr. Santhosh, Mr. Shetty and I also thank non teaching staff of the School of Chemistry.

I thank Department of Atomic Energy for the financial support in the form of Dr. K.S. Krishnan fellowship. I thank University authorities for providing infrastructure facilities.

I am grateful to all my family members who supported and encouraged all these years.

I take this opportunity to thank my uncle Ch. R.K. Murthy, aunt Jayasree and family who made my stay in the campus a memorable one.

The single largest contribution in shaping me what I am today comes from the faith, hope and pride of my parents and sisters. It is their love that keeps me going and I take this opportunity to offer my heartfelt thanks to them.

Part of the work presented in the Thesis has been published as follows:

- 1 Effect of β - cyclodextrin on intramolecular charge transfer emission of 4-aminophthalimide, T. Soujanya, T.S.R. Krishna and A. Samanta, *J. Photochem. Photobiol. A: Chem.*, 66, 185, **1992**.
- 2 The nature of 4-aminophthalimide - cyclodextrin inclusion complexes, T. Soujanya, T.S.R. Krishna and A. Samanta, *Phys. Chem.*, 96, 8544, **1992**.
- 3 Dipole moment change of NBD group upon excitation studied using solvatochromic and quantum chemical approaches: Implications in membrane Research, S. Mukherjee, A. Chattopadhyay, A. Samanta and T. Soujanya, *J. Phys. Chem.*, 98, 2809, **1994**.
- 4 AMI study of the twisted - intramolecular - charge - transfer phenomenon in p-(N,N-dimethylamino)benzonitrile, T. Soujanya, G. Saroja and A. Samanta, *Chem. Phys. Lett.*, 236, 503, **1995**.
- 5 Excited state dipole moments of some coumarin dyes from a solvatochromic method using the solvent polarity parameter, E_T^N , M. Ravi, T. Soujanya, A. Samanta and T. P. Radhakrishnan, *J. Chem. Soc. Faraday Trans.*, 91, 1995) 2739.
- 6 Role of nonfluorescent twisted - intramolecular - charge - transfer state on the Photophysical behavior of aminophthalimide dyes, T. Soujanya, R. W. Fessenden and A. Samanta, *J. Phys. Chem.*, 100, 3507, **1996**.

INTRODUCTION

1.1. Charge Separation in Donor - Acceptor Molecules

Separation of charge is the basis of numerous transformations of interest in chemistry and biochemistry. Over the past two decades there has been considerable effort in understanding the photoinduced charge separation reactions¹ as a means of storing the solar energy.² This includes attempts to mimic the long - range separation of charge in plants during photosynthesis using model systems.³ Separation of charge is also known to play a crucial role in the visual process.⁴ Development of organic conductors, superconductors and nonlinear optical materials⁵ is based primarily on charge transfer phenomenon.

Mulliken introduced the concept of charge transfer states to describe the spectral and bonding characteristics of molecular complexes formed between an electron donor and an acceptor.⁶ Weller was first to show that a charge transfer complex can be formed between an excited state and a ground state species.⁷ Such complexes are termed as exciplexes.⁸ When both the electron donor and acceptor groups belong to the same molecule and the molecular lability permits an overlap of the donor and acceptor orbitals through space, of intramolecular charge transfer complex or exciplex can be observed.⁹ In systems with limited conformational flexibility, where through - space interaction of the donor and acceptor orbitals is precluded, charge separation can take place as a result of the through-bond interaction of the donor and acceptor orbitals.⁹ Model compounds

containing donor-acceptor pairs held at a fixed distance and orientation coupled through n - or σ - bond have been used to study the free energy, distance and orientation effects on the rate of electron transfer process.¹⁰ A number of systems are reported in the literature in which electron transfer processes take place over very large distances at lightning speed and with high efficiencies.¹¹ One such example can be found in the photosynthetic reaction centres of certain photosynthetic bacteria.¹²

The available Photophysical techniques such as steady state and time-resolved fluorescence and transient absorption studies allow the charge separated states to be detected. An especially powerful, inexpensive tool is provided if the charge separated systems are fluorescent; because, due to highly polar nature of charge separated systems, internal and environmental influences affect this fluorescence in a characteristic way, yielding detailed information on the thermodynamic, kinetic and other Photophysical and photochemical properties of such species.

In recent years, it has been shown that when the donor and acceptor groups are linked by flexible bonds in a π -conjugated network, the charge transfer process is often associated with twisting of a portion of the molecule relative to the rest of the system.¹³⁻¹⁵ This has led to the concept of twisted intramolecular charge transfer (TICT) phenomenon introduced by Grabowski and co-workers.¹³⁻¹⁴ The TICT concept is extremely helpful in rationalising the Photophysical and photochemical behaviour of a wide variety of donor-acceptor systems.¹³⁻²¹ The application of TICT exhibiting molecules in the construction of efficient fluorescent dyes, fluorescent pH or ion indicators, in photosynthesis,

light harvesting, energy storage processes and cis-trans isomerisation of donor-acceptor substituted olefins have been discussed in several articles on this phenomenon.^{13,21}

Even though the TICT model was originally proposed to account for dual fluorescence of a compound, it was soon realised that TICT states could be nonfluorescent and responsible for rapid nonradiative decay of numerous important dyes leading to intramolecular fluorescence quenching.^{22,25} Since, a low-lying TICT state, whether fluorescent or not, plays a crucial role in dictating the fluorescence efficiency of the dye systems by providing an additional decay channel, it is necessary that the presence of such *nonfluorescent* or *hidden* TICT states adjacent to the emitting state of the donor-acceptor systems is carefully searched for. This knowledge is absolutely essential in designing efficient tailor-made fluorescent materials.

1.2. Motivation of the Present Work

In the present thesis we have addressed ourselves to some problems related to the excited state charge transfer and twisting phenomena. The first problem concerns with the identification of *hidden* or *nonfluorescent* states in 4-aminophthalimide (AP) and 4-(N,N-dimethylamino) phthalimide (DAP). Aminophthalimides are known as highly fluorescent dyes.²⁶ However, no analysis of the Photophysical behaviour of these systems has so far been undertaken to determine the influence of the rotary decay mode, if any, on the radiative efficiencies of these molecules. Even though twisting is commonly observed in compounds containing dialkylamino groups, there are systems where twisting of the unsubstituted amino group leads to TICT formation.²⁷ In AP and

DAP, the donor group (amino or dimethylamino group) is linked to a common acceptor, phthalimido group by a single bond. Therefore, twisting of the donor group could be a possible decay route for the emitting state. We have studied this aspect using conventional fluorescence techniques. The electron donating strength of the donor groups in two compounds is different. In addition, methyl groups in DAP are likely to interact sterically more strongly with the *peri* hydrogens of the aromatic ring. Both these factors are likely to favour a low energy twisted state in DAP. Therefore, a detailed comparative study of the fluorescence properties of the two compounds has been made.

The solvatochromic fluorescence properties of the aminophthalimide dyes point to possible application of these systems as probes for microscopic polarity in organised systems. Therefore, a study of the microheterogeneous structures of cyclodextrins using aminophthalimide probes has been undertaken. There are two main objectives behind this investigation. Firstly, it is of interest to see how the hydrophobic pockets of the host molecules alter the fluorescence of the guest molecules. Secondly, whether it is possible to make any prediction on the structural aspect of the guest-host complex from fluorescence measurements. In addition, we were also interested in finding out whether cyclodextrins can restrict the rotary motion of the amino or dimethylamino group. Preliminary investigations of the Photophysical behaviour of two systems have also been carried out in micellar environments.

The results of theoretical calculations often help interpretation of the experimental data in terms of a speculated mechanism. Since a comparative study of the Photophysical behaviour of AP and DAP suggested possible involvement of a TICT state, we thought it appropriate to investigate theoretically the properties of the TICT state. We had to resort to calculations based on a semi-empirical method instead of an *ab initio* one because of limitations in computational facilities. Austin Model 1 (AMI) method is possibly the best suited for the calculation of the ground state properties of the molecules.²⁸ Some recent reports suggest that the calculated excited state properties are also in good agreement with the experimental data.²⁹ We have carried out a detailed calculation based on AMI method on p-(N,N-dimethylamino)benzonitrile, the most extensively studied molecule from TICT point of view, primarily to test the predictive ability of the method. Having verified that the results of this calculation are in agreement with the experimental results, we subsequently calculated the properties of the TICT states of AP and DAP which helped us rationalising the difference in behaviour of the two compounds in terms of a twisting mechanism.

A knowledge of the excited state charge distribution and dipole moment is helpful in determining the nature of the fluorescent states of the donor-acceptor molecules. Even though equipment-intensive methods like fluorescence polarisation,³⁰ electric dichroism,³¹ stark splitting of rotational levels³² and microwave conductivity or absorption³³ are considered to be more accurate, the most popular method for experimental determination of the excited state dipole moment is based on the analysis of the solvatochromism of the absorption and fluorescence maxima. In the method suggested by Lippert and Mataga, the

Stokes shift of the absorption and fluorescence maxima is related to the dipole moment change on excitation and solvent polarity function involving the dielectric constant and refractive index.^{34,35} The main difficulty in the quantitative estimation of the change in dipole moment on excitation using the above method is due to the uncertainty in the value of the Onsager cavity radius. In the absence of any clear guidelines for the selection of the cavity radius of a particular system, the choice is often arbitrary and hence the determined dipole moment change values are far from accurate. We address to the Onsager radius problem using a few 7-nitrobenz-2-oxa-1,3-diazol-4-yl (NBD) derivatives of different length. The fluorescent NBD probes are widely used to label the lipids to study a variety of processes such as membrane fusion, lipid motion, organisation of lipids and proteins in membranes, etc.³⁶ A combination of theoretical results and experimental data led us to conclude that the cavity radius is to be estimated from the distance between the two centres involved in the charge separation process, the length of the molecule is unimportant in dictating the excited state dipole moment.

Finally, we have addressed to one problem that concern with the nature of the emitting states in six structurally related coumarin derivatives, a number of which are capable of exhibiting TICT phenomenon.²² In this study, we have estimated the excited state dipole moments of the fluorescent states of the compounds using a recently suggested solvatochromic method in which Stokes shift is correlated with a microscopic solvent parameter, E_T^N instead of solvent polarity function defined in terms of macroscopic parameters such as dielectric constant and refractive index.³⁷

1.3. Layout of the thesis

The second Chapter presents a brief overview of the TICT phenomenon. The third Chapter provides details of theoretical and experimental methodologies. Chapter IV describes the results of theoretical calculations of ground and excited state properties of DMABN. Chapter V deals with the investigations carried out on AP and DAP. This includes Photophysical studies in homogeneous media, theoretical studies on TICT phenomenon and studies in microheterogeneous media Chapter VI contains two sections The first section is concerned with the selection of Onsager cavity radius in systems with a common chromophoric group and different length. The next section of this Chapter illustrates the application of the modified Lippert equation in obtaining excited state dipole moments of the fluorescent states of some coumarin derivatives Chapter VII presents a summary of the results.

1.4. References

- 1 a) *Photoinduced Electron Transfer*, MA. Fox, M. Chanon, eds. parts A-D, Elsevier: New York, **1988**; b) D. Gust, T.A. Moore, *Science*, 244, 35, **1989**, c) *Photoinduced Electron Transfer*, parts I to V, In *Topics in Current Chemistry*, J. Mattay, ed. Springer-Verlag: New York, **1991**; d) H. Kurreck, M. Huber, *Angew. Chem. Int. lid. Engl.* 34, 849, 1995.
- 2 a) V. Balzani, F. Scandola, In *Photochemical Conversion and Storage of Solar Energy*, J S. Conolly, ed. Chapter 4, Academic Press: New York, **1981**; b) G. Jones 11, R.J. Butler, *Sol. Energy.*, 29, 579, **1982**; c) K. Honda, A. Fujishima, T. Watanabe, In *Solar Hydrogen Energy Systems*, T. Ohta, ed. Pergaman Press: Oxford, p 137, **1982**, d) R. Memming, In *Photochemical*

Conversion and Storage of Solar energy, E. Pelizzetti, M. Schiavello, eds. Kluwer: Holland, p 193, **1991**.

- 3 a) J. Deisenhofer, O. Epp, K. Mikki, R. Huber and H. Michel, *J. Mol. Biol.*, **180**, 385, **1984**; b) J. Deisenhofer, H. Michel, *Science*, **45**, 1463, **1989**, c) D. Gust, T.A. Moore, A.L. Moore, *Acc. Chem. Res.*, **26**, **198**, **1993**, d) A. Bard, M.A. Fox, *Acc. Chem. Res.*, **28**, **141**, **1995** and references therein.
- 4 L. Salem, *Science*, **191**, 822, **1976**.
- 5 a) D.S. Chemla, J. Zyss, *Nonlinear Optical Materials of Organic Molecules and Crystals*, Academic Press: New York. **1987**; b) H.S. Nalwa, T. Watanabe, S. Miyata, In *Photochemistry and Photophysics*, J.F. Rabek, ed. Vol. 5, p 103, CRC press: Boca Raton, **1991**; c) *Molecular Nonlinear Optics*, J. Zyss, ed. Academic Press: New York, **1993**; d) D.B. Shelton, J.E. Rice, *Chem. Rev.*, **94**, 3, **1994**; e) A.W. Sleight, *Acc. Chem. Res.*, **28**, 103, **1995**
- 6 R.S. Mulliken, *J. Am. Chem. Soc.*, **72**, 600, **1950**, **74**, 811, **1952**, *J. Phys. Chem.*, **56**, 801, **1952**.
- 7 H. Leonhardt, A. Weller, *Ber. Bunsenges. Phys. Chem.*, **67**, 791, **1963**.
- 8 a) I. Forster, *Angew. Chem. Int. Ed. Engl.*, **8**, 333, **1969**, b) *The Exciplex*, M. Gordon, W.R. Ware, eds. Academic Press: New York, **1975**.
- 9 a) J.B. Birks, *Photophysics of Aromatic Molecules*, New York: Wiley, **1970**, b) H. Beens, A. Weller, In *Organic Molecular Photophysics*, J.B. Birks, ed. Wiley: London, Vol. 2, p 159, **1975**.
- 10 a) M.R. Wasielewski, *Chem. Rev.*, **92**, 435, **1992**; b) M.A. Fox, *Chem. Rev.*, **92**, 365, **1992**.
- 11 a) M. Lendon, J. Miller, *J. Am. Chem. Soc.*, **107**, 7811, **1985**; b) H. Overing, M. Paddon-Row, M. Heppenes, A. Oliver, E. Cotsaris, J. Ver Hoeven, N.

- Hush, *J. Am. Chem. Soc.*, **109**, 3258, **1987**; c) N. Hush, M. Paddon-Row, E. Cotsaris, H. Overing, *Chem. Phys. Lett.*, **117**, **18**, **1985**; d) K.D. Jordan, M. Paddon-Row, *Chem. Rev.*, **92**, 395, **1992**.
- 12 J. Deisenhofer, H. Michel, *Angew. Chem. Int. Ed. Engl.*, **28**, 829, **1989**.
- 13 a) K. Rotkiewicz, K.H. Grellmann, Z.R. Grabowski, *Chem. Phys. Lett.*, **19**, 315, **1973**, b) K. Rotkiewicz, Z.R. Grabowski, A. Krowczynski, W. Kuhnle, *J. Lumin.*, **12/13**, 877, **1976**.
- 14 a) Z.R. Grabowski, K. Rotkiewicz, A. Siemiarczuk, D.J. Cowley, W. Baumann, *Nouv. J. Chim.*, **3**, 443, **1979**; b) J. Karpluk, Z.R. Grabowski, F.C. De Schryver, *Proc. Ind. Acad. Sci.*, **KM**, 133, **1992**; c) Z.R. Grabowski, J. Dobkowski, *Pure Appl. Chem.*, **55**, 245, **1983**.
- 15 W. Rettig, *Angew. Chem. Int. Ed. Engl.*, **25**, 971, **1986**.
- 16 E. Lippert, W. Rettig, V. Bonacic-Koutecky, F. Heisel, J.A. Mierke, *Adv. Chem. Phys.*, **68**, 1, **1987**.
- 17 W. Rettig, In *Modern Models of Bonding and Delocalisation; A Series in Molecular Structure and Energetics*, J.F. Liebman, A. Greenberg, eds. Vol. 6, Chapter 5, VCH: New York, p 229, **1988**.
- 18 W. Rettig, W. Baumann, In *Photochemistry and Photophysics*, J. F. Rabek, ed. Vol. 6, CRC press: Boca Raton, p 79, **1992**.
- 19 W. Rettig, *Proc. Ind. Acad. Sci.*, **104**, 89, **1992**.
- 20 K. Bhattacharyya, M. Chowdhury, *Chem. Rev.*, **93**, 507, **1993**.
- 21 W. Rettig, In *Top. Curr. Chem.*, J. Mattay, ed. Vol.169, p 254, **1994**.
- 22 a) G. Jones II, W.R. Jackson, A.M. Halpern, *Chem. Phys. Lett.*, **72**, 391, **1980**, b) G. Jones II, W.R. Jackson, C. Choi, W.R. Bergmark, *J. Phys. Chem.*, **89**, 294, **1985**.

- 23 a) M. Vogel, W. Rettig, U. Fiedeldei, H. Baumgaertel, *Chem. Phys. Lett.*, **148**, 347, **1988**, b) M. Vogel, W. Rettig, R. Sens, K.H. Drexhage, *Chem. Phys. Lett.*, 147, 461, **1988**.
- 24 T. Carstens, K. Kobs, *J. Phys. Chem.*, **84**, 1871, **1980**.
- 25 J.D. Simon, S.G. Su, *J. Chem. Phys.*, **89**, 908, **1988**.
- 26 a) N.G. Bakhshiev, *Opt. Spektrosk.*, **12**, 1557, **1962**; *ibid.* **12**, 350, **1962**; b) W.R. Ware, S.K. Lee, G.J. Brant, P.P. Chow, *J. Chem. Phys.*, 54, 4729, **1971**; c) Y.T. Mazurenko, *Opt. Spectrosk.*, 36, 283, **1974**; d) S.W. Yeh, L.A. Philips, S.P. Webb, L.F. Buhse, J.H. Clark, *Ultrafast Phenomena, IV*, D.A. Auston, K.B. Eisenthal, eds. Springer: Berlin, p 359, **1987**; e) T. Hagan, D. Pilloud, P. Suppan, *J. Chem. Soc. Faraday Trans., I*, 83, 497, **1987**; f) V. Nagarajan, A.M. Brearley, T.J. Kang, P.F. Barbara, *J. Chem. Phys.*, 86, 3183, **1987**; g) H. Langhals, *Anal. Lett.*, 23, 2243, **1991**; h) N.A. Nemkovich, V.I. Tomin, A.N. Rubinov, In *Topics in Fluorescence Spectroscopy*, J.R. Lakowicz, ed. Vol. 2, p 367, Plenum: New York, **1991**; i) N.A. Nenikovich, W. Baumann, H. Reis, N. Detzer, *Photochem. Photobiol., A: Chem.*, 89, 127, **1995**
- 27 a) B.S. Vogt, S.G. Schulman, *Chem. Phys. Lett.*, 89, 320, **1982**; b) W. Rettig, A. Klock, *Can. J. Chem.*, 63(7), 1649, **1985**.
- 28 a) M.J.S. Dewar, W. Thiel, *J. Am. Chem. Soc.*, 99, 4899, **1977**; b) M.J.S. Dewar, E.G. Zoebisch, E.F. Healy, J.J.P. Stewart, *J. Am. Chem. Soc.*, **107**, 3902, **1985**; c) M.J.S. Dewar, K.M. Dieter, *J. Am. Chem. Soc.*, 108, 8075, **1986**
- 29 a) P.K. McCarthy, G.J. Blanchard, *J. Phys. Chem.*, 97, 12205, **1993**; b) M.A. Awad, P.K. McCarthy, G.J. Blanchard, *J. Phys. Chem.*, 98, 1454, **1994**.

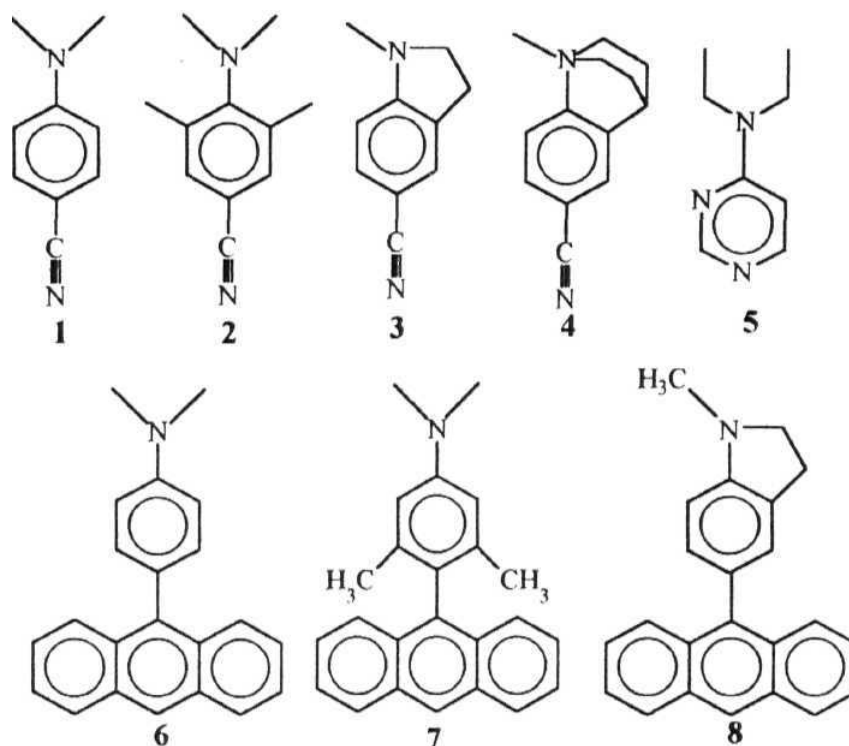
- 30 a) J. Czekalla, *Z. Electrochem.*, 64, 1221, 1960; b) W. Liptay, *Z. Naturforsch.*, 18a, 705, 1963.
- 31 a) W. Liptay, J. Czekalla, *Z. Naturforsch.*, **15a**, 1072, 1960, b) J. Czekalla, W. Liptay, K.O. Meyer, *Ber. Bunsenges. Phys. Chem.*, 67, 465, 1963, c) W. Liptay, *Angew. Chem.*, **81**, 195, 1969; d) W. Liptay, In *Excited States*, E.C. Lim, ed. Academic Press: New York, Vol. 1, p 129, 1974.
- 32 a) DE. Freeman, W. Klemperer, *J. Chem. Phys.*, 45, 52, 1966; b) DE. Freeman, J.R. Lombardi, W. Klemperer, *J. Chem. Phys.*, 45, 58, 1966.
- 33 a) R.J. Visser, P.C.M. Weisenborn, C.A.G.O. Varma, MP. deHaas, J.M. Wannan, *Chem. Phys. Lett.*, KM, 38, 1984; b) S.A. Jonker, J.M. Warman, *Chem. Phys. Lett.*, 183, 36, 1991; c) R.W. Fessenden, P.M. Carton, H. Paul, H Shimamori, *J. Phys. Chem.*, **83**, 1676, 1979.
- 34 a) E.Z. Lippert, *Naturforsch.*, WA, 541, 1955, *Z. Electrochem.*, 61., 962, 1957, b) E. Lippert, W. Luder, H. Boos, *Adv. Mol. Spectros.*, 6, 125, 1956.
- 35 a) N. Mataga, Y. Kaifu, M. Koizumi, *Bull. Chem. Soc. Jpn.*, 28, 690, 1955, b) N. Mataga, Y. Torihashi, *Bull. Chem. Soc. Jpn.*, 36, 356, 1963; c) N. Mataga, *Bull. Chem. Soc. Jpn.*, 36, 620, 654, 1963.
- 36 a) T. Arvinte, A. Cudd, K. Hildenbrand, *Biochim. Biophys. Acta*, **860**, 215, 1986; b) A. Chattopadhyay, E. London, *Biochim. Biophys. Acta*, 938, 24, 1988; c) A. Chattopadhyay, *Chem. Phys. Lipids*, 53, 1, 1990.
- 37 M. Ravi, T.P. Radhakrishnan, A. Samanta, *J. Phys. Chem.*, 98, 9133, 1994.

TICT PHENOMENON : AN OVERVIEW

Since the Thesis deals with donor-acceptor systems capable of exhibiting the twisted intramolecular charge transfer (TICT) process, we provide necessary background information describing the salient features of this phenomenon in this Chapter. The information provided herein should not be treated as an exhaustive review on this topic.

2.1. The TICT concept

More than three decades ago, Lippert reported that *p*-(N,N-dimethylamino)benzonitrile (DMABN) exhibits dual fluorescence in polar solvents.¹ He originally proposed the *normal* short-wavelength band (B band) to originate from a relatively nonpolar state (1L_b state in Platt's nomenclature²) and the *anomalous* long-wavelength one (A band) to originate from a polar state (1L_a state). The polarity dependence of the fluorescence was attributed to the solvent induced reversal of the ordering of two close-lying excited states of DMABN. However, Lippert's proposal could not account for identical fluorescence polarisation of both the bands in glycerol along the axis connecting the amino and cyano groups.³ Studies on model compounds with pre-twisted and rigidised geometries such as 1-8 led Grabowski and coworkers to introduce the TICT concept for a more complete description of the dual-fluorescence of DMABN and similar donor-acceptor molecules.³⁻⁸



According to this concept, electronic excitation promotes planar DMABN to a locally excited (LE) state with geometry and dipole moment similar to those in the ground state. In polar solvents, an electron is transferred on excitation from the donor to the acceptor and the donor group undergoes a twist. This internal twisting makes the donor orbital orthogonal to the acceptor orbital ensuring complete electron transfer. The resulting state is therefore highly polar and known as TICT state. Thus, according to this concept two emissions in DMABN originate from the LE state and the TICT state. This phenomenon is schematically illustrated in fig. 2.1.

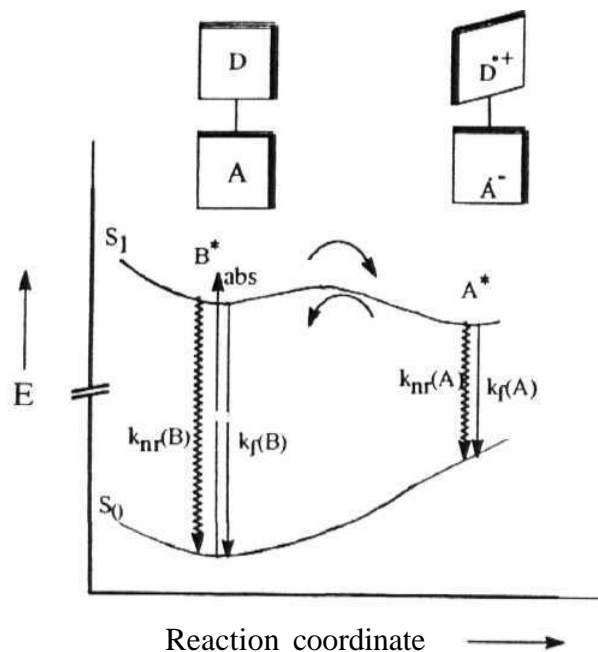
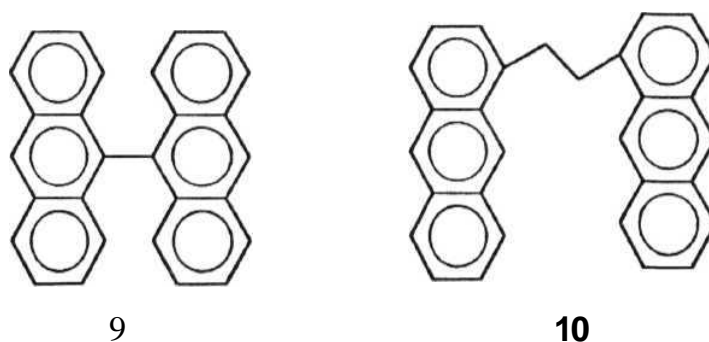


Fig.2.1. Schematic representation of the TICT phenomenon.

It is important to note that while maximum overlap between the donor and acceptor moieties in exciplexes and excimers leads the charge transfer, it is the minimum overlap between the two moieties that results in the formation of the TICT state. The effect of minimum and maximum overlap on the fluorescence bands is illustrated with the help of the systems, **9** and **10**.⁹⁻¹¹



Due to through - space overlap and charge separation between two anthracene rings, the excited state of 10 is slightly polar and fluorescence spectra exhibits small red shifts. On the other hand 9 with maximum charge separation due to orthogonal conformation, shows strong solvatochromic red shifts.

2.1.1. *Alternative mechanisms*

A number of alternative mechanisms were proposed to account for the dual-fluorescence of DMABN. Khalil et al assigned the long-wavelength band of DMABN to excimer formation.¹² Chandross and later Visser et al observed quenching of the B band of DMABN with increase in the amount of a polar solvent constituent in a mixture.¹³ From a linear correlation of the ratio of the intensity of the two bands with the concentration of polar solvent, the specific formation of a 1:1 exciplex with polar solvent molecule was suggested. Specific solvation with the water molecules was also considered as a possibility. Kosower et al concluded that the A band arises from species protonated in the excited state.¹⁴ However, this mechanism could not explain the presence of the A band in rigorously dried aprotic solvents, in the gas phase¹⁵ and also in hydrocarbon solvents, where specific interactions are not possible.^{15,16}

Recently, Zachariasse et al have proposed solvent-induced pseudo-Jahn-Teller coupling of two close-lying excited states with an amino-nitrogen inversion as the promoting mode¹⁷ to account for the orbital-decoupling of the donor and acceptor groups in the excited state leading to maximum charge transfer in aminobenzonitriles.¹⁷ However, this model has been contradicted in some recent papers.^{18,19} Very recently, it has been concluded from an *ab initio* calculation on aminobenzonitriles that bending of the cyano group rather than

twisting of the amino group is the intramolecular motion which is responsible for the stabilisation of the charge transfer state.²⁰ However, this mechanism can not account for the TICT phenomenon in symmetric aryls which do not possess a cyano group or other group that can bend in the excited state.²¹⁻²²

2.1.2. Supporting data

The TICT model is backed up by several key experiments: a) model compounds where the twisting of the dialkylamino group is blocked by molecular bridging do not exhibit the long-wavelength band. Model compounds for which^{6,23,24} the planar conformation is made unavailable by steric hindrance and which exist in perpendicular conformation in the ground state, display only the long-wavelength band^{6,25,26} b) excited state dipole moment is consistent with a large degree of intramolecular charge separation^{27,31} c) observation of TICT emission in the gas phase¹⁵ and d) radical anion in transient absorption experiment.³¹⁻³³ The TICT model is backed up by an enormous amount of data on a wide variety of systems which can be found in several review articles that appeared on this topic.³⁴⁻⁴⁰

2.2. Properties of the TICT state

The most important feature of the TICT states is the charge separation, which, amounts to transfer of one unit of electronic charge from the donor to the acceptor.⁵⁸ This charge separation is detectable experimentally either by measurement of the dipole moment of the TICT state or by direct observation of charge separated species. A large variation of dipole moment of the twisted state of DMABN, ranging from as high as 23 D to as low as 12.2 D is reported in the literature.²⁷⁻³⁰

Since the TICT emission originates from a state where the donor and acceptor orbitals are decoupled from each other, it is an overlap forbidden transition and the intensity of this emission is expected to be small. However, by coupling to suitable vibrations this transition borrows intensity which accounts for many systems with appreciable TICT fluorescence quantum yields.³⁴

2.3. Factors influencing the TICT process

A number of external and internal factors influence the TICT formation rate. Among the external factors, viscosity and the polarity of the solvent, temperature and pressure are important. The electron donor and the acceptor strength of the substituents, ground state twist angle, rotating volume of the twisting moiety and molecular shape are some of the internal factors which determine the rate of TICT state formation.

2.3.1. Nature of the substituent

A change in the donor or acceptor strength has profound effect on the potential surfaces which ultimately govern any reaction dynamics. Replacement of a weak acceptor with a strong one results in reversal of the nature of B and A excited states.^{16,41} Thus on going from cyano (11) to alkoxycarbonyl (12) derivatives, the nature of the B state changes from 1L_b to 1L_a . Since both 1L_a and TICT states are of same symmetry species, B and A bands originate from the same potential energy surface. The relevant region of the potential surfaces is shown schematically in fig. 2.2.

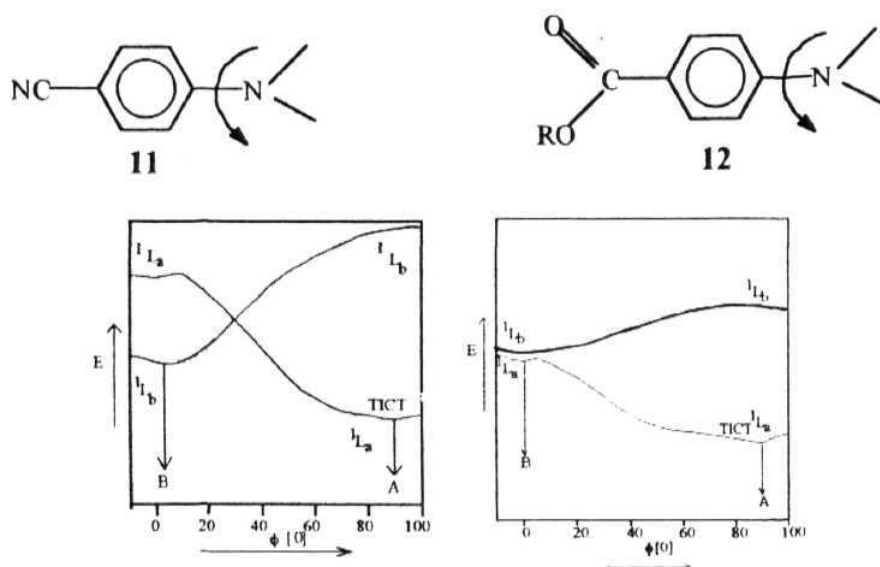
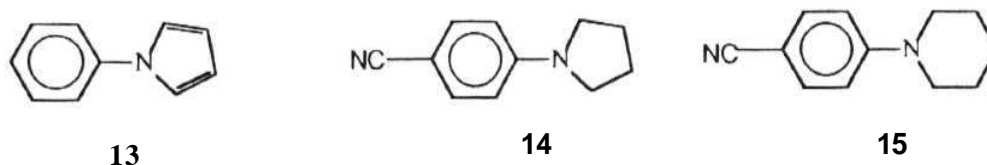


Fig. 2.2. Schematic representation of the potential surfaces in p-substituted dialkylanilines

In the case of cyano derivatives, the two states (1L_a and 1L_b) approach each other and interact vibronically via an asymmetric vibration. The adiabatic potential along the asymmetric normal mode is thus transformed into a diabatic double minimum potential on the lower surface.²⁵ This results in an upward-directed cone on the lower surface and downward-directed cone on the upper surface centered at the crossing point where the twist angle has the critical value ϕ_{cr} . This is known as *conical intersection*.⁴² Thus in cyano derivatives, the crossing of the two states causes conical intersection at the critical twist angle ϕ_{cr} which necessitates coupling with a **non-totally** symmetric vibration or with solvent for transition to the TICT state. Therefore, DMABN shows TICT fluorescence only in polar solvents.⁷ For alkoxy carbonyl derivatives, this coupling is not necessary. The experimental consequence is a readily observable TICT fluorescence even in non polar environment and an increase in the rate

constant for TICT formation for ester derivatives.^{16,43,44} If the donor strength is weakened by replacing the dimethylamino group with an amino group, TICT state would be higher in energy with respect to the LE state.⁴⁵ On the other hand, replacement of dialkylamino group by heterocyclic aromatic systems such as pyrrole in 13 as shown below, has strong tendency towards TICT formation even though it has relatively weak acceptor group.⁴⁶



The enhancement of the relative intensity of the A band (ϕ_A/ϕ_B) from 0.7 in 14 to 6.7 in 15 is interpreted in terms of an increase of the donor strength as measured from their ionisation potential values (8.39 eV for 14 and 8.28 eV for

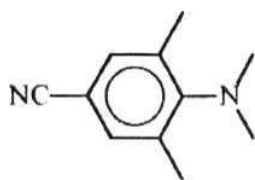
The energy of the TICT state is commonly expressed in terms of the ionisation potential of the donor, $IP(D)$ and electron affinity of the acceptor, $EA(A)$ as follows.³⁴

$$E_{TICT} = IP(D) - EA(A) + C + E_{SOLV} \quad 2.1$$

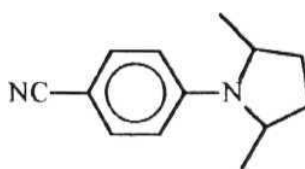
Where, C is the coulomb energy which stabilises the radical cation and radical anion formed as a result of transfer of electron. E_{SOLV} is the solvation energy provided by surrounding solvent molecules around the radical ion pair.

2.3.2. Ground state twist angle

Ground state twist angle also plays a decisive **role** in TICT formation process. In the case of sterically hindered dialkyl anilines²⁵, such as, 16 and 17,



16



17

the LE state can not be reached at the planar conformation and this leads to strong preference for TICT formation even in the gas **phase**.¹⁵ The critical twist angle which controls the rate of TICT formation depends on the ground state twist angle as evident from the comparison of the TICT formation rates in 14 and 15.^{25,47} Due to steric repulsion in 15, the ground state twist angle is 30°. Consequently, **15** starts its reactive motion on the **S₁** surface much closer (than in 14) to the critical twist angle ϕ_{cr} , where the downward slope of the TICT potential starts. As a result, the TICT formation rate in 15 is larger by a factor of about 10 in polar media.

2.3.3. Effect of solvent polarity

The appearance of the long-wavelength fluorescence band of DMABN only in polar solvents indicates that the polarity of the media plays an important role in determining the dynamics of the TICT formation and decay processes. The TICT formation rate is determined by two factors; molecular relaxation rate and solvent relaxation rate. When solvation is slower than the molecular relaxation rate, the emission exhibits a time-dependent Stokes shift or dynamic Stokes shift.⁴⁸ However, when molecular relaxation rate is slower than the

solvent relaxation rate, then static polarity shift is expected. For DMABN, Hicks et al observed that the TICT formation rate is slower than the rate of solvent relaxation and therefore the molecule shows static polarity effect.⁴⁹ Eisenthal et al performed a series of experiments on DMABN in iso-viscous mixtures of different polarities⁴⁹ and found that there is a linear relationship between the TICT rate and the solvent polarity parameter, $E_T(30)$.⁵⁰ To account for this observation, a polarity dependent activation barrier for the TICT process was proposed. An empirical relation between the barrier height (E_a) and a microscopic solvent polarity parameter, $E_T(30)$ was proposed to explain the experimental results quantitatively.

$$E_a = E_a^0 - A[E_T(30) - 30] \quad 2.2$$

where $E_T(30)$ is the absorption energy (in kcal mol⁻¹) of the betaine dye (details are given in Chapter III) in a given solvent.⁵⁰ E_a^0 is activation energy in a hydrocarbon solvent having an $E_T(30)$ of 30 kcal mol⁻¹. A is a measure of how strongly the barrier height changes with solvent polarity. The TICT formation rate, k_T is given by,

$$k_T = C \exp \{ A[E_T(30) - 30] / RT \} \exp (-E_a^0 / RT) \quad 2.3$$

which accounts for the linear relation between $\ln k_T$ and $E_T(30)$. C is the Arrhenius pre-exponential factor. The concept of the polarity dependent barrier has been tested on many other molecules such as sulfones,⁵¹ aniline sulfonates⁵² and rhodamines.⁵³

Although the TICT formation rate is **enhanced** on increase of polarity, it has been observed that the TICT fluorescence yield of DMABN pass through a maximum which has been explained in terms of two competitive processes, formation and nonradiative decay of the TICT state, both of which are accelerated with increase in solvent **polarity**.⁵⁴

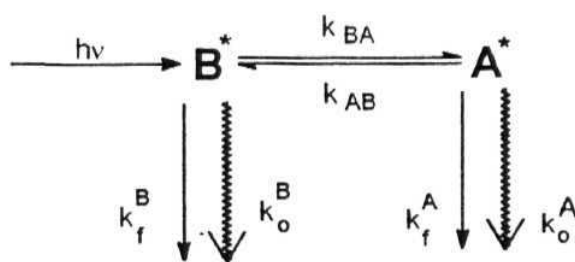
2.3.4. Effect of viscosity

The effect of viscosity on the yield of TICT emission depends on many factors such as ground state twist angle, rotating volume of the twisting moiety, molecular shape, etc. For DMABN, the rotating group (NMe₂) is rather small and hence the TICT formation does not involve significant displacement of solvent molecules. Thus the solvent offers little friction on the twisting motion in DMABN and the TICT process in DMABN is found to be almost independent of viscosity upto a moderate viscosity.⁴⁹ However, for systems with larger rotating groups (e.g. toluidino group in (p-toluidino)naphthalenesulfonate), an increase in viscosity is shown to retard the TICT process even at low viscosity.⁵² The retarding influence of viscosity on twisting process can always be expected in media of large viscosities.^{55,63} This has been substantiated by a study on 12 in polymer solution.⁵⁵ In highly viscous polymer media, 12 is found to exist as different ground state rotamers. Excitation of different rotamers leads to different ratios of the intensities of the LE and TICT emission.⁵⁵ The sensitivity of the TICT emission to polymer environment has been utilised to probe mobilities of polymer segments⁵⁷⁻⁶² and to monitor the kinetics of polymerisation.⁶³

2.3.5. Effect of temperature

The variation of temperature provides a convenient way of bringing substantial changes in the polarity of the medium without changing the polarity dependent studies on the kinetics of the TICT process.

Since the polarity of the solvent increases as the temperature is lowered, the activation barrier for the TICT process decreases at low temperatures. Eisenthal et al observed an increase in rate of formation of TICT state for DMABN with decrease in temperature (350-250 K)⁴⁹ for this reason. The observed dependence of the fluorescence quantum yield as a function of temperature can be described by means of the kinetic scheme (Scheme 2.1) developed by Grabowski and co-workers⁵ This kinetic model includes equilibration rate constants, k_{BA} (forward reaction) and k_{AB} (backward reaction) as well as the rate constants for the radiative (k_f^B , k_f^A) and nonradiative decay (k_o^B and k_o^A) to the ground state. The scheme as shown below, has three temperature dependent rate constants (k_{BA} , k_{AB} , k_f^A).



Scheme 2.1. Kinetic scheme for adiabatic photoreaction

The quantum yield of the B band is strongly temperature dependent and shows a minimum at a certain temperature called T_M . Above this temperature, excited B and A states reach a **thermodynamic** equilibrium $B^* \rightleftharpoons A^*$ during their lifetime. Upon **further** increase of the temperature, this equilibrium is shifted toward B^* , resulting in an increase of the total fluorescence quantum yield, because the deactivation of A^* , unlike that of B^* occurs mainly via nonradiative processes. The slight increase of the quantum yield of the A fluorescence with increase in temperature is attributed to the forbidden nature of TICT— \bullet ground state transition (upper vibrational levels of the TICT state are significantly populated at higher temperatures i.e., hot fluorescence).⁶⁴ The temperature dependent behaviour of 12 has also been explained using the same kinetic scheme.¹⁶

2.3.6. *Effect of pressure*

The application of pressure provides a convenient way of making substantial changes in the solvent viscosity and dielectric constant, while only slightly changing the solvent structure. Thus, pressure provides a way to change the environment of a solute molecule in a continuous and controlled fashion. Since TICT formation involves twisting of flexible bonds, variation of pressure is expected to bring significant changes on TICT rate. Studies on the effect of pressure on DMABN⁶⁵⁻⁶⁹ and 4,4'-diaminodiphenyl sulfone (DAPS)⁶⁸ revealed that the formation of the TICT state does strongly depend on viscosity. The viscosity independent rate of TICT process for DMABN as reported by Eisenthal and co-workers⁴⁹ has been attributed to very narrow range of viscosities used in their experiments. Effect of pressure on 12 bonded to polymer chain has been **studied**.⁶⁹ The ratio of the intensities of TICT and nonpolar

emission was found to decrease with increase in the external pressure in solution and to a greater extent when 12 is bonded to polymer chain. This is ascribed to a decrease of the free volume for rotation with increase in pressure.

2.4. Theoretical approaches to the TICT phenomenon

Theoretical studies on TICT process can be broadly classified into two types. The first one is based on stochastic models in which the overall rate is determined using statistical mechanical models.⁷⁰⁻⁷⁵ The interaction between the solute and the surrounding solvent molecules is described by generalised Langevin equation (GLE) considering the effect of solvent as a time-dependent friction term. Although solvent is considered as a continuous medium in most of these studies,⁷¹ in some recent studies there has been an attempt to take the solvent structure into account.⁷⁵ Recently, the mechanism of solvent assisted intramolecular charge transfer in DMABN has been theoretically studied by Rettig et al using stochastic model.⁷⁵ In this model, the dynamics of interconversion between the planar and perpendicular conformer is described as a diffusional process coupled to a solvent polarisation coordinate. The model provides a satisfactory description of all static and dynamic fluorescence spectral features available from experiments. The success of this model in interpretation of the experimental behaviour not only gives support to the TICT hypothesis of a conformational change accompanying the charge transfer process but also to the reliability of the Debye-Onsager description of the solvent properties. The success and limitations of the various stochastic models have been summarised in several recent publications.⁷⁰⁻⁷⁵

The second approach is based on quantum chemical calculations of the potential energy surface with twist angle as the reaction coordinate.^{18-20,76-83} The semi-empirical calculations based on various methods such as INDO,⁷⁸ MNDO,⁸¹ CNDO^{77,79,82} and AM1¹⁸ methods and *ab initio* studies^{19,20,80,83} at various levels have been performed to explain the anomalous behaviour of DMABN and similar systems. A majority of these calculations at various levels although favours TICT model, a few theoretical studies proposing alternative mechanisms are also reported. The successes and limitations of the above methods are discussed in Chapter IV.

2.5. Variety of TICT systems

Since the discovery of dual emission in DMABN, a wide variety of compounds have been examined where TICT is reported. Apart from aromatic amines and aryl-anilines, several nitriles, aldehydes, esters, nitro compounds, hetero-aromatics, biaryls, sulfones, stilbenes, aryldisilanes, triphenyl phosphines, etc have been shown to exhibit TICT phenomenon.³⁴⁻⁴⁰ TICT compounds can be categorised into *emissive TICT compounds* and *non emissive TICT compounds*.

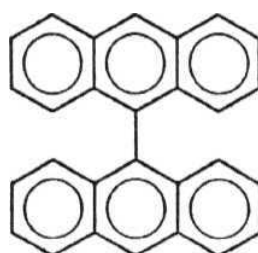
Among the TICT compounds, **18**,⁸⁴ is a highly symmetric dimer of DMABN with topology A-D-D-A and has very high excited state dipole moment. The ground state dipole moment of **18** is zero because of cancellation of the dipole moments of the two halves in an anti parallel arrangement. However, unlike that in DMABN, twisting of the dimethylamino group in **18** is very difficult because of the six-membered ring. The dual fluorescence and high

dipole moment observed for this compound possibly result from a chair to boat conformational change of the piperazine ring. This aspect needs further investigation.

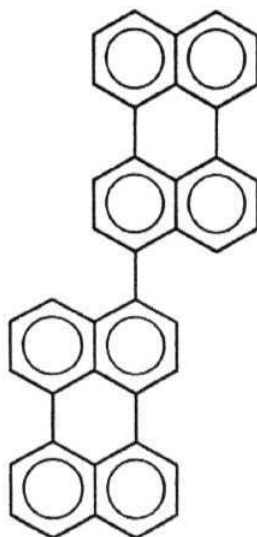


18

Push-Pull stilbenes or diphenyl polyenes form another interesting class of compounds where TICT formation competes or assists in the cis-trans isomerisation.⁸⁵⁻⁸⁶ In this class of compounds the dual fluorescence is generally not observed. This is attributed to very low energy gap between LE and TICT states. As a result the rate of formation of the TICT state from the LE state is too fast to resolve two bands even in picosecond time scale regime. However it has been shown that the rate of TICT state formation can be slowed down by lengthening the polyenic chain. Rulliere et al were able to resolve dual fluorescence in donor-acceptor systems linked to butadiene and hexatriene.⁸⁶

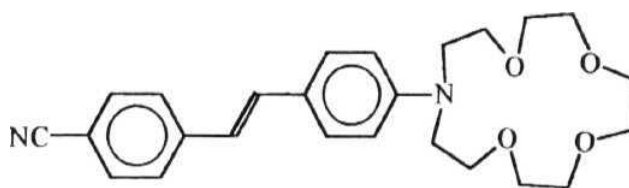


19



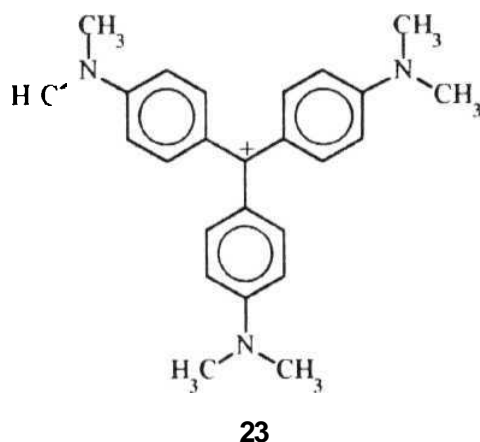
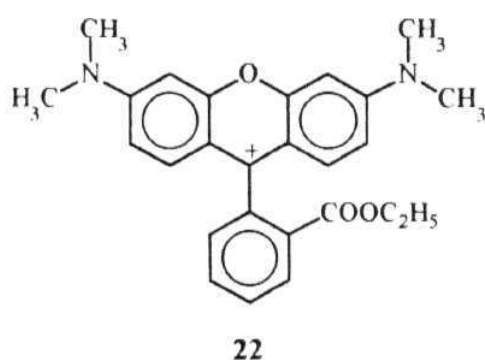
20

Symmetric biaryls such as 19 and 20 are nice examples of TICT systems because the ground state is non polar and highly symmetric yet form a very polar TICT state upon **excitation**.³⁴ The best known example is perhaps **19**.⁸⁷ Another interesting class of TICT compounds is molecules with crown ether function, which form complex with metal ions, and they have different emission properties in the **complexed** and uncomplexed state.⁸⁸ This type specific ion probes may find application in medicine, biology and analytical chemistry.



21

A large number of molecules are known where the TICT states are found to be nonfluorescent and responsible for rapid nonradiative decay of numerous important dyes leading to intramolecular fluorescence quenching.^{89,90} A number of coumarin dyes fall in this class of systems.⁸⁹ The Photophysical behaviour of rhodamine dyes has also been explained in terms of nonradiative TICT state.⁹⁰ Intramolecular fluorescence quenching in triphenylmethane (TPM) dyes is also documented.⁴⁵ The quenching process in TPM dyes such as 23 and malachite green is believed to be linked to a twisting relaxation of the dimethylanilinogroups.



2.6. References

- 1 a) E Lippert, W. Luder, F. Moll, W. Nagele, H. Boos, H Prigge, IS. Blankenstein, *Angew. Chem.*, 73, 695, 1961; b) E. Lippert, W. Luder, H. Boos, In *Advances in Molecular Spectroscopy*, A. Mangini, ed Pergamon Press: Oxford, 1962

- 2 **J.R. Platt**, *J. Chem. Phys.*, **17**, 484, **1949**.
- 3 K. Rotkiewicz, K.H. Grellmann, Z.R. Grabowski, *Chem. Phys. Lett.*, 19315, **1973**
- 4 a) K. Rotkiewicz, Z.R. Grabowski, A. Krowczynski, W. Kuhnle, *J. Lumin.*, **12/13**, 877, **1976**, b) A. Siemiarczuk, Z.R. Grabowski, A. Krowczynski, M. Asher, M. Ottolengui, *Chem. Phys. Lett.*, **51**, 315, **1977**.
- 5 Z.R. Grabowski, K. Rotkiewicz, W. Rubaszewska, E. Kirkor-Kaminska, *Acta. Phys. Pol.*, A54, 767, **1978**.
- 6 Z.R. Grabowski, K. Rotkiewicz, A. Siemiarczuk, *J. Lum.*, **18/19**, 420, **1979**.
- 7 Z.R. Grabowski, K. Rotkiewicz, A. Siemiarczuk, D.J. Cowley, W. Baumann, *Nouv. J. Chim.*, **3**, 443, **1979**.
- 8 a) J. Karpluk, Z.R. Grabowski, F.C. De Schryver, *Proc. Ind. Acad. Sci.*, **104**, 133, **1992**; b) Z.R. Grabowski, J. Dobkowski, *Pure Appl. Chem.*, 55, 245, **1983**
- 9 T. Hayashi, N. Mataga, Y. Sakata, S. Misumi, N. Morita, J. Tanaka, *J. Am. Chem. Soc.*, 98, 5910, **1976**.
- 10 R.J. Visser, P.C.M. Weisenborn, P.J.M. Vankan, B.H. Huizer, C.A.G.O. Varma, J.M. Warman, M.P. de Haas, *J. Chem. Soc. Faraday. Trans.*, **281**, 689, **1985**.
- 11 T. Hayashi, T. Suzuki, N. Mataga, Y. Sakata, S. Misumi, *J. Phys. Chem.*, **81**, 420, 1977.
- 12 O.S. Khalil, R.H. Hofeldt, S.P. McGlynn, *Chem. Phys. Lett.*, **J7**, 497, **1972**.
- 13 a) E.A. Chandross, *In The Exciplex*, M. Gordon, W.R. Ware, eds. Academic Press: New York, 187, **1975**, b) R.J. Visser, C.A.G.O. Varma, *J. Chem. Soc. Faraday Trans.*, 2, 76, 453, **1980**; c) R.J. Visser, C.A.G.O. Varma, J. Konijnenberg, P.C.M. Weisenborn, *J. Mol. Struct.*, **Hi**, 105, **1984**; d) **R.J.**

- Visser, P.C.M. Weisenborn, C.A.G.O. Varma, *Chem. Phys. Lett.*, **113**, 330, **1985**
- 14 E.M. Kosower, H. Dodiuk, *J. Am. Chem. Soc.*, 98, 924, **1976**.
- 15 a) K. Rotkiewicz, W. Rubaszewska, *J. Lumin.*, **21**, 221, **1982**; b) K. Rotkiewicz, W. Rubaszewska, *Chem. Phys. Lett.*, 70, 444, **1980**; c) H. Bischof, W. Baumann, N. Detzer, K. Rotkiewicz, *Chem. Phys. Lett.*, **116**, 180, **1985**, d) J. Herbich, F.P. Salgado, R.P.H. Rettschnick, Z.R. Grabowski, II. Wojtowicz, *J. Phys. Chem.*, 95, **3491**, **1991**.
- 16 G. Wermuth W. Rettig, E. Lippert, *Ber. Bunsenges. Phys. Chem.*, **85**, 64, **1981**
- 17 a) W. Schuddeboom, S.A. Jonker, J.M. Warman, U. Leinhos, W. Kuhnle, K.A. Zachariasse, *J. Phys. Chem.*, 96, 10809, **1992**; b) K A. Zachariasse, TV. Haar, A Hebecker, U. Leinhos, W. Kuhnle, *Pure Appl. Chem.*, 65, 1745, **1993**
- 18 AD. Gorse, M. Pesquer, *J. Phys. Chem.*, 99, 4039, **1995**.
- 19 L.S. Andres, M. Merchan, B.C). Roos, R. Lindh, *J. Am. Chem. Soc.*, 117, 3189, **1995**.
- 20 AL. Sobolewski, W. Domcke, *Chem. Phys. Lett.*, 250, 428, **1996**.
- 21 W. Rettig, M Zander, *Ber. Bunsenges. Phys. Chem.*, 87, 1143, **1983**.
- 22 M. Zander, W. Rettig, *Chem. Phys. Lett.* **110**, 38, **1984**.
- 23 a) W. Rettig, *J. Phys. Chem.*, 86, 1970, **1982**; b) W. Rettig, R. Gleiter, *J. Phys. Chem.*, 89, 4676, **1985**.
- 24 W. Rettig, K. Rotkiewicz, W. Rubaszewska, *Spectrochim. Acta.*, 40A, 241, **1984**
- 25 G. Wennuth, W. Rettig, *J. Phys. Chem.*, 88, 2729, **1984**.
- 26 W. Rettig, F. Marschner, *Nouv. J. Chim.*, 7, 425, **1983**.

- 27 a) B. Koutek, *Collect. Czech. Chem. Commun.*, 43, 2368, **1978**. b) M.P. de Hass and J.M. Warman, *Chem. Phys.*, 73, 35, **1982**.
- 28 a) J. Czekalla, W. Liptay and K.O. Meyer, *her. Bunsenges. Phys. Chem.*, 67, 465, **1963**; b) H. Labhart, *Advan. Chem. Phys.*, 13, 179, **1967**; c) W. Liptay, *Angew. Chem.*, 81, 195, **1969**; d) W. Liptay, *In Excited States*, E.C. Lim, ed, Academic Press: New York, Vol. 1, p 129, **1974**, e) H. Labhart, *Advan. Chem. Phys.* 13, 179, 1990.
- 29 a) W. Baumann, *Ber. Bunsenges. Phys. Chem.*, 80, 31, **1976**; b) W. Baumann, H. Dickens, *ibid.* 81, 786, **1977**; c) W. Baumann, *J. Mol. Struct.*, 47, 237, 1978; d) S.A. Jonker, J.M. Warmann, *Chem Phys. Lett.*, 185, 36, **1991**; f) W. Baumann, H. Bischof, J.C. Frohling, C. Brittinger, W. Rettig, K. Rotkiewicz, *J. Photochem. Photobiol. A; Chem.*, 64, 49, 1992.
- 30 P. Suppan, *J. Lumin.*, 33, 29, **1985**.
- 31 C. Rulliere, Z.R. Grabowski, J. Dobkowski, *Chem. Phys. Letts.*, 137, 408, **1987**
- 32 T. Okada, N. Mataga, W. Baumann, A. Siemiarczuk, *J. Phys. Chem.*, 91, 4490, **1987**.
- 33 T. Okada, N. Mataga, W. Baumann, *J. Phys. Chem.*, 91, 760, **1987**.
- 34 W. Rettig, *Angew. Chem. Int. Ed. Engl.*, 25, 971, **1986**.
- 35 E. Lippert, W. Rettig, V. Bonacic-Koutecky, F. Heisel, J.A. Mische, *Adv. Chem Phys.*, 68, 1, **1987**.
- 36 W. Rettig, *In Modern Models of Bonding and Delocalisation; Series: Molecular Structure and Energetics*, J.F. Liebman, A. Greenberg, eds. Vol. 6, Chapter 5, VCH: New York, p 229, **1988**.
- 37 W. Rettig, W. Baumann, *In Photochemistry and Photophysics*, J. F. Rabek, ed. Vol. 6, CRC press: Boca Raton, p 79, **1992**.

- 38 W. Rettig, *Proc. Ind. Acad. Sci.*, KM, 89, **1992**.
- 39 K. Bhattacharyya, M. Chowdhury, *Chem. Rev.*, 93, 507, **1993**.
- 40 W. Rettig, In *Top. Curr. Chem.*, J. Mattay, ed. Vol.169, p 254, **1994**.
- 41 E. Lippert, A.A. Ayuk, W. Rettig, *Ber. Bunsenges. Phys. Chem.*, 85, 553, **1981**
- 42 a) H. Koppel, L.S. Cederbaum, W. Domcke, S.S. Shaik, *Angew. Chem.*, 95, 221, **1983**; b) H. Koppel, W. Domcke, L.S. Cederbaum, *Adv. Chem. Phys.*, 57, 59, **1984**.
- 43 a) K. Rotkiewicz, Z.R. Grabowski, J. Jasny, *Chem. Phys. Lett.*, 34, 55, **1975**;
b) D. Huppert, S.D. Rand, P.M. Rentzepis, P.F. Barbara, W.S. Struve, Z.R. Grabowski, *J. Chem. Phys.* 75, 5714, **1981**; c) Y. Wang, M. McAuliffe, F. Novak, K.B. Eisenthal, *J. Phys. Chem.*, 85, 3736, **1981**.
- 44 W. Rettig, G. Wermuth, *J. Photochem.* 28, 351, **1985**.
- 45 M. Vogel, W. Rettig, *Her. Bunsenges. Phys. Chem.*, 89, 962, **1985**.
- 46 W. Rettig, F. Marschner, *Nouv. J. Chem.*, 14, 819, **1990**.
- 47 a) W. Rettig, *J. Lumin.*, 26, 21, **1981**; b) W. Rettig, *Ber. Bunsenges. Phys. Chem.* 95, 259, **1991**.
- 48 P.F. Barbara, W. Jarzeba, *Adv. Photochem.* 15, 1, **1990**.
- 49 a) J.M. Hicks, M.T. Vandersall, Z. Babarogic, K.B. Eisenthal, *Chem. Phys. Lett.*, 116, 18, 1985; b) K.B. Eisenthal In *Ultrashort Light Pulses, Topics in Applied Physics*, W. Kaiser, ed. Springer-Verlag: Vol.60, New York, **1988**,
c) J.M. Hicks, M.T. Vadersall, E.V. Sitzmann, K.B. Eisenthal, *Chem. Phys. Lett.*, **135, 413, 1987**.
- 50 C. Reichardt, *Solvents and Solvent Effects in Organic Chemistry*, VCH: Weinheim, **1988**
- 51 J.D. Simon, S.G. Su, *J. Phys. Chem.*, 94, 3656, **1990**, 90, 6475, **1986**.

- 52 a) K. Das, N. Sarkar, D. Nath, K. Bhattacharyya, *Spectrochim. Acta.*, **48A**, **1701**, **1992**; b) T.L Chang, H.C. Cheung, *Chem. Phys. Lett.*, **173**, 343, **1990**.
- 53 a) M. Vogel, W. Rettig, U. Fiedeldei, H. Baumgaertl, *Chem. Phys. Lett.*, **148**, 347, **1988**; b) M. Vogel, W. Rettig, R. Sens, K.H. Drexhage, *Chem. Phys. Lett.*, **147**, 461, **1988**.
- 54 a) R.J. Visser, C.A.G.O. Varma, *J. Chem. Soc. Faraday Trans. 2*, **76**, 453, **1980**; b) A. Nag, T. Kundu, K. Bhattacharyya, *Chem. Phys. Lett.*, **160**, 257, **1989**; c) C.C. Dubroca, S.A. Lyazidi, P. Cambou, A. Peirigua, Ph. Cazeau, M. Pesquer, *J. Phys. Chem.*, **93**, 2347, **1989**.
- 55 a) R. Hayashi, S. Tazuke, C.W. Frank, *Macromolecules*, **20**, 983, **1987**; b) R.K. Guo, S. Tazuke, N. Kitamura, *J. Phys. Chem.*, **94**, 1404, **1990**.
- 56 K.A. Al-Hassan, T. Azumi, *Chem. Phys. Lett.*, **146**, 121, **1988**.
- 57 S. Tazuke, R.K. Guo, R. Hayashi, *Macromolecules*, **21**, 729, **1989**.
- 58 a) C. C. Dubroca, A. Peirigua, M. BenBrahim, G. Nouchi, Ph. Cazeau, *Chem. Phys. Lett.*, **157**, 393, **1989**; b) *Proc. Ind Acad Sci.*, **104**, 209, **1992**.
- 59 K.A. Al-Hassan, T. Azumi, *Chem. Phys. Lett.*, **163**, 129, **1989**.
- 60 K.A. Al-Hassan, T. Azumi, *Chem. Phys. Lett.*, **179**, 195, **1991**.
- 61 S. Tazuke, R.K. Guo, *Macromolecules*, **23**, 719, **1990**.
- 62 S. Tazuke, R.K. Guo, T. Ikeda, *J. Phys. Chem.*, **94**, 408, **1990**.
- 63 J. Paczkowski, CD. Neckers, *Macromolecules*, **24**, 3013, **1991**.
- 64 M.V. Auweraer, Z.R. Grabowski, W. Rettig, *J. Phys. Chem.*, **95**, 2083, **1991** and references therein.
- 65 J.M. Lang, Z.A. Dreger, H.G. Drickamer, *J. Phys. Chem.*, **98**, 11308, **1994**.
- 66 M. Lang, Z.A. Dreger, H.G. Drickamer, *Chem. Phys. Lett.*, **243**, 78, **1995**.
- 67 K. Hara, W. Rettig, *J. Phys. Chem.*, **96**, 8307, **1992**.
- 68 D. S. Bulgarevich, O. Kajimoto, K. Hara, *J. Phys. Chem.*, **99**, 13356, **1995**.

- 69 R. Hayashi, S. Tazuke, C.W. Frank, *Chem. Phys. Lett.*, **L35**, 122, 1987.
- 70 a) B. Bagchi, G.R. Fleming, *J. Phys. Chem.*, **94**, 9, **1990**; b) B. Bagchi, *Annu. Rev. Phys. Chem.*, **40**, 115, **1989**; c) A. Chandra, B. Bagchi, *Adv. Chem. Phys.*, **80**, **1**, **1991**; d) M. Maroncelli, *J. Chem. Phys.*, **94**, 2084, **1991**; e) S.C. Tucker, D.G. Truhler, *J. Am. Chem. Soc.*, **112**, 3347, **1990**.
- 71 a) G.R. Fleming, P.G. Wolynes, *Physics Today*, **36**, **1990**, b) M. Maroncelli, J. McInnis, G.R. Fleming, *Science*, **243**, 1674, **1989**.
- 72 a) H.J. Kim, J.T. Hynes, *J. Phys. Chem.* **94**, 2736, **1990**; *J. Chem. Phys.*, **93**, 5211, **1990**; b) D. A. Zichi, J.T. Hynes, *J. Chem. Phys.*, **88**, 2513, **1988**.
- 73 A. Wallqvist, G. Martyna, B.J. Berne, *J. Phys. Chem.*, **92**, 1721, **1988**.
- 74 a) M. Rao, B.J. Berne, *J. Phys. Chem.*, **85**, 1498, **1981**; b) C.F. Chapman, R.S. Fee, M. Maroncelli, *J. Phys. Chem.*, **94**, 4929, **1990**.
- 75 A. Polimeno, A. Barbon, P.L. Nordio, W. Rettig, *J. Phys. Chem.*, **98**, 12158, **1994**
- 76 O.S. Khalil, J.L. Meeks, S.P. McGlynn, *Chem. Phys. Lett.*, **39**, 457, 1976.
- 77 W. Rettig, V. Bonacic-Koutecky, *Chem. Phys. Lett.*, **62**, 115, **1979**.
- 78 J. Lipinsky, H. Chojnacki, K. Rotkiewicz, Z.R. Grabowski, *Chem. Phys. Lett.*, **70**, 449, **1980**.
- 79 a) J.P. Lafemina, C.B. Duke, A. Paton, *J. Chem. Phys.*, **87**, 2151, **1987**; b) J.P. Lafemina, G.K. Schenter, *J. Chem. Phys.*, **94**, 7558, **1991**.
- 80 S. Kato, Y. Amatatsu, *J. Phys. Chem.*, **92**, 7241, **1990**.
- 81 D. Majumdar, R. Sen, K. Bhattacharyya, S.P. Bhattacharyya, *J. Phys. Chem.*, **95**, 4324, **1991**.
- 82 S. Marguet, J.C. Mialocq, P. Millie, G. Berthier, F. Momicchioli, *Chem. Phys.*, **160**, 265, **1992**.
- 83 V. Bonacic-Koutecky, J. Michl, *J. Am. Chem. Soc.*, **93**, 507, **1993**.

- 84 J.P. Launay, M. Sowinska, L. Leydier, A. Gourdon, E. Amouyl, M.L. Boillot, F. Heisel and J.A. Miehe, *Chem. Phys. Lett.*, 160, 89, **1989**.
- 85 a) J.F. Letard, R. Lapouyade, W. Rettig, *J. Am. Chem. Soc.*, JJ_5, 2441, **1993**; b) E. Gilabert, R. Lapouyade, C. Rulliere *Chem. Phys. Lett.*, 82, 185, **1991**; c) J.F. Letard, R. Lapouyade, W. Rettig, *Chem. Phys. Lett.*, 222, 209, **1994**; d) Y. Maeda, T. Okada, N. Mataga, *J. Phys. Chem.*, 88, 2714, **1984**.
- 86 J. M. Vallet, F. Dupuy, R. Lapouyade, C. Rulliere, *Chem. Phys. Lett.*, 222, 571, **1994**
- 87 a) N. Nakashima, M. Murakawa, N. Mataga, *Bull. Chem. Soc. Jpn.*, 49, 854, **1976**; b) M. Migira, T. Okada, W. Rettig, *J. Phys. Chem.*, 93, 3383, **1989**; c) M. Migira, T. Okada, N. Mataga, Y. Sakata, S. Misumi, N. Nakashima, K. Yoshihara, *Bull. Chem. Soc. Jpn.*, 54, 3301, **1993**; d) W. Rettig, M. Zander, *Her. Bunsenges. Phys. Chem.*, 87, 1143, **1983**; e) A.S. Leitis, C. Monte, A. Roggan, W. Rettig, P. Zimmermann, J. Heinze, *J. Chem. Phys.*, 93, 4543, **1990**; f) H. Lueck, M.W. Windsor, W. Rettig, 94, 4550, **1990**.
- 88 a) J. Bourson, B. Valeur, *J. Phys. Chem.*, 93, 3871, **1989**; b) J.F. Letard, R. Lapouyade, W. Rettig, *Pure Appl. Chem.*, 65, 1705, **1993**; c) P.H. Cobbold, T.J. Rink, *Biochem J.*, 248, 313, **1987**.
- 89 a) G. Jones II, W.R. Jackson, A.M. Halpern, *Chem. Phys. Lett.*, 72, **391**, **1980**; b) G. Jones II, W.R. Jackson, C. Choi, W.R. Bergmark, *J. Phys. Chem.*, 89, 294, **1985**.
- 90 a) M. Vogel, W. Rettig, U. Fiedeldei, H. Baumgartel, *Chem. Phys. Lett.*, 148, 347, **1988**; b) M. Vogel, W. Rettig, R. Sens, K.H. Drexhage, *Chem. Phys. Lett.*, 147, 461, **1988**.

EXPERIMENTAL AND THEORETICAL DETAILS

In this Chapter, the details of experimental and theoretical procedures that have been followed in this investigation are presented. In the experimental section, the method of preparation and purification of the materials, instrumental details and methodologies for Photophysical investigations are described. The theoretical section outlines a summary of various semi-empirical methods and is followed by a description of the actual procedure for our AMI calculations.

3.1. Experimental

3.1.1. Materials preparation and purification

3.1.1.1. Purification of materials

4-aminophthalimide (AP), obtained from Kodak, was recrystallised several times from ethanol-water mixture. Thin, fine yellow crystals thus obtained were used for all the experiments. Laser grade coumarin dyes (**C1**, **C102**, **CT20**, **C152**, **C153**, **C154**) were obtained from Kodak and used without any further purification. *p*-(N,N-Dimethylamino)benzomtrile (Aldrich) was recrystallised several times from ethanol-water mixture before use. α -, and γ - cyclodextrins were received from Aldrich and used without any further purification. β -Cyclodextrin (Aldrich) was recrystallised twice from water before use. Sodiumdodecylsulfate (SDS) and cetyltrimethylammonium bromide (CTAB) were received from Aldrich and TRITON X-100 from Sigma and were used without any further purification.

Quinine Sulfate monohydrate (Aldrich) was recrystallised several times from water-ethanol mixture before experiment.

Extremely pure and dry solvents are essential for spectroscopy investigation involving dipolar species as contamination of the solvent by polar impurities such as water affects the spectral behaviour of the compounds significantly. As the quality of the solvents received (procured locally) was far from spectral grade, extreme care was taken for the purification and drying of the solvents in view of solvatochromic nature of the spectral bands of the compounds studied. Each solvent was purified by a standard procedure¹, which is outlined below. Only freshly purified solvents were used for measurements.

Hexane, toluene, benzene, tetrahydrofuran (THF), 1,4-dioxane and diethylether: The drying of these solvents was attained by distilling the solvent containing the blue ketyl formed by the reaction of sodium with a small amount of benzophenone.

Carbon tetrachloride (CCl_4): Distilled carbon tetrachloride was shaken with calcium chloride and then fractionally distilled once again over phosphorous pentoxide.

Ethyl acetate: First the solvent was washed with calcium chloride and dried by shaking with magnesium Sulfate. Finally, the solvent was fractionally distilled over phosphorous pentoxide.

Dichloromethane (DCM): Pre-dried with calcium chloride and distilled from phosphorous pentoxide. The solvent was stored away from light in a dark coloured bottle with molecular sieves.

Acetone: Small quantities of potassium permanganate was added several times to acetone at reflux, until a violet colour persisted. This was followed by drying with potassium carbonate and distillation.

Acetonitrile: Most of the water in acetonitrile was removed by shaking the solvent with activated silica gel. Subsequent stirring with calcium hydride until no further hydrogen was evolved left only traces of water. The acetonitrile was then fractionally distilled by refluxing over calcium hydride.

Methanol and ethanol: To 50-75 ml of alcohol, clean, dry magnesium turnings (5 g) and iodine (0.5 g) were added and warmed until the iodine disappeared and all the magnesium converted to corresponding oxide. To this, one litre of methanol or ethanol was added, refluxed for 2-3 hours and fractionally distilled.

iso-Propanol: Refluxed with calcium oxide for three hours and then distilled. The distillate was then dried over calcium hydride.

t-Butanol: Pre-dried with calcium oxide and then fractionally distilled. Dried further by distilling at reflux from magnesium activated with iodine.

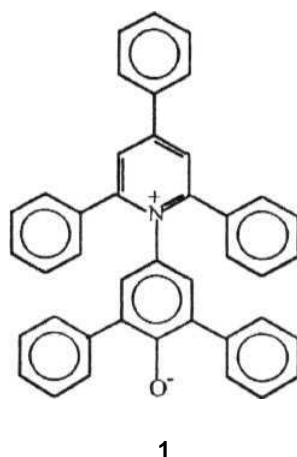
Glycerol: Glycerol was used without any further purification.

Water; Water was triply distilled for all experiments in aqueous solution.

The extent of dryness of each solvent was checked by monitoring the wavelength of the absorption maximum of a polarity sensitive betaine dye 1 in the given solvent and comparing the same with the literature value for the solvent.² 1 was introduced by Dimorth and Reichardt as a *polarity indicator* of the solvent in view of remarkable sensitivity of the charge transfer absorption band of the dye on the solvent polarity². Based on the absorption energy of the longest wavelength solvatochromic absorption band of the dye, a solvent polarity scale in terms of a polarity parameter, $E_T(30)$ was defined:

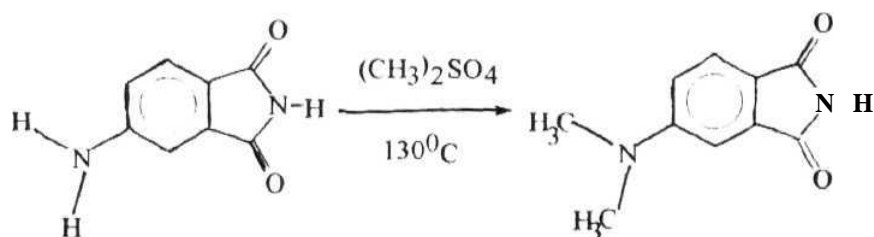
$$E_T(30)(\text{kcal mol}^{-1}) = 28591 / \lambda_{\text{max}}(\text{nm}) \quad \mathbf{3.1}$$

Where $E_T(30)$ is the transition energy of 1 measured in kcal mol^{-1} at room temperature (25° C) and normal pressure (1 bar) and λ_{max} is the wavelength of the absorption maximum in nanometers. We compared the measured $E_T(30)$ values of the solvents with the literature $E_T(30)$ values of the respective solvents to determine the extent of contamination by polar impurities. 1 was a kind gift from Prof. C. Reichardt of Philipps University and was used without any further purification.



3.1.1.2. Synthesis of 4-(*N,N*-dimethylamino)phthalimide (DAP)

DAP was synthesised from AP according to the following scheme:



Scheme 3.1

To one gm of AP (6.2 mM) taken in a 50 ml round bottomed flask, 2.75 ml of acid-free distilled dimethylsulfate (treated with K_2CO_3 followed by distillation at $175^\circ C$) was added dropwise. Then the reaction mixture was refluxed for one hour at $130^\circ C$ in oil bath. After 15 mts. of cooling, the reaction mixture was added to water and filtered. The solid thus obtained was purified by column chromatography using silica gel column and eluted with ethyl acetate and hexane

mixture. Finally, DAP was recrystallised from ethyl acetate. The purity of the compound was verified by IR, NMR and CHN analysis.

Melting Point: 210 - 212°C

IR: (KBr, cm^{-1}) 1050, 1700, 1640.

NMR: (δ) 3.1 (s, 6H), 6.9 (d, 1H), 7.5 (s, 1H), 7.6 (d, 1H).

CHN analysis: calculated for $\text{C}_{10}\text{H}_{10}\text{N}_2\text{O}_2$: C, 63; H, 5.3; N, 14.73. Found: C, 62; H, 5.44; N, 13.24.

3.1.2. Solution preparation procedure for spectral measurements

Dilute solutions (O.D \approx 0.2 at the longest wavelength absorption maximum which corresponded to a concentration of $\approx 6 \times 10^{-5}$ M) were used for the measurement of absorption, fluorescence and fluorescence excitation spectra in homogeneous media.

For studies in aqueous solutions the following procedure was adopted. A stock solution of the compound under study was prepared in triple-distilled water. For partially soluble compounds, solutions were sonicated for 30 mts. to one hour and allowed to settle for 30 minutes. This was followed by repeated filtration of the solution so as to avoid any undissolved solute particles. The solution was then diluted to give O.D of \sim 0.2 at the longest wavelength absorption maximum. Required amount of cyclodextrin or surfactant was added to this solution for studies in microheterogeneous media and steady state or time-resolved measurement was performed. At higher concentration of the cyclodextrins (particularly with β -cyclodextrin), solutions were sonicated for 30

minutes and kept aside for 15 minutes to see whether there is any precipitation on cooling.

3.1.3. Measurement of fluorescence quantum yields (ϕ_f)

Quinine Sulfate was used as the reference compound for fluorescence quantum yield measurements of all the samples ($\phi_f = 0.55$ in 1N H₂SO₄).³ Fluorescence quantum yields were estimated by measurements of the areas under the fluorescence spectra using the following expression.⁴

$$\phi_{\text{sample}} = \frac{I_{\text{sample}} \times \text{O.D}_{\text{standard}}}{I_{\text{standard}} \times \text{O.D}_{\text{sample}}} \times \phi_{\text{standard}} \quad 3.2$$

Where I is the area under the emission spectral curve, O.D is the optical density of the compound at the exciting wavelength. For actual measurements, optically matched solutions of the reference compound and the sample were used and areas were determined by weighing. No solution of O.D more than 0.2 at the exciting wavelength was used and no correction for the solvent refractive indices was made.

3.1.4. Measurement of dipole moment change on excitation ($\Delta\mu$)

Although a number of expressions have been proposed to describe the effect of solvent polarity on the absorption and emission spectra of a

compound⁵⁻⁶ the most widely used expression is one based on early experiments of Lippert and Mataga.⁵ Onsager's reaction field theory provides the basic framework for the equation, which assumes the fluorophore as a point dipole situated in the centre of a spherical cavity, known as Onsager cavity, in a homogeneous and continuous dielectric medium.⁷ According to this model, the fluorophore-solvent interaction is given by the interaction of the dipole in the cavity with its own reaction field arising from the polarisation of the surrounding dielectric by the dipole. According to Lippert-Mataga equation,⁵ the energy difference between the absorption and fluorescence maximum of any compound ($\bar{\nu}_a - \bar{\nu}_f/\text{cm}^{-1}$) in a given solvent is related to the solvent polarity function Δf as shown below.

$$\bar{\nu}_a - \bar{\nu}_f = \frac{2(\mu_e - \mu_g)^2}{hca^3} \Delta f + \text{constant} \quad 3.3$$

Where, Δf is equal to $[(\epsilon-1)/(2\epsilon+1) - (n^2-1)/(2n^2+1)]$, h is the Planck constant, c is velocity of light, a is the Onsager cavity radius and μ_g and μ_e are the ground and excited dipole moments of the molecule, ϵ is the dielectric constant and n is the refractive index of the solvent. The solution of this equation requires the use of measurable parameters such as the Onsager cavity radius, the absorption and fluorescence band maxima in solvents of varying polarities. $\Delta\mu$ was estimated from the slope of the plot of $\bar{\nu}_a - \bar{\nu}_f$ vs Δf .

The reliability of the measured value of the change in dipole moment on excitation using Lippert-Mataga equation is highly dependent on the choice of the Onsager radius. When a given compound has acceptable solubility only in limited

number of solvents the number of data points are few and this makes statistical analysis less reliable. Another disadvantage with this solvatochromic procedure is that in mixed solvents one needs to measure the dielectric constant and refractive index of several mixtures of different compositions or these values have to be approximated from empirical rules. Very recently, Ravi et al has suggested a modified equation (equn. 3.4) for the determination of the change in dipole moment on excitation, in which the Stokes shift is correlated with a microscopic solvent polarity parameter.⁸ It is known that Stokes shift data show a better correlation with microscopic solvent polarity parameter, $E_T(30)$ or E_T^N (as defined below) than with bulk polarity functions such as Δf .⁹

The modified equation, believed to eliminate some of the disadvantages associated with the measurement of the change in dipole moment using Lippert-Mataga equation, is

$$\Delta \bar{\nu} = 11307.6 [(\Delta \mu / \Delta \mu_D)^2 (a_D / a)^3] E_T^N + \text{constant.} \quad 3.4$$

$$\text{where, } E_T^N = [E_T(\text{solvent}) - E_T(\text{TMS})] / [E_T(\text{water}) - E_T(\text{TMS})] \quad 3.5$$

$E_T(\text{solvent})$, $E_T(\text{TMS})$, $E_T(\text{water})$ are the $E_T(30)$ values of the solvent, tetramethylsilane and water respectively.

The derivation of equn. 3.4 is based on the following arguments. The linear relation between the Stokes shift $\nu(m,s)$ of a molecule (m) in solvent (s) and the solvent polarity function $X(s)$ can be represented as

$$Y(m,s) = B(m) X(s) + Y(m,g) \quad 3.6$$

where, $Y(m,g)$ is a constant independent of the solvent and $B(m)$ is the regression coefficient given by $B(m) = 2(\Delta\mu)^2/hca^3$.

For 1, the ground state dipole moment (15 D) is much higher than the excited state dipole moment (6 D).² Assuming therefore, a negligible shift of the fluorescence band one can write $Y(m,s) = \bar{\nu}$ -constant. Substitution of this on equn. 3.6 yields

$$\bar{\nu}_a - \text{constant} = [2(\Delta\mu_D)^2 / hca_D^3]X(s) + Y(m,g) \quad 3.7$$

where $\Delta\mu_D$ is the change in dipole moment on excitation of the dye 1 (9 D) and a_D is its Onsager radius. Using the definition of $E_T(30)$ in terms of $\bar{\nu}_a$, the following equation can be written,

$$X(s) = 349 [hca_D^3 / 2(\Delta\mu_D)^2]E_T(30) + Y'(m,g) \quad 3.8$$

To avoid dimensionality problem, when the normalised value of $E_T(30)$, namely E_T^N is used,

$$X(s) = 11307.6 [hca_D^3 / 2(\Delta\mu_D)^2] E_T^N + Y''(m,g) \quad 3.9$$

Thus this treatment provides an expression for $X(s)$ which when substituted back into equn. 3.6 gives the working expression as shown in equn. 3.4. This equation illustrates the linear correlation of Stokes shift with solvent polarity function, E_T^N . The $\Delta\mu$ values can be obtained from a plot of the Stokes shift versus E_T^N . An Onsager radius of 6.2 Å for the dye is recommended for $\Delta\mu$ calculations which corresponds to half the distance between the amino nitrogen atom and the carbonyl oxygen atom in **the** optimised **structure**.

3.1.5. Calculation of radiative and nonradiative lifetimes

The radiative rate constants, k_R^{SB} of AP and DAP in different solvents have been calculated using Strickler-Berg equation¹⁰

$$\frac{1}{\tau_0} = k_R^{SB} = 2.88 \times 10^{-9} \times n^2 \langle \bar{\nu}^{-3} \rangle_{Av}^{-1} \frac{(g_l)}{(g_u)} \int \epsilon \, d\ln \bar{\nu} \quad 3.10$$

Where n is the refractive index of the solvent, g_l and g_u are the multiplicities of the lower and upper states and

$$\langle \bar{\nu}^{-3} \rangle_{Av}^{-1} = \frac{\int I(\nu) d\nu}{\int \nu^{-3} I(\nu) d\nu} \quad 3.11$$

τ_0 , **the** reciprocal of the radiative rate constant, represents the radiative lifetime of **the** excited state which is related to the actual lifetime (τ) as

$$\tau = \phi_f \times \tau_o \quad 3.12$$

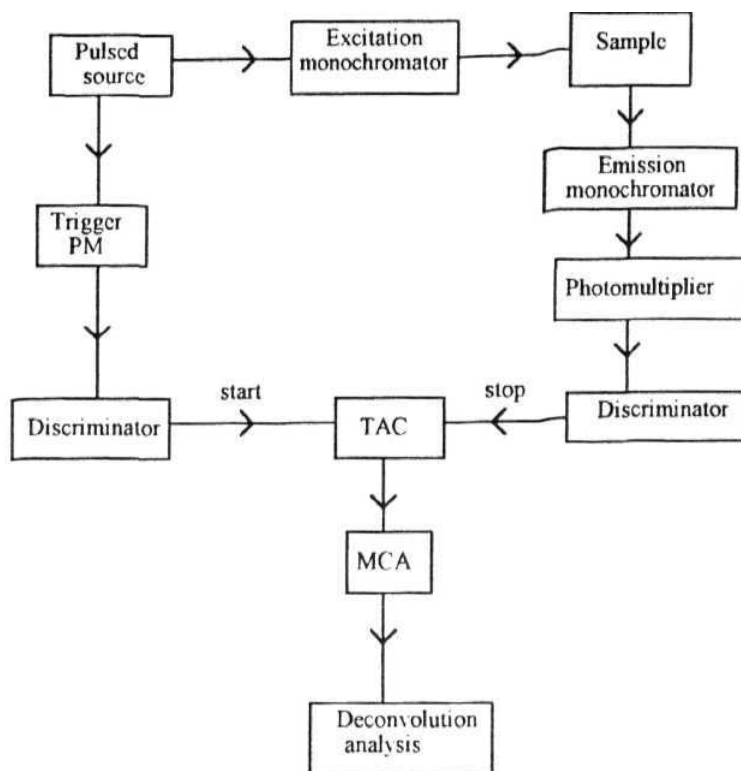
The radiative rate constants calculated by the **Strickler-Berg** formula (equn. 3.10) were compared with the same determined independently from the measured values of ϕ_f and τ using equn. 3.12. The nonradiative rate constants (k_{nr}) were estimated by the following equation.

$$k_{nr} = (1 - \phi_f) / \tau \quad 3.13$$

3.1.6. Instrumentation

The absorption spectra were recorded either on a Perkin-Elmer Lambda-3B or a JASCO model 7800 spectrophotometer. The fluorescence spectra were recorded on a Hitachi F-3010 or a JASCO FP 777 spectrofluorimeter. The fluorescence spectra were not corrected for the instrumental response.

The fluorescence lifetimes were measured on PTI or IBH 5000 single-photon-counting spectrometer.¹¹ A schematic diagram of the set-up of the instrument is shown below.



A hydrogen flash-lamp of pulse-width 1.6 ns was employed as the excitation source. The lamp was operated at a frequency of 40 MHz. A part of the incident pulse train was focused on a photomultiplier tube (1P28) and the photomultiplier signal was fed into a constant-fraction-discriminator (CFD) to discriminate the background noise and generate a precise timing pulse. The output of CFD served as the START pulse of the time-to-amplitude converter (TAC). The first fluorescence photon reaching the detection photomultiplier (Hamamatsu 3235) generated a pulse which, after passing through CFD (for reasons already described) served as the STOP signal for the TAC. The time-difference between the START and the STOP signal was due to the time taken for the pulses to travel through the cables/electronics and for the excited state to

relax and emit a photon. The TAC converted the time-difference to a voltage which was then fed into a multi-channel analyser (MCA). The MCA was operated in the pulse-height-analysis mode and counts were recorded in each voltage channel. Repetitive laser-pulsing and emitted photon collection produced a histogram of voltage against counts in MCA. This provided the time-profile of the fluorescence intensity. For recording the lamp profile, a scatterer (dilute solution of magnesium oxide in water) was placed in place of the sample and the same procedure was repeated.

When the decay time is long compared to the decay time of the excitation pulse, the excitation may be described as a delta function. However, when the lifetime is short, distortion of the experimental data occurs, by the finite decay time of the lamp pulse and response time of the photomultiplier and associated electronics. Since the measured decay function was a convolution of the true fluorescence decay, it was necessary to analyse the data by deconvolution in order to estimate the fluorescence lifetime.

The lifetime was calculated with the help of the convolution integral,

$$f(t') = \int_0^{t'} y(t) P(t' - t) dt \quad 3.14$$

where $f(t')$ is the fluorescence intensity at any time t' . $Y(t)$ is the intensity of the exciting light at time t , $P(t'-t)$ is the response function of the experimental system.

The values of $f(t)$ and $Y(t)$ as a function of time measured in MCA were fed into a computer (IBM PC clone, 80486, 50 MHz) to determine T . We used **IBH** program to analyse multiexponential decays. The **deconvolution** program was based on least square iterative method.

An excitation pulse was recorded and then deconvolution started with mixing of the excitation pulse and a projected decay to form a new reconvoluted set. This data was compared with the experimentally obtained data and the difference between data points summed generating the χ^2 function for the fit. The deconvolution proceeded through a series of such iterations until an insignificant change occurs between iterations. The quality of the fit was assessed by inspection of reduced χ^2 , plot of weighted residuals and autocorrelation functions of the residuals. The data points and the fitted curve were finally recorded by a plotter.

Standard error limits involved in various measurements are,

λ_{max} (absorption / fluorescence)	$\pm 1 \text{ nm}$
ϕ_f	$\pm 10 \%$
$\tau (> 1 \text{ ns})$	$\pm 5 \%$
$T (< 1 \text{ ns})$	$\pm 15 \%$

3.2. Theoretical

3.2.1. Semi-empirical calculations

Quantum chemical calculations are generally based on either an *ab initio* or a semi-empirical method¹². The oldest and simplest semi-empirical method of quantum chemistry, utilising the so-called pi-electron approximation is that of Huckel, usually referred to by the abbreviation HMO (Huckel Molecular Orbital method). The counterpart of the traditional Huckel method represented by the so-called Extended Huckel Theory (EHT) was proposed by R. Hoffmann in 1963. Other than EHT method, we can distinguish the NDDO (neglect of diatomic differential overlap), CNDO (complete neglect of differential overlap) and INDO (intermediate neglect of differential overlap) schemes introduced in 1965 by Pople and his co-workers.¹⁴ These schemes represent the highest degree of sophistication in the present day semi-empirical methods. These schemes are obtained by various approximations involved in the reduction of the non-empirical Hartree-Fock equation. Among the INDO-type methods one should consider the semi-empirical approach due to Dewar et al and known as MINDO (modified intermediate neglect of differential overlap) schemes.¹⁶ Confidence in a semi-empirical procedure is strengthened by demonstration of its ability to reproduce experimental results unrelated to those used in determining the parameters in it. One of the major assets of MINDO/3 and MNDO was their demonstrated ability to reproduce the ground state properties of molecules of all kinds.^{15,16}

MINDO/3 has proved very effective in studies of a wide variety of hydrocarbons. Problems arise, however, in the case of molecules containing

heteroatoms because of the neglect of one-centre overlap in the INDO approximation on which MINDO/3 is based.¹⁶ To overcome this weakness, a new parametric quantum mechanical molecular model, AM1 (Austin Model 1) based on NDDO approximation is described by Dewar et al.¹⁷ Calculations on 167 test molecules indicate that AM1 represents a real improvement over MNDO, with no increase in the computing time. The specific failings in MNDO have been at least moderated while the average error for molecules of other kinds has also been reduced. The main gains are the ability of AM1 to reproduce hydrogen bonds and the promise of better estimates of activation energies for reactions and is also found to be an effective method for studying processes involving deprotonation of neutral molecules. Recent AM1 results on some large polar systems indicate that this method is capable of predicting the excited state properties fairly well.¹⁸

Using the program, PCMODEL, which enables us to draw the molecule, the geometry of the molecules were first roughly optimised using the MMX force field and generated the corresponding Cartesian coordinates. A more precise geometry optimisation was then achieved using the AM1 Hamiltonian of the MOPAC program. MOPAC (ver. 5.0) is a general purpose semi-empirical molecular orbital package for the study of chemical reactions. Subsequently unrestricted ground state optimisation for various twist angles (at every ten degrees) of the amino or dialkylamino group with respect to plane of ring was performed. The gradient norms for each geometry were monitored to test the successful convergence by using the keyword PRECISE. While these calculations were performed on personal computers, the excited state calculations were performed on a DEIL microvax 3300 computer. For every twist angle of the

ground state geometry, excited state calculations were performed using the keywords, AM1, C.I.=16, MICROS=128, EXCITED, MECl (multi electron configuration interaction). The keyword C.I.=16 allows us to use eight Highest Occupied Molecular Orbitals (HOMO) and eight Lowest Unoccupied Molecular Orbitals (LUMO). Option MICROS=128 generates 128 microstates, each state formed with excitation of one electron from each of the eight HOMOs to one of the eight LUMOs. Only singly excited configurations were considered. Output of each calculation gives us the heat of formation, dipole moment, ionisation potential and gas phase energy.

3.2.2. Calculation of Solvation Energies

The solvation energies of different electronic states have been taken into account in our calculations within the basic framework of Onsager's theory.⁷ The energy of a dipole $\vec{\mu}$, in the reaction field R is given by

$$E = \vec{\mu} \cdot \mathbf{R} \quad 3.15$$

When a molecule with a permanent dipole strength $\vec{\mu}$ is surrounded by other molecules, the inhomogeneous field of the permanent dipole polarises its environment. The resulting inhomogeneous polarisation of the environment will give rise to a field at the dipole, which is called the reaction field, R and is given by,

$$\bar{R} = \frac{2}{a^3} f \bar{\mu} \quad 3.16$$

where f is factor of the reaction field, $\bar{\mu}$ is the solute dipole causing polarisation of the cavity of radius, a . When the solvent is fully equilibrated, f is given by $f(\epsilon) = [(c - 1)/(2c + 1)]$. But if the dipole moment of the solute changes so rapidly that the solvent dipoles cannot reorient although its electrons are polarised, then f is given by $f(n) = (n^2 - 1)/(2n^2 + 1)$. The solvation energy of a fully relaxed state of dipole $\bar{\mu}_i$ has been calculated using the relation,⁷

$$\Delta E_{fs} = -\frac{2\bar{\mu}_i^2}{a^3} \left(\frac{\epsilon - 1}{2\epsilon + 1} \right) \quad 3.17$$

where $\bar{\mu}_i$ represents the dipole about which the solvent is fully equilibrated. If the change of dipole moment of solute from $\bar{\mu}_i$ to $\bar{\mu}_f$ is very fast, then the solvent molecules do not have sufficient time to reorient themselves within the electronic excitation. Then one has to calculate the energy for the partially solvated state. The solvation energy of a partially solvated state has been calculated using the following relation.¹⁹

$$\Delta E_{ps} = -\frac{2}{a^3} \bar{\mu}_f \bar{\mu}_i \left(\frac{\epsilon - 1}{2\epsilon + 1} - \frac{n^2 - 1}{2n^2 + 1} \right) - \frac{2\bar{\mu}_f^2}{a^3} \left(\frac{n^2 - 1}{2n^2 + 1} \right) \quad 3.18$$

Thus in order to calculate the transition energy for absorption, the solvation energy of the LE state was calculated by using **equn. 3.18**. Since the fluorescence lifetime of most of the molecules is longer than the relaxation time of the solvent, the emitting states can be assumed to be fully solvated. Therefore, the solvation energy of the state from where the emission originates is calculated by using the **equn. 3.17** and for the final state the solvation energy calculated using **equn. 3.18**.

3.3. References

- 1 D.D. Perrin, W.L.F. Armarego, D.R. Perrin *Purification of Laboratory Chemicals*, II edition, Pergamon Press: New York, **1986**.
- 2 C. Reichardt, *Solvents and Solvent Effects in Organic Chemistry*, chapter 7, VCH: Weinheim, **1988** and references therein.
- 3 W.H. Melhuish, */. Phys. Chem.*, 64, 762, 1960.
- 4 E. Austin, M. Gouterman, *Bioinor. Chem.*, 9, 281, **1978**.
- 5 a) E.Z. Lippert, *Z Naturforsch*, **10A**, 541, **1955**, b) N. Mataga, Y. Kaifu, M. Koizumi, *Bull. Chem. Soc. Jpn.*, 29, 465, **1956**.
- 6 B. Koutek, *Collect. Czech. Commun.*, 43, 2368, **1978**.
- 7 C.J.F. Bottcher, *Theory of Electric Polarisation*, Vol.1, Elsevier: Amsterdam, p 153, **1973**.
- 8 M. Ravi, A. Samanta, T.P. Radhakrishnan, */. Phys. Chem*, 98, 9133, **1994**.
- 9 a) V. Nagarajan, A.M. Brearly, T. Kang, P.F. Barbara, */. Chem. Phys.*, 86, 3183, **1987**; b) G.S. Cox, P.J. Hauptman, N.J. Turro, *J. Photochem. Photobiol.*, 39, 597, **1984**.

- 10 S.J. Strickler, R.A. Berg, *J. Chem. Phys.*, 37, **814**, **1962**.
- 11 a) D. V. O'Connor, D. Phillips, *Time-Correlated Single Photon Counting*, Academic Press: New York, **1984**; b) J.R. Lakowicz, In *Topics in Fluorescence Spectroscopy*, J.R. Lakowicz, ed. Vol.1, Plenum Press; New York, **1991**.
- 12 J. Sadlej, In *Semi-empirical Methods of Quantum Chemistry*. Ellis-Horwood; Poland, **1985** and references therein.
- 13 a) R. Hoffmann, *J. Chem. Phys.*, 39, 1397, **1963**; b) *ibid*, 40, 2047, **1964**.
- 14 J.A. Pople, D.L Beveridge, P.A. Dobosh, *J. Chem. Phys.*, 47, 2026, **1967**.
- 15 R.C Bingham, M.J.S. Dewar, D.H. Lo, *J. Am. Chem. Soc*, 97, 1285, 1294, 1302, 1307, **1975**.
- 16 M.J.S. Dewar, W. Thiel, *J. Am. Chem. Soc*, 99, 4899, 4907, **1977**.
- 17 a) M.J.S. Dewar, E.G. Zoebisch, E.F. Healy, J.J.P. Stewart, *J. Am. Chem Soc*-, 107, 3902, **1985**, b) M.J.S. Dewar, K.M. Dieter, *J. Am. Chem. Soc*, 108, 8075, **1986**.
- 18 a) P.K. McCarthy, G.J. Blanchard, *J. Phys. Chem.*, 97, 12205, **1993**; b) M.M. Awad, P.K. McCarthy, G.J. Blanchard *J. Phys. Chem.*, 98, 1454, **1994**.
- 19 D. Mazumdar, R. Sen, K. Bhattacharyya, S.P. Bhattacharyya, *J. Phys. Chem.*, 95, 4324, **1991**.

A STUDY OF THE TICT PHENOMENON IN AMINOBENZONITRILES BY AMI METHOD

In this Chapter, we present the results of a theoretical investigation based on semi-empirical AMI method on one of the most extensively studied systems that exhibit the TICT phenomenon, p-(dimethylamino)benzonitrile (DMABN).¹⁻² We also describe the results on a structurally similar molecule, p-aminobenzonitrile (ABN) which does not exhibit dual fluorescence.³⁻⁵

4.1. Introduction

The system which received the maximum attention as far as the TICT phenomenon is concerned is undoubtedly DMABN. As this molecule provides a testing ground for quantum chemical methods, a large number of calculations based on either *ab initio*⁶⁻¹⁰ or semi-empirical method¹¹⁻¹⁶ have been performed on DMABN right from the introduction of the TICT concept by Grabowski and co-workers² till very recently to test the validity of the TICT mechanism or the predictive ability of a particular method.

Rettig et al carried out *ab initio* and CNDO/S calculations in late seventies in order to understand the origin of multiple fluorescence in DMABN and related molecules.¹² The results of this calculation are qualitative due to the limited number of configurations used. Also, the role of the solvent which is so

crucial was not taken into consideration in this calculation. Lipinski et al performed INDO-CI calculations only at two extreme **geometries**.¹³ Lafemina et al applied CNDO/S3 method on DMABN and related **molecules**.¹⁴ However, they also did not take into account the solvent stabilisation of the TICT state while carrying out the calculation. Lower level *ab initio* calculations based on SCF-MO method have also been performed on DMABN by Kato and Amatatsu.⁷ *Ab initio* calculations at higher level have been **carried** out for smaller molecules such as **aminoborane**.⁸ A more detailed semi-empirical calculation based on MNDO and CNDO/S-CI methods on DMABN in which a number of excited states are considered and the solvation phenomenon is taken into account has been performed by Bhattacharyya et al.¹⁵ Although this method explains a number of experimental features of DMABN, it fails to take into account some of the experimental data. Recently *ab initio* calculations using the complete active space (CAS) SCF method in combination with multiconfigurational second order perturbation theory (CASPT2) have been performed on aminobenzonitriles which accounts for most of the experimental features of the two molecules in terms of the TICT **model**.⁹ Further, it is shown in this calculation that the recently proposed N-inversion mechanism of Zachariasse and co-workers³ can not be considered as an alternative to the TICT model. The major drawbacks of this calculation are perhaps nonconsideration of the role of solvent and the data limited to few dihedral angles. In a very recent *ab initio* calculation on benzonitrile and aminobenzonitriles the possibility of the bending of the cyano group as the intramolecular coordinate (which was mentioned in the early work of Rotkiewicz et al¹ and studied later by a semi-empirical method (INDO/S) by Lewis and co-worker¹¹) has been **investigated**.¹⁰ It is concluded that bending of the cyano group, in other words, change of

hybridisation of the carbon atom in the acceptor group (cyano group in this particular case) from sp to sp^2 leads to stabilisation of the charge transfer state. However, the effect of the solvent is not included in these calculations. Also, the conclusion that rehybridisation is responsible for stabilisation of the charge transfer state can not explain the anomalous behaviour of many systems such as, biaryls.¹⁷

The following investigation on DMABN using the AM1 method has been carried out for the following reasons. First, we were in search of a quantum chemical method that would allow us to calculate the excited state properties of DMABN donor-acceptor molecules reasonably well. While doing so we kept in mind the limited computational facilities which were available with us. When we noted that AM1 is possibly the best semi-empirical method available for the calculation of ground state properties¹⁸ and came across some papers in which the excited state properties of some systems have been calculated and shown to be in agreement with experimental data,¹⁹ we decided to test the predictive ability of the method on DMABN and ABN (two structurally very similar molecules, yet quite different Photophysical properties) as no calculations based on this method was performed on these systems till then. Subsequent to communication of our results for publications, a paper in which the same method (using different CI and solvation model) has been applied to DMABN appeared in print.¹⁶ We included ABN as another system for investigation as its fluorescence properties are quite different from that of DMABN. The method, if capable of explaining the difference in properties of the two structurally similar compounds, could be applied to other systems of interest for apriori prediction of

the possible role of a rotary decay mechanism. This was our second objective for carrying out this calculation.

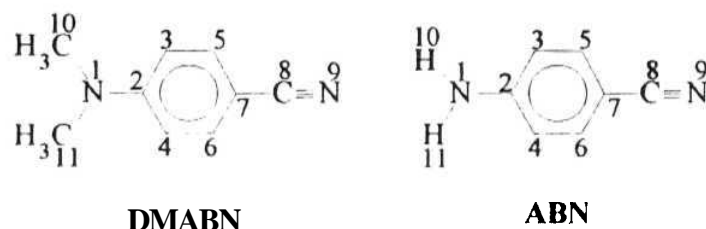


CHART 4.1

4.2. Ground state properties

The calculated bond lengths and bond angles of the fully optimised planar and perpendicular conformations of ABN and DMABN in the ground state are shown in Tables 4.1. The charge densities for the planar conformers of the two molecules are shown in fig. 4.1. Although the **AM1** calculated geometrical parameters are not significantly different from those obtained by **MNDO** calculations,¹⁵ a number of ground state properties are found to be quite different in these two methods. The most notable of them is the ground state dipole moment of DMABN. The **AM1** calculated dipole moment of the minimum energy conformer (planar form) is 5.71 D, whereas that obtained by the **MNDO** method is close to 4 D.¹⁵ The experimentally obtained dipole moment of DMABN (5.5 D)²⁰ is much closer to the **AM1** calculated value (5.7 D). For ABN, the calculated dipole moment is found very similar (5.45 D). The calculated charge densities at different atoms of the two molecules, shown in fig. 4.1, are very similar to expect any difference in their dipole moment values.

Table 4.1. AM1 calculated geometrical parameters for the planar and perpendicular conformers of ABN and DMABN in the ground state.^a

ABN			DMABN		
Geometrical parameters	0°	90°	Geometrical parameters	0°	90°
r(1-2)	1.3730	1.3969	r(1-2)	1.3885	1.4115
r(2-3)	1.4194	1.4128	r(2-3)	1.4211	1.4122
r(2-4)	1.4213	1.4131	r(2-4)	1.4210	1.4123
r(3-5)	1.3857	1.3897	r(3-5)	1.3860	1.3903
r(4-6)	1.3851	1.3903	r(4-6)	1.3861	1.3908
r(5-7)	1.4032	1.4012	r(5-7)	1.4016	1.4011
r(6-7)	1.4034	1.4010	r(6-7)	1.4181	1.4010
r(7-8)	1.4185	1.4208	r(7-8)	1.4181	1.4210
r(8-9)	1.1640	1.1636	r(8-9)	1.1639	1.1636
r(1-10)	0.9858	0.9820	r(1-10)	1.4324	1.4247
r(1-11)	0.9859	0.9820	r(1-11)	1.4324	1.4247
0(1-2-3)	121.11	120.87	0(1-2-3)	121.14	120.64
0(1-2-4)	121.01	120.82	0(1-2-4)	121.14	120.78
0(2-3-5)	120.72	120.92	0(2-3-5)	120.83	120.61
0(7-5-3)	120.62	120.12	0(7-5-3)	120.74	120.23
0(2-4-6)	121.00	120.67	0(2-4-6)	121.82	120.62
0(4-6-7)	120.32	120.31	0(4-6-7)	120.74	120.18
0(8-7-5)	120.30	120.14	0(8-7-5)	120.42	120.12
0(9-8-7)	180.00	180.00	0(9-8-7)	180.00	179.98
0(10-1-2)	120.14	119.55	0(10-1-2)	120.20	118.89
0(11-1-2)	120.15	119.56	0(11-1-2)	120.20	118.87

atoms numbering are as per the Chart 4.1. Bond lengths (r) and bond angles (0) are expressed in Å and deg. respectively.

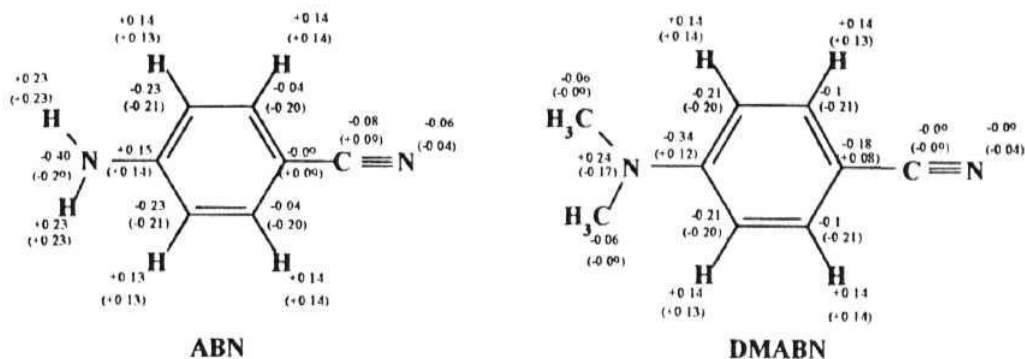


Fig. 4.1. Electronic charge densities in the ground and excited state of DMABN and A BIN. The excited state charge densities are shown in parenthesis.

According to the MNDO results, the ground state energy of an isolated DMABN molecule is minimum for a conformation with twist angle of around 50° and the minimum shifts to a twist angle of 30° in a solvent of dielectric constant of 80^{15} . This result is in sharp contrast with our AM1 results which indicate that the planar form (twist angle of 0°) is the most stable conformation of both DMABN and ABN irrespective of the solvent polarity. Based on the overwhelming experimental data which unequivocally point to a planar ground state of DMABN²¹ we conclude that the AM1 method provides a more realistic picture of the ground state of DMABN. While no structural data available for ABN to suggest a planar conformation, very similar ground state dipole moments of ABN and DMABN, and theoretical results obtained by other methods support our conclusion.^{4,9}

Another prediction of the MNDO method is that the twisting of the dimethylamino group is essentially free in the ground state (the energy difference between the perpendicular and the minimum energy form is only 0.04 eV)¹⁵. If that was the case then one would have expected existence of several conformers in the ground state which would have resulted in significant broadening of the absorption spectrum; distinct absorption to the TICT state could also have been observed. This is, however, contrary to the experimental observations.^{1,2}

On the other hand, it can be seen from figs. 4.2 and 4.3 (where the variation of the ground state energies of ABN and DMABN are shown as a function of the twist angles) that the AM1 calculated ground state energies of both the compounds increase monotonically as the twist angle is increased from 0° to 90°. The energy differences between the planar and perpendicular conformers of ABN and DMABN in the gas phase were found to be 0.38 eV and 0.29 eV respectively. These barriers are too high to expect any noticeable amount of the twisted conformer in the ground state at room temperature in the gas phase. This conclusion is again consistent with the experimental observation that twisting of the dimethylamino group is only an excited state phenomenon.^{1,2}

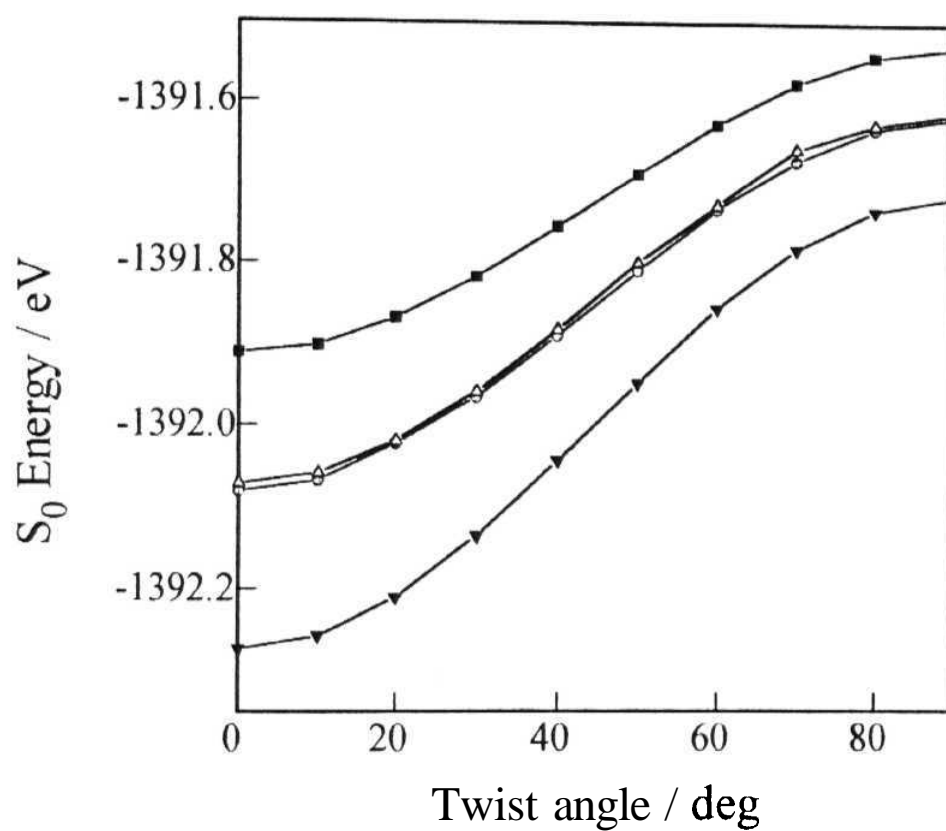


Fig.4.2. Variation of the ground state energy of ABN as a function of the twist angle in the gas phase (•), dioxane (Δ), THF (•) and acetonitrile(▼).

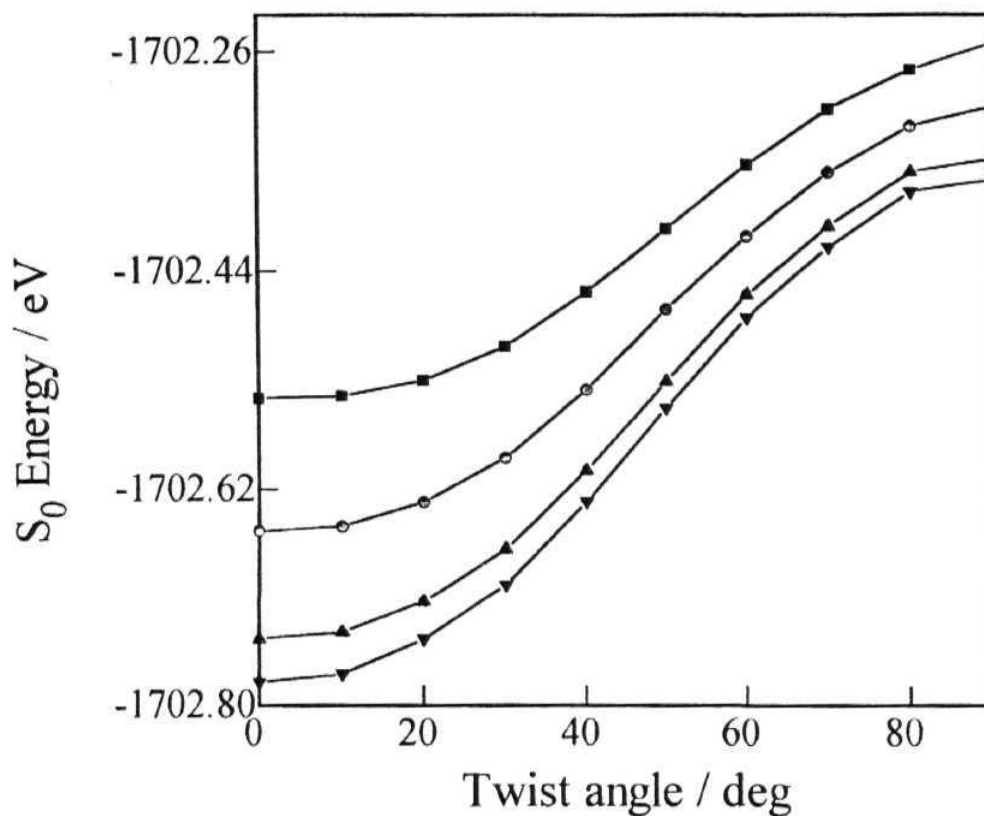


Fig.4.3. Variation of the ground state energy of DMABN as a function of the twist angle in gas phase (•), dioxane (◐), THF (▲) and acetonitrile(▼).

As it is necessary to have a knowledge of the dipole moments of different conformers of ABN and DMABN in order to find out the effect of solvent on the energy profiles, we have calculated the dipole moments (μ_g) of different conformers of ABN and DMABN which are presented in Table 4.2 along with the heats of formation (AHf) data.

Table 4.2. Heats of formation (ΔH_f) and dipole moment (μ_g) values of ABN and DMABN at different twist angles in the ground state.

Twist angle (deg)	ABN		DMABN	
	ΔH_f kcal mol ⁻¹	Debye	ΔH_f kcal mol ⁻¹	μ_g Debye
0	51.22	5.45	61.41	5.70
10	51.45	5.40	61.47	5.65
20	52.21	5.29	61.74	5.45
30	53.37	5.10	62.36	5.21
40	54.80	4.86	63.33	4.87
50	56.32	4.60	64.50	4.49
60	57.76	4.34	65.71	4.17
70	59.93	4.11	66.81	3.93
80	59.70	3.97	67.59	3.71
90	59.96	3.91	68.13	3.94

The solvated ground state energies of the two compounds in **1,4-dioxane** ($\epsilon=2.21$), THF ($\epsilon=7.58$) and acetonitrile ($\epsilon=35.94$) have been calculated on estimation of the solvation energies of different conformers with the help of eqn. 3.17 using the dipole moment values from Table 4.2. The solvated energy profiles are also shown in figs. 4.2 and 4.3. It can be seen that with increase in the solvent polarity, the planar conformer is stabilised relative to the twisted conformer (since the dipole moments of ABN and DMABN, as shown in Table 4.2, decrease with increase in twist angle). This results in an increase in the energy gap between two conformers from 0.29 eV in gas phase to 0.39 eV in acetonitrile for DMABN and 0.38 eV in gas phase to 0.55 eV in acetonitrile for ABN, making twisting more difficult in a polar solvent.

4.3. Excited state properties

4.3.1. Dipole moments

The dipole moments of different conformers of the two molecules in the lowest excited singlet state are presented in Table 4.3 along with the heats of formation values. It can be seen from the Table that as the twist angle is increased from 0° there is a gradual decrease in the dipole moment. However, the dipole moment starts increasing sharply from a twist angle of 40° for DMABN and 60° for ABN. This indicates that at around 40° and 60° the nature of the electronic state is changed. Similar reversal of the electronic state is reported in the literature.¹³

Table 4.3. Heats of formation (ΔH_f) and dipole moments (μ_e) of ABN and DMABN for different twist angles in the lowest singlet excited state.

Twist angle deg	ABN		DMABN	
	ΔH_f kcal mol ⁻¹	μ_e Debye	ΔH_f kcal mol ⁻¹	μ_e Debye
0	136.30	6.70	145.79	7.69
10	136.55	6.67	145.89	7.65
20	137.50	6.57	146.24	7.53
30	139.00	6.37	147.10	7.35
40	141.02	6.10	148.08	8.76
50	143.37	5.77	147.78	9.75
60	144.86	7.39	146.99	11.16
70	146.32	8.46	145.83	12.61
80	147.85	10.35	144.88	13.59
90	149.16	12.87	143.77	14.10

The calculated dipole moments of the LE and twisted states of DMABN are 7.69 and 14.1 D, respectively and for ABN the respective values are 6.70 D and 12.87 D. The dipole moments of ABN in the LE and TICT states agree fairly well with the same obtained by other theoretical methods⁹⁻¹⁰ and experimental measurements.⁴ The dipole moments of DMABN obtained from various methods are summarised in Table 4.4. It can be seen that the experimental values of μ_g and $\mu_e(\text{LE})$ vary within a small range depending on the technique used. However, a large variation of the experimental dipole moment of the twisted state from 23 D to 12.2 D is reported in the literature.^{4,9-16,20-24} Our value (14.1 D) is in fair agreement with the experimental dipole moment obtained by direct methods such as electrochromic fluorescence measurements²² or time-resolved microwave conductivity measurements. We would also like to note that although the dipole moments obtained by the AMI and INDO¹³ methods are almost identical, that obtained by the CNDO/S-CI is significantly higher (18.66 D).¹⁵

Table 4.4. Experimental and theoretical dipole moments of DMABN in the ground, LE and TICT states.

Dipole moment	expt. ^a	INDO ^b	CNDO/S ^c	ab initio ^d	AMI ^e
$\mu_g(S_0)$	5-7	6.6	≈ 4.00	6.4	5.75
$\mu_e(\text{LE})$	8-11	9.0	5.61	6.33	7.69
$\mu_e(\text{TICT})$	14-23	14.0	18.66	15.5	14.1

^a from ref. 1, 3, 20-24, ^b ref. 13, ^c ref. 15, ^d ref. 8, ^e this study

4.3.2. Excited state energies and barrier to twisting

The variation of the lowest excited singlet state energy as a function of the twist angle is shown in fig. 4.4 for ABN and in fig. 4.5 for DMABN. In the case of ABN, the gas phase excited state energy increases monotonically with the twist angle. In polar solvents, however, the twisted conformer is significantly stabilised. The barrier involved in the twisting process appears too high (0.45 eV) for this molecule to expect any population of the TICT state at room temperature. This possibly accounts for the absence of dual emission in ABN.³⁻⁵ The interesting point about the excited state profile of DMABN is that, contrary to its behaviour in the ground state, the energy passes through a maximum. Secondly, we find that twisting in the excited state is associated with a barrier of 0.1 eV. The barrier height is almost four times the available thermal energy at room temperature explaining why the TICT emission of DMABN is not observed in the gas phase or in highly non-polar solvents.²⁵ As far as the origin of the barrier is concerned, we believe that the barrier is due to the crossing of two zeroeth-order electronic states. This is evident from the variation of the excited state dipole moments of different conformers presented in Table 4.4. The effect of solvation on the excited state energy profiles is also shown in the same figures. The TICT state is further stabilised relative to the LE state in a polar solvent. This behaviour is exactly opposite to what has been observed in the ground state. One important point to note in this context is that according to this calculation although the TICT state is significantly stabilised in polar media, the barrier to the twisting process does not show any noticeable change when the polarity of the medium is changed. This is contrary to experimental observations.²⁶

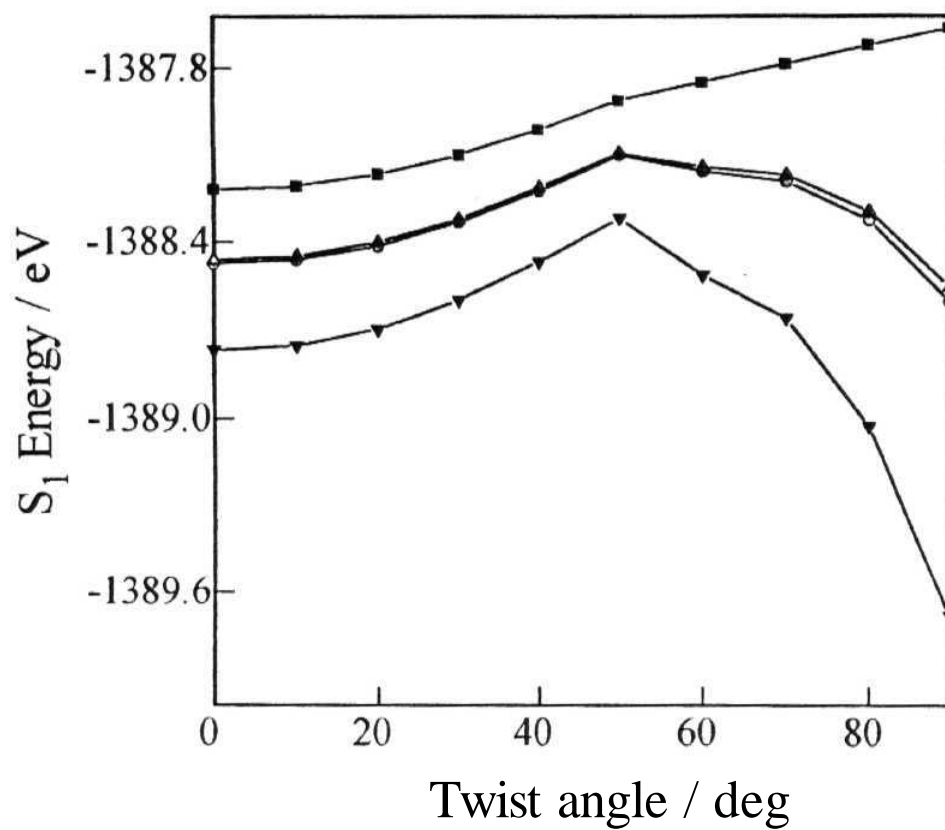


Fig.4.4. Variation of the first excited state energy of ABN as a function of the twist angle in the gas phase (○), dioxane (▲), THF (■) and acetonitrile (▼).

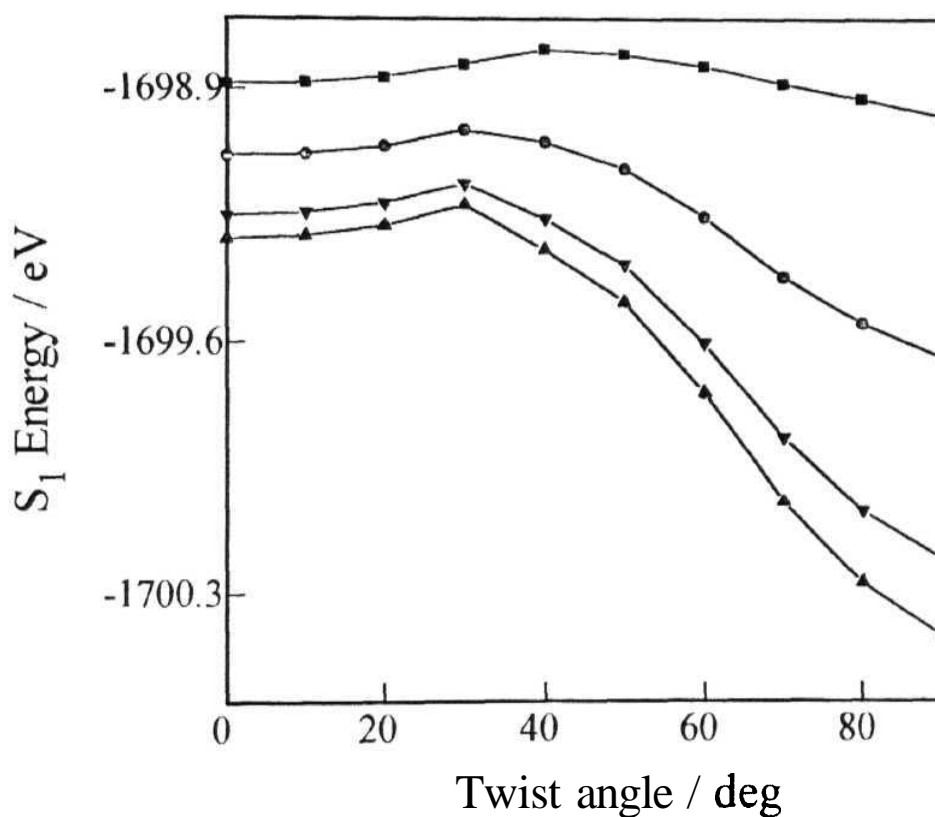


Fig.4.5. Variation of the first excited state energy of DMABN as a function of the twist angle in gas phase (■), dioxane (●), THF (▼) and acetonitrile(▲).

4.3.3. Absorption spectra

During (he time scale of absorption, the solvent molecules surrounding the dipole **can** not reorient. Therefore, the transition energies for absorption are calculated as the difference in energy of the fully solvated ground state and partially solvated excited state in the planar conformation. The gas phase

absorption energy is calculated as 3.66 eV for DMABN and 3.8 eV for ABN. On solvation, the transition energy of DMABN decreases to 3.57 eV, 3.54 eV and 3.53 eV in 1,4-dioxane, tetrahydrofuran and acetonitrile respectively. The calculated gas phase absorption energy of ABN (3.8 eV) agrees reasonably well with the experimental value in heptane (4.0 eV).³ The experimental absorption energies of DMABN as measured by us from the onset of the absorption band, are presented in Table 4.5 along with the theoretically calculated values for comparison. It can be seen that the AM1 calculated absorption energies are in good agreement with the experimental values.

Table 4.5. Theoretical and experimental transition energies of DMABN in the gas phase and in some selected solvents.

Medium	Absorption energy		TICT emission energy	
	theo. (eV)	exp. ^a (eV)	theo. (eV)	exp. ^b (eV)
Gas phase	3.66	-	3.28	-
1,4-dioxane	3.57	3.80	2.66	2.95
THF	3.54	3.80	2.15	2.83
Acetonitrile	3.53	3.72	1.94	2.60

^aMeasured from the onset of the absorption spectra, ^bsee text for measurement details.

4.3.4. Fluorescence spectra

As mentioned earlier, the TICT emission energies of DMABN in various solvents are estimated from the energy difference between the fully solvated excited state (because the lifetime of the TICT state of DMABN (1-3 ns)¹ is much longer than the relaxation time of the solvents), calculated using equn 3.17, and the partially solvated ground state, calculated using equn. 3.18. The gas phase TICT emission energy of DMABN is calculated as 3.28 eV. As can be seen from the Table 4.5, the emission energy is lowered considerably in polar media due to large dipole moment of the TICT state. In order to compare our results with experimental values we have measured the TICT emission energies from the fluorescence maxima. The maxima appear at 2.95 eV, 2.83 eV and 2.60 eV in 1,4-dioxane, tetrahydrofuran and acetonitrile respectively. Although the agreement between the experimental and theoretical numbers is fairly satisfactory in non-polar solvent such as dioxane; in polar media, some variation is noticeable. However, we are not sure whether the onset of the emission band or the emission maxima is to be considered as the transition energy. If the excited state energy is determined from the onset of emission spectra instead of the band maxima then the theoretically predicted numbers will differ significantly from the experimental ones. However, in the absence of precise information on the experimental 0-0 transition energy it is difficult to judge how close the theoretical prediction is. A reasonably good agreement between the theoretical and experimental data in non-polar solvents and increasingly larger deviation in polar media suggests that the solvation energy calculated by us using Onsager continuum model may not provide a true picture of the solvation of a highly dipolar species. We also note that as the solvation energy is critically

dependent on the Onsager cavity radius, the predictions would be quite different if a cavity radius different from ours is chosen.

4.4. The limitations of the method

Even though all the ground state and a number of excited state properties, calculated by the AMI method, are in accordance with the experimental data and the method offers an explanation for the absence of TICT emission in ABN, the method has its drawbacks. The polarity dependence of the barrier height, as proposed by Eisenthal and co-workers,²⁶ cannot be explained satisfactorily. The observed barrier for the ICT \rightarrow TICT process in the gas phase (0.1 eV) for DMABN is found almost constant with increase in solvent polarity. One reason could be that the solvation model used here is not very appropriate for the estimation of barrier height. However, a recent AMI calculations, where a supposedly better 'solvaton model' has been used, could not produce any better result to account for the polarity dependent energy barrier for the ICT \rightarrow TICT process.¹⁶ It is to be noted that the CNDO method also fails in this aspect.¹⁵ This is suggestive of the fact that the barrier height obtained from one-dimensional quantum mechanical calculations may not be the actual transition state. Instead, the transition state may receive considerable stabilisation from solvent shell reorganisation thus making the barrier height dependent on the polarity of the media.

Despite these limitations **we find** that AM I method in combination with the present model of solvation is capable of predicting the excited state properties of DMABN and ABN reasonably well. Therefore, the use this method to examine other systems where the role of the rotary decay mechanism is **unknown**, is justified. However, we feel it necessary to have a model more sophisticated than the present one to account for the solvent dependence of the short-lived excited species.

4.5. References

- 1 K. Rotkiewicz, K.H. Grellmann, Z.R. Grabowski, *Chem. Phys. Lett.*, **19**, 315, **1973**.
- 2 a) Z.R. Grabowski, K. Rotkiewicz, A. Siemiarczuk, D.J. Cowley, W. Baumann, *Nouv. J. Chim.*, **3**, 443, **1979**, b) W. Rettig, *Angew. Chem. Int. Ed. Engl.*, **25**, 971, 1986; c) E. Lippert, W. Rettig, V. Bonacic-Koutecky, F. Heisel, J.A. Mielke, *Adv. Chem. Phys.*, **68**, **1**, **1987**.
- 3 a) U. Leinhos, W. Kuhnle, K.A. Zachariasse, *J. Phys. Chem.*, **95**, 2013, **1991**; b) K.A. Zachariasse, T.V. Haar, A. Hebecker, U. Leinhos, W. Kuhnle, *Pure Appl. Chem.*, **65**, 1745, **1993**.
- 4 W. Schuddeboom, S.A. Jonker, J.M. Warman, U. Leinhos, W. Kuhnle, K.A. Zachariasse, *J. Phys. Chem.*, **96**, 10809, **1992**

- 5 a) EM. Gibson, AC. Jones, AG. Taylor, W.G. Bouwman, D. Phillips, J. Sandell, *J. Phys. Chem.*, 92, 5449, **1988**; b) S. Ram, J.S. Yadav, D.K. Rai, *Indian J. Phys.*, 59b, 19, **1985**.
- 6 OS. Khalil, J.L. Meeks, S.P. McGlynn, *Chem. Phys. Lett.*, 39, 457, **1976**.
- 7 S. Kato, Y. Amatatsu, *J. Phys. Chem.*, 92, 7241, **1990**.
- 8 V. Bonacic-Koutecky, J. Michl, *J. Am. Chem. Soc.*, 93, 507, **1993**.
- 9 L.S. Andres, M. Merchan, B.O. Roos, R. Lindh, *J. Am. Chem. Soc.*, 117, 3189, 1995.
- 10 AL. Sobolewski, W. Domcke, *Chem. Phys. Lett.*, 250, 428, **1996**.
- 11 F.D. Lewis, B. Holman III, *J. Phys. Chem.*, 84, 2326, **1980**.
- 12 W. Rettig, V. Bonacic-Koutecky, *Chem. Phys. Lett.*, 62, 115, **1979**.
- 13 J. Lipinsky, H. Chojnacki, K. Rotkiewicz, Z.R. Grabowski, *Chem. Phys. Lett.*, 70, 449, 1980.
- 14 J.P. Lafemina, C.B. Duke, A. Paton, *J. Chem. Phys.*, 87, 2151, **1987**.
- 15 D. Majumdar, R. Sen, K. Bhattacharyya, S.P. Bhattacharyya, *J. Phys. Chem.*, **95, 4324, 1991**.
- 16 A.D. Gorse, M. Pesquer, *J. Phys. Chem.*, 99, 4039, **1995**.
- 17 W. Rettig, M. Zander, *Ber. Bunsenges. Phys. Chem.*, 87, 1143, **1983**; b) M. Zander, W. Rettig, *Chem. Phys. Lett.*, 110, 602, **1984**.
- 18 a) M.J.S. Dewar, E.G. Zoebisch, E.F. Healy, J.J.P. Stewart, *J. Am. Chem. Soc.*, 107, 3902, **1985**; b) M.J.S. Dewar, K.M. Dieter, *J. Am. Chem. Soc.*, 108, 8075, **1986**, c) D. Chen, R. Sadygov, E.C. Lim, *J. Phys. Chem.*, 98, 2018, **1994**.

- 19 a) P. K. McCarthy, G. J. Blanchard, *J. Phys. Chem.*, **97**, 12205, 1993; b) M. M. Awad, P. K. McCarthy, G. J. Blanchard, *J. Phys. Chem.*, **98**, 1454, 1994.
- 20 P. Suppan, *J. Lumin.*, **33**, 29, **1985**.
- 21 A. Gourdon, J. P. Launay, M B. Doeuff, F. Heisel, J. A. Mieke, E. Amouyal, M. L. Boillot, *Photochem. Photobiol. A: Chem.*, **77**, 13, 1993.
- 22 a) J. Czekalla, W. Liptay and K.O. Meyer, *Her. Bunsenges. Physik Chem.*, **67**, 465, **1963**; b) H. Labhart, *Adv. Chem. Phys.*, **13**, 179, **1967**, c) W. Liptay, *Angew. Chem.*, **81**, 195, **1969**; d) W. Liptay, In *Excited States*, E.C. Lim, ed, Academic Press: New York, Vol. 1, p 129, **1974**; e) H. Labhart, *Adv. Chem. Phys.* **13**, 179, **1990**.
- 23 a) W. Baumann, *Ber. Bunsenges. Phys. Chem.*, **80**, 31, **1976**; b) W. Baumann, H. Dickens, *ibid.* **81**, 786, **1977**; c) W. Baumann, *J. Mol. Struct.*, **47**, 237, **1978**, d) H. Bischof, W. Baumann, N. Detzer, K. Rotkiewicz, *Chem. Phys. Lett.*, **116**, 180, 1985; e) S.A Jonker, J.M. Warmann, *Chem Phys. Lett.*, **185**, 36, **1991**; f) W. Baumann, H. Bischof, J.C. Frohling, C. Brittinger, W. Rettig, K. Rotkiewicz, *J. Photochem. Photobiol., A: Chem.*, **64**, 49, **1992**; g) MP. de Hass, J.M Warmann, *Chem. Phys.*, **73**, 35, **1982**, h) J.M. Warmann, MP. de Hass, In *Pulse radiolysis*, Y. Tabata, ed. CRC Press: Boca Raton, ch. 6, **1991**.
- 24 a) E. Lippert, W. Luder, H. Boos, In *Advances in. Molecular. Spectroscopy.*, A. Mangini ed. Pergamon Press: New York, **1962**; b) B. Koutek, *Collect. Czech. Chem. Commun.*, **43**, 2368, **1978**.
- 25 J. Herbich, P.F. Salgado, R.P.H. Rettschnick, Z.R. Grabowski, H. Wojtowicz, *J. Phys. Chem.*, **95**, 3491, **1991**.

26 a) J.M. Hicks, M.T. Vandersall, Z. Babarogic, K.B. Eisenthal. *Chem. Phys. Lett.*, 116, 18, 1985; b) K.B. Eisenthal *In Ultrashort Light Pulses, Topics in Applied Physics*, W. Kaiser, ed. Springer-Verlag: Vol. 60, New York, 1988; c) J.M. Hicks, M.T. Vadersall, E.V. Sitzmann, K.B. Eisenthal, *Chem. Phys. Lett.*, 135, 413, **1987**.

PHOTOPHYSICAL STUDIES ON AMINOPHTHALIMIDES

A comparative study of the Photophysical characteristics of two aminophthalimide dyes, 4-aminophthalimide (AP) and 4-N,N~dimethylamino phthalimide (DAP) in homogeneous media is described in the first section of this Chapter. The next section deals with an investigation of the behaviour of these systems in microheterogeneous media.

5.1. Photophysical behaviour of AP and DAP in homogeneous media

A large number of dyes which find application as fluorescence probes for the microenvironments in organised media such as cyclodextrins, micelles, membranes, polymers, surfaces, etc. are bichromophoric systems comprising of electron donor and acceptor groups.¹⁻¹³ The sensitivity of the fluorescence band positions and quantum yields on the polarity of the media in these systems results from intramolecular charge transfer character of the emitting state. A greater solvent sensitivity is expected for systems with low-lying TICT states in view of larger dipole moment associated with such states resulting from complete transfer of electron from the donor to the acceptor group.¹⁴ While the TICT state in DMABN is fluorescent,¹⁴ it need not be so in other systems.¹⁵ Since the π -systems of the donor and the acceptor are decoupled from each other in the twisted conformation, the TICT fluorescence is overlap forbidden unless other effects such as vibronic interaction make it allowed. It is important to realise that whether fluorescent or not, a low-lying TICT state is expected to

play a crucial role in dictating the fluorescence efficiency of the flexible dye systems by providing an additional decay **channel**.¹⁵ It is therefore pertinent to **carefully** examine the possibility of the presence of such non-fluorescent TICT state adjacent to the (LE) state. This knowledge will help designing efficient dye systems. With this view we have examined the Photophysical properties of two structurally similar dyes, AP and DAP shown in Chart 5.1. While there is no literature report on **studies** involving DAP, few scattered studies on **aminophthalimides**, however, have been **reported**.¹⁶⁻¹⁸

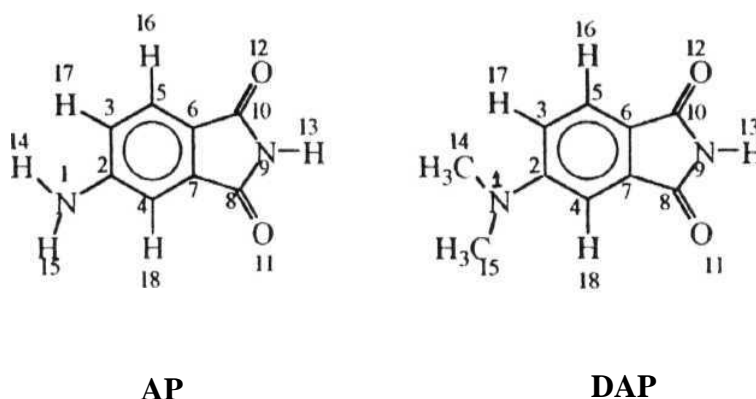


CHART 5.1

5.1.1. Spectral Data

The absorption and fluorescence spectra of AP are characterised by broad structureless bands whose locations are determined predominantly by the polarity of the media. Some representative absorption and fluorescence spectra of AP are shown in figs. 5.1 and 5.2 respectively. With increase in polarity of the medium, both the absorption and fluorescence spectra shift to longer wavelengths. However, the spectral shift is significantly larger for fluorescence than that for absorption. This is consistent with the observations of Barbara and

co-workers that the excited state of AP is more polar than the ground state.¹⁹ The spectral data of AP in various solvents (selected so as to cover a wide range of polarity) are presented in Table 5.1. It can be seen from the Table that the bathochromic shift is more pronounced in protic solvents, and this behaviour can not be correlated solely to the polarity of the media. The fact that acetonitrile is more polar than *t*-butanol (as measured either by the microscopic solvent polarity parameter, $E_T(30)$ or by the dielectric constant),²⁰ and yet the spectra are red-shifted in the latter solvent, points to specific hydrogen bonding interaction of the fluorophore with the protic solvents such as alcohols and water.

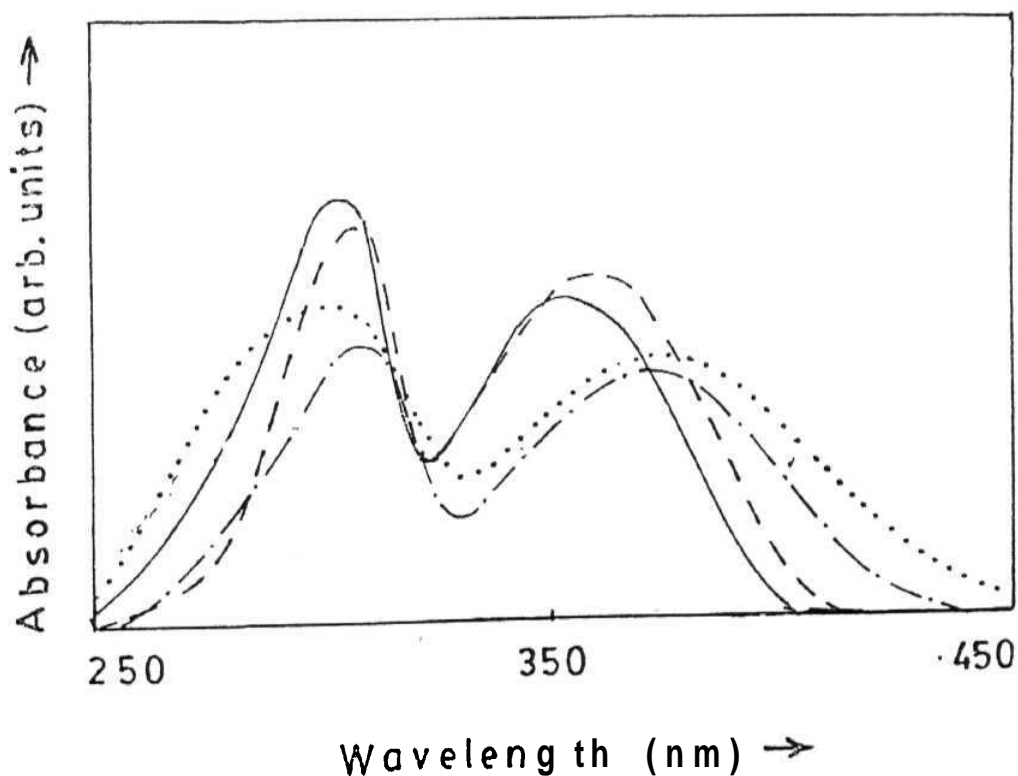


Fig.5.1. Absorption spectra of AP in dioxane (—), acetonitrile (—), methanol (---) and water (···). To avoid overlapping, only few spectra are shown.

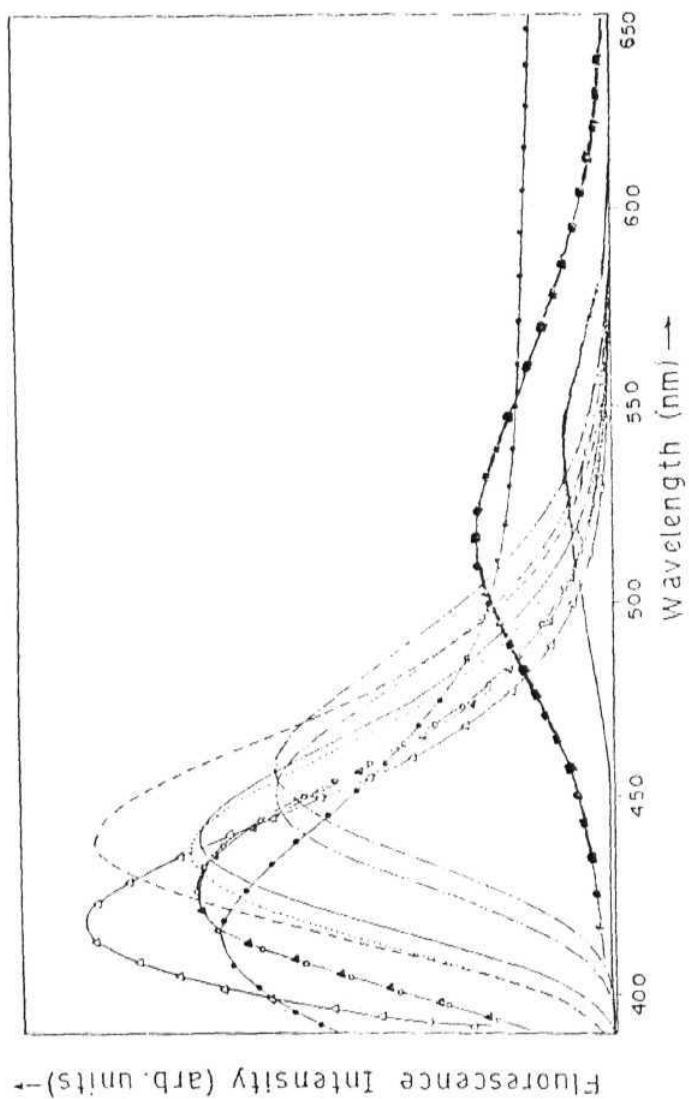


Fig.5.2. Fluorescence spectra of AP in hexane (Δ - Δ), CCl_4 (\circ - \circ), toluene (\square - \square), benzene (\blacktriangle - \blacktriangle), dioxane (\bullet - \bullet), THF (---), DCM (···), acetone (-·-·-), acetonitrile (- - - -), methanol (- - -) and water (—). The excitation wavelength was 360 nm.

Table 5.1. Summary of the spectral properties of AP in different solvents

Solvent	$E_T(30)^a$	Dielectric constant ^b	Refractive Index ^b		ν_{abs} (cm ⁻¹)	$\bar{\nu}_{flu}^{max d}$ (cm ⁻¹)
Hexane	31.0 ^b	1.88	1.3749	-0.0013	28985	24390
CCl ₄	32.4 ^b	2.23	1.4602	0.0102	28777	24213
Benzene	34.6	2.27	1.5011	0.0016	28653	23629
Toluene	34.2	2.38	1.4969	0.0219	28523	23485
1,4-Dioxane	35.9	2.21	1.4224	0.0204	28409	22989
Diethylether	34.2	4.20	1.3524	0.1625	28571	23529
THF	37.5	7.58	1.4072	0.2095	28011	22472
DCM	41.7	8.93	1.4242	0.2171	28169	22346
Acetone	43.1	20.56	1.3587	0.2840	28011	21882
Acetonitrile	45.9	35.94	1.3441	0.3047	28011	21834
<i>t</i> -Butanol	43.5	12.42	1.3877	0.2514	27027	19920
<i>Iso</i> -Propanol	49.0	19.92	1.3772	0.2640	27248	19802
Methanol	55.8	32.66	1.3284	0.3086	27174	19305
Water	63.1 ^b	78.30	1.3330	0.3199	27174	18519

^a measured from the longest wavelength band maximum of the betaine dye dissolved in **respective solvent**.

^b from ref. 20. ^c as defined in equn. 3.3. ^d excited at 360 nm.

The spectral features of DAP are very similar to those of AP, as evident from the representative absorption and fluorescence spectra of DAP shown in figs. 5.3 and 5.4 respectively. The spectral data of DAP are compiled in Table 5.2. A comparison of the spectral data of AP and DAP reveals that in a given solvent the spectral maximum for DAP is red shifted with respect to that for AP. This behaviour is consistent with the inductive effect of the **alkyl** groups.

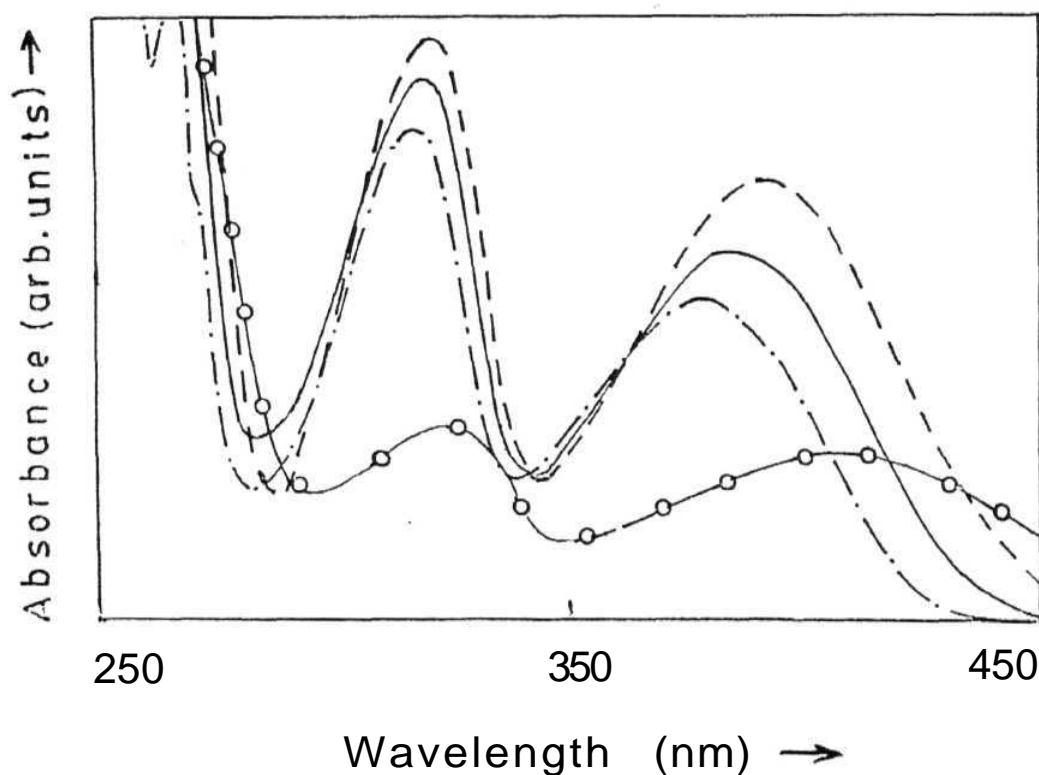


Fig.5.3. Absorption spectra of DAP in dioxane (---), acetonitrile (—), methanol (—) and water (○—). To avoid overlapping, only few spectra are shown.

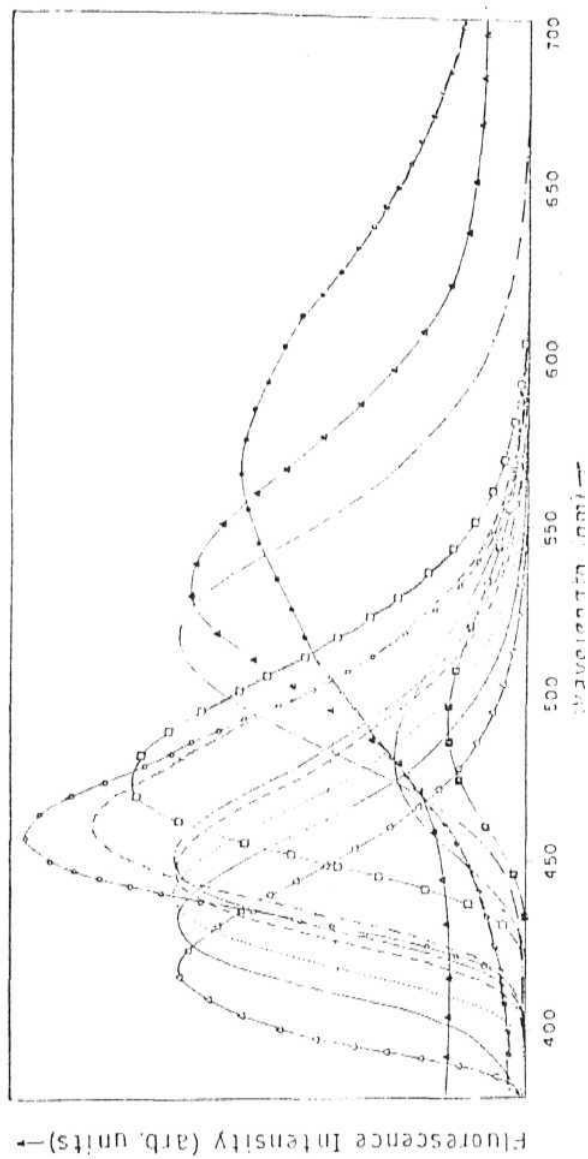


Fig.5.4. Fluorescence spectra of DAP in hexane ($\Delta\Delta\Delta$), CCl_4 (—), diethylether (\cdots), toluene (---), benzene (-.-.), dioxane ($\circ\circ\circ$), THF ($\square\square\square$), DCM ($\diamond\diamond\diamond$), acetone ($\triangle\triangle\triangle$), acetonitrile ($\times\times\times$), methanol ($\circ\circ\circ$), t-butanol ($\square\square\square$) and water ($\diamond\diamond\diamond$). The excitation wavelength was 370 nm.

Table 5.2. Summary of the spectral properties of DAP in different solvents

Solvent	$E_T(30)^a$	Dielectric constant ^b	Refractive Index ^b	Δf^c	$\bar{\nu}_{abs}^{max} d$ (cm ⁻¹)	$\bar{\nu}_{em}^{max}$ (cm ⁻¹)
Hexane	31.0b	1.88	1.3749	-0.0013	27473	23992
CCl ₄	32.4b	2.23	1.4602	0.0102	26455	21882
Benzene	34.3	2.27	1.5011	0.0016	26267	22183
Toluene	33.9	2.38	1.4969	0.0219	26455	22341
1,4-Dioxane	36.0	2.21	1.4224	0.0204	26455	22123
Diethylether	34.5	4.20	1.3524	0.1625	26954	22727
THF	37.4	7.58	1.4072	0.2095	26525	21786
DCM	40.7	8.93	1.4242	0.2171	25641	21231
Acetone	42.2	20.56	1.3587	0.2840	26178	20704
Acetonitrile	45.6	35.94	1.3441	0.3047	25773	20408
<i>t</i> -Butanol	43.3	12.42	1.3877	0.2514	25873	19011
<i>Iso</i> -Propanol	48.5	19.92	1.3772	0.2640	25707	19120
Methanol	55.4	32.66	1.3284	0.3086	25253	18727
Water	63.1b	78.30	1.3330	0.3199	24500	17794

^a measured from the longest wavelength band maximum of the betaine dye dissolved in **respective solvent**

^b from ref. 20. ^c as defined in eqn. 3.3. ^d Excited at 370 nm.

We have examined the correlation of the wavenumbers of the fluorescence maxima (only non-hydrogen bonding solvents were considered for reasons stated above) of the two compounds with both the bulk solvent polarity function, dielectric constant (ϵ), and microscopic solvent polarity function, $E_T(30)$ in an attempt to find out which one better represents the polarity around the fluorophores. The correlations with ϵ are shown in figs. 5.5 for AP and in fig. 5.6 for DAP and those with $E_T(30)$ are illustrated in figs. 5.7 and 5.8 for AP and DAP respectively. A superior correlation of the emission maxima with the microscopic solvent polarity function, $E_T(30)$ compared to the bulk polarity function (ϵ) is clearly evident from these plots. This points to the efficacy of $E_T(30)$ to describe the microscopic environment of molecular dipoles in solution.^{19,21}

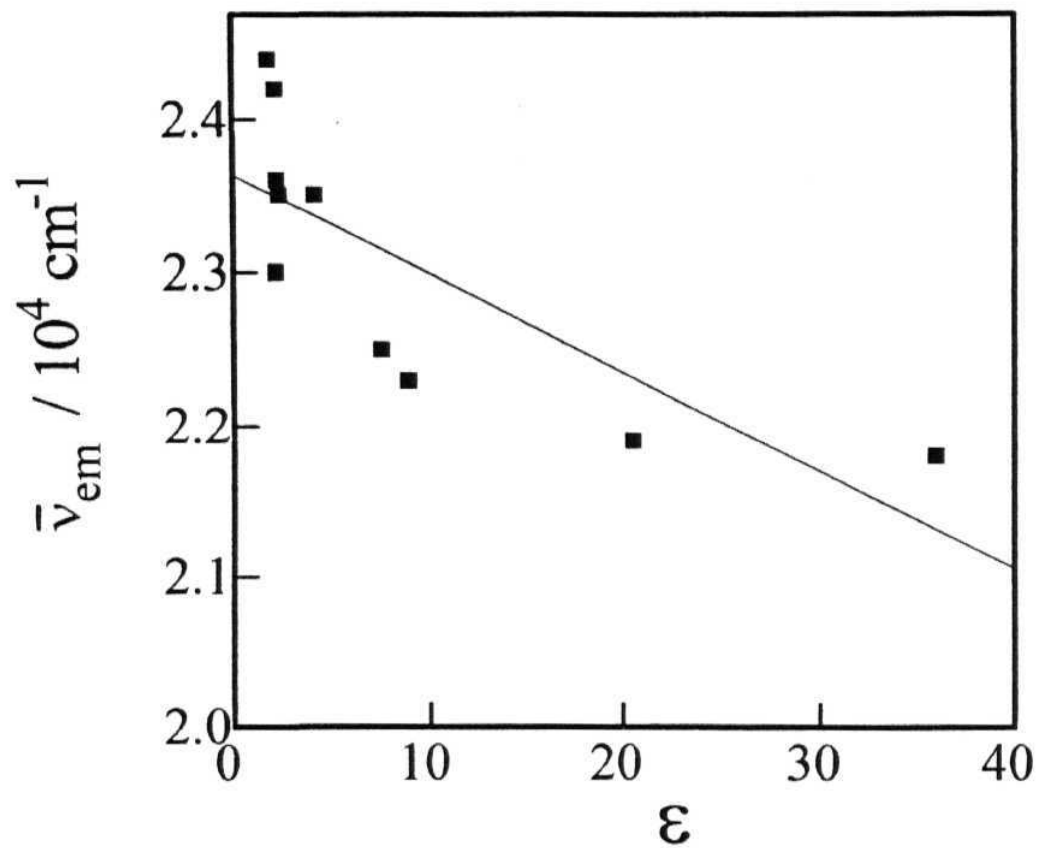


Fig.5.5.Plot of the wavenumbers of the fluorescence maxima of AP with solvent dielectric constant ($r=0.7818$).

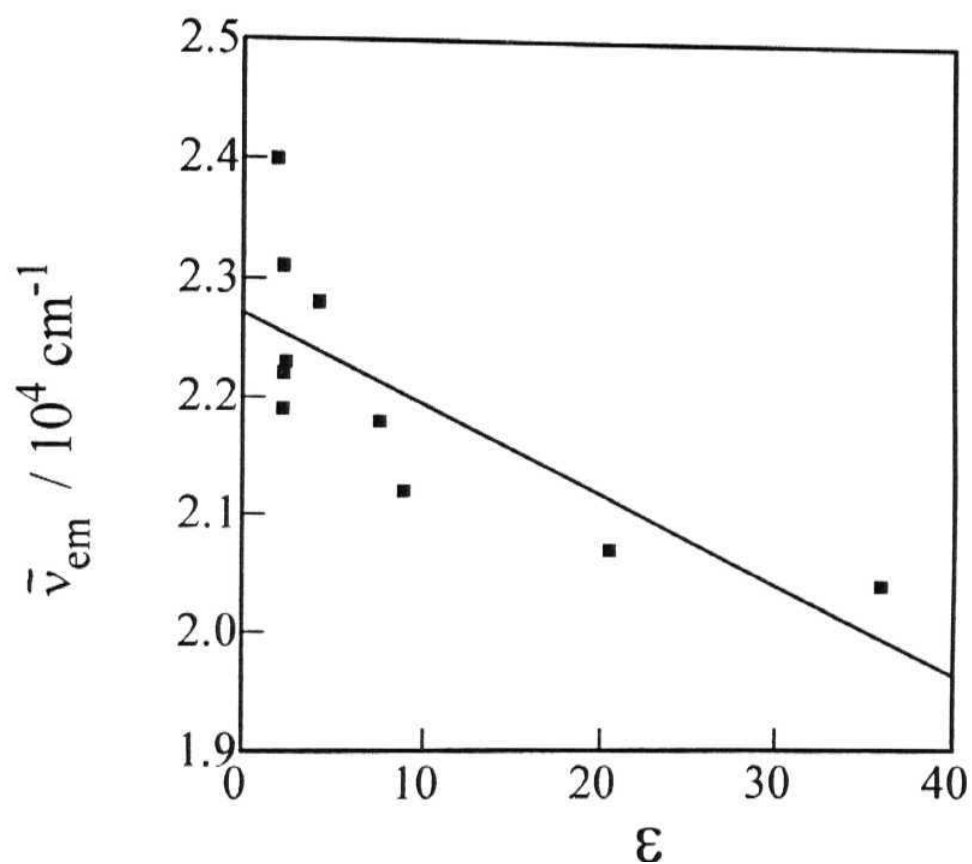


Fig.5.6. Plot of the wavenumbers of the fluorescence maxima of DAP with solvent dielectric constant ($r=0.7818$).

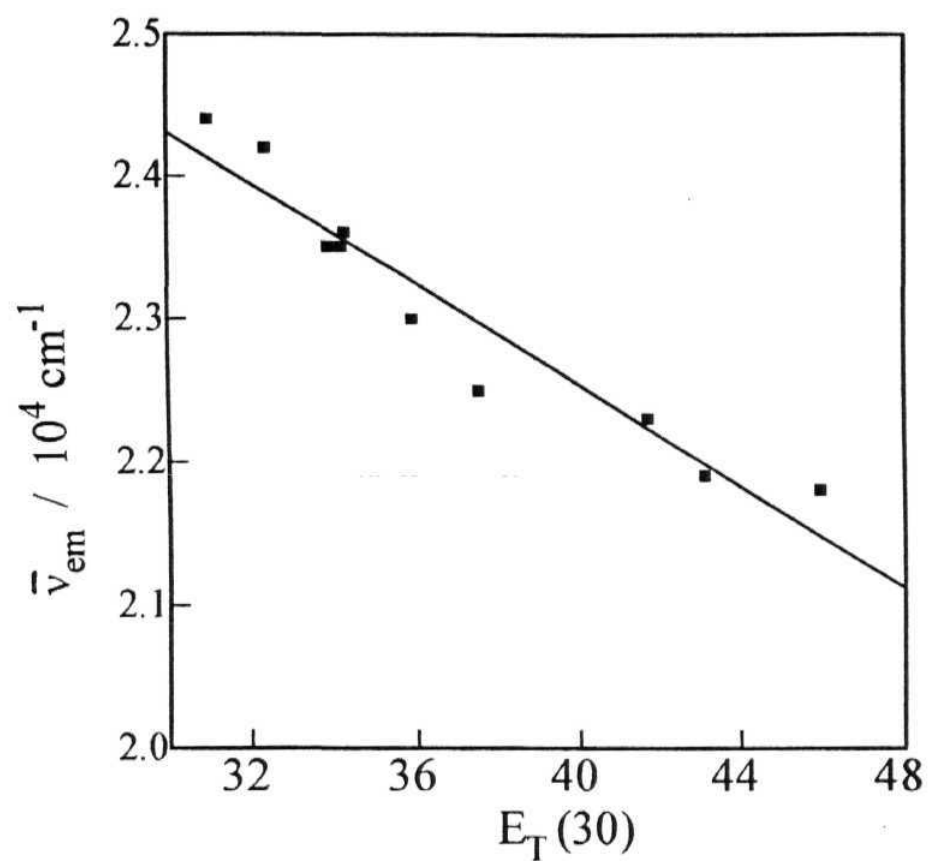


Fig.5.7. Plot of the wavenumbers of the fluorescence maxima of AP with the $E_T(30)$ values of the solvent ($r=0.9593$).

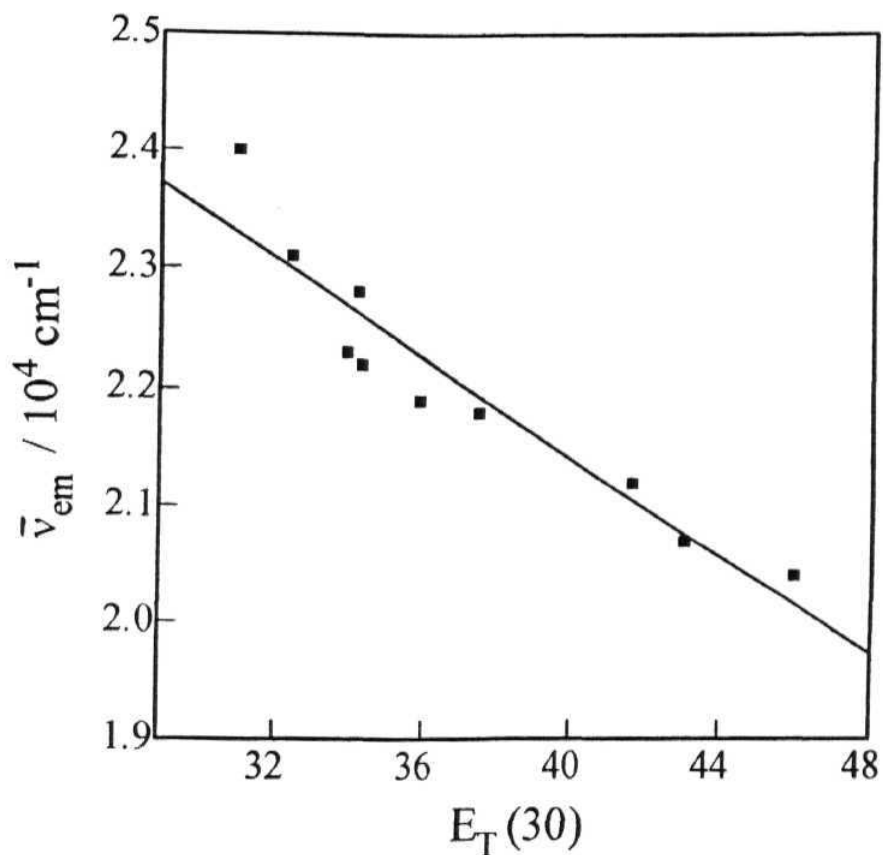


Fig.5.8. **Plot** of the wavenumbers of the fluorescence maxima of DAP with the $E_T(30)$ value of the solvents ($r=0.9488$)

*S. I. 2. Dipole moment **change** on excitation ($\Delta\mu$)*

In order to quantify the extent of charge transfer on electronic excitation and to determine the nature of the emitting state (whether LE state with charge transfer character or a fully charge separated TICT state) we have calculated the dipole moment changes on excitation using Lippert-Mataga equation.²² One

needs to have a knowledge of the Onsager cavity radius in order to calculate $\Delta\mu$. It can be seen that for many systems, 40% of the long axis is used for this purpose²³, in some cases, effective radii based on density is used²⁴ and in some other cases the choice is rather **arbitrary**.²⁵ We have used half of the distance between the amino nitrogen (**N-1**) and the carbonyl oxygen (O-12), across which the charge separation occurs, as the cavity radius. The basis of this choice of the cavity radius is discussed briefly in Chapter I and more elaborately in Chapter VI. This distance, estimated from the **AM1** optimised structures of the molecules, is 6.70 Å for AP and 6.74 Å for DAP. Therefore, the Onsager cavity radii used for $\Delta\mu$ estimation were 3.35 Å and 3.37 Å for AP and DAP respectively. The plots based on Lippert-Mataga equation are shown in figs. 5.9 and 5.10 respectively for AP **and** DAP. A linear regression analysis of the plots shown in figs. 5.9 and 5.10 ($r = 0.91$ and 0.92 for AP and DAP respectively) yielded $\Delta\mu$ of 3.8 D and 4.1 D for AP and DAP respectively. Since the change of dipole moment on excitation is small in both cases it is quite likely that the emission originates from LE state. **It** may be noted that while the measured $\Delta\mu$ value of AP is in excellent agreement with that obtained (3.2 D) by Suppan;¹⁷ a widely different $\Delta\mu$ value (6.3 D) is also reported by **them**.¹⁸ However, the latter value, measured from **thermochromic** shift of the fluorescence spectra, may not be reliable since the method is **applicable** only for molecules with μ_e of 10 D^{17,18}

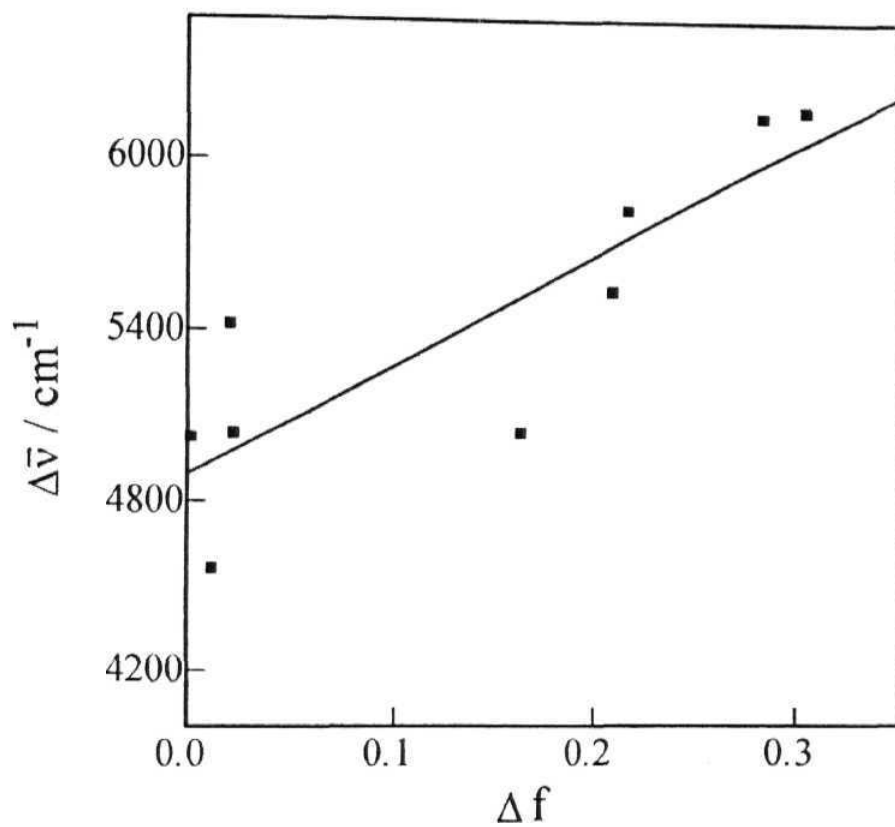


Fig.5.9. Plot of Stokes shift ($\Delta\bar{\nu}$) versus Δf for AP (**$r=0.9073$**) based on Lippert Mataga equation.

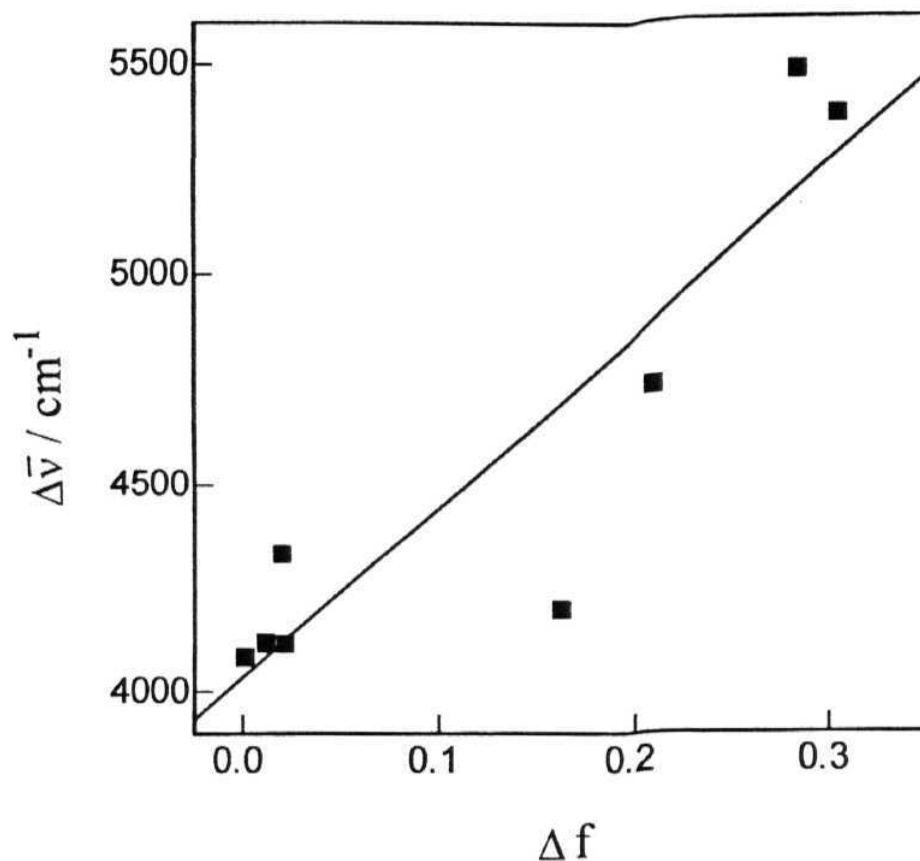


Fig.5.10. Plot of Stokes shift ($\Delta\bar{\nu}$) versus Δf for DAP ($r=0.9196$) based on Lippert Mataga equation.

5.7.3. Fluorescence quantum yields, lifetimes, radiative and nonradiative rate constants

The fluorescence quantum yield of AP remains more or less constant in the range 0.6 to 0.7 with increase of solvent polarity in aprotic solvents. However as seen from the Table 5.3, in protic solvents significant decrease of

quantum yield (0.63 in **acetonitrile** to 0.01 in water) resulting from hydrogen bonding interaction between the probe and solvents is **observed**. This is presumably due to reduction of S_1-S_0 and/or S_1-T_1 energy gaps as a result of stabilisation of the emitting state on hydrogen bonding interaction, which according to the energy gap law, favours the nonradiative **processes**.²⁶ Similar reduction in quantum yield is observed for DAP in protic solvents.

It is interesting to note that although the fluorescence quantum yield of AP remains almost constant in aprotic solvents, the structurally similar compound, DAP shows considerable different behaviour for which a reduction of the fluorescence yield with increase in the polarity of medium is observed even in aprotic media. It can be seen from the fluorescence quantum yield data presented in Table 5.3 that the fluorescence quantum yield of DAP in acetonitrile is nearly **one-fifth of** that in 1,4-dioxane.

The fluorescence lifetimes (T) of the two compounds have been determined from the measured fluorescence decay curves. The fluorescence decays were found to be single exponential in all the solvents. Biexponential fitting of the decay curves did not result in improvement of χ values. The measured T values are collected in Table 5.3 and two representative decay curves of AP and DAP in dioxane along with the fitted curves and standard deviations are shown in figs. 5.11 and 5.12 respectively. It can be seen from Table 5.3 that the variation of lifetimes with the polarity of the medium parallels the variation of quantum yields.

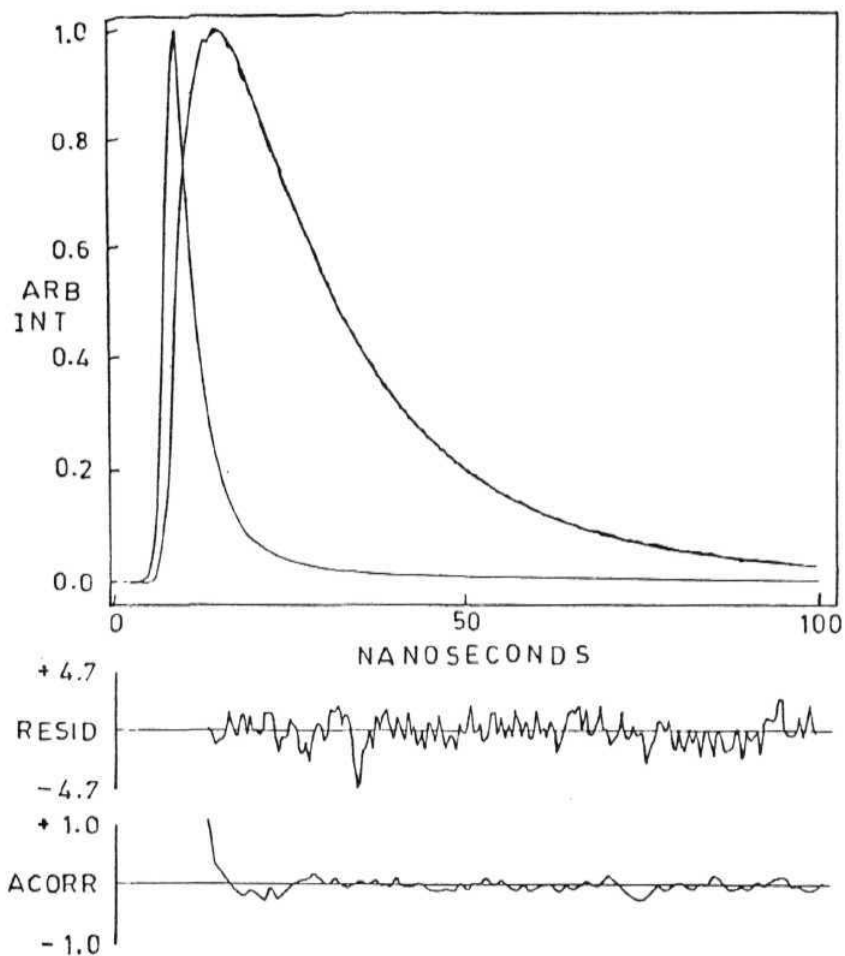


Fig.5.11. The exciting lamp profile, fluorescence decay curve **and** the fitted curve of AP in **dioxane**, $\lambda_{\text{exc}} = 360$ nm.

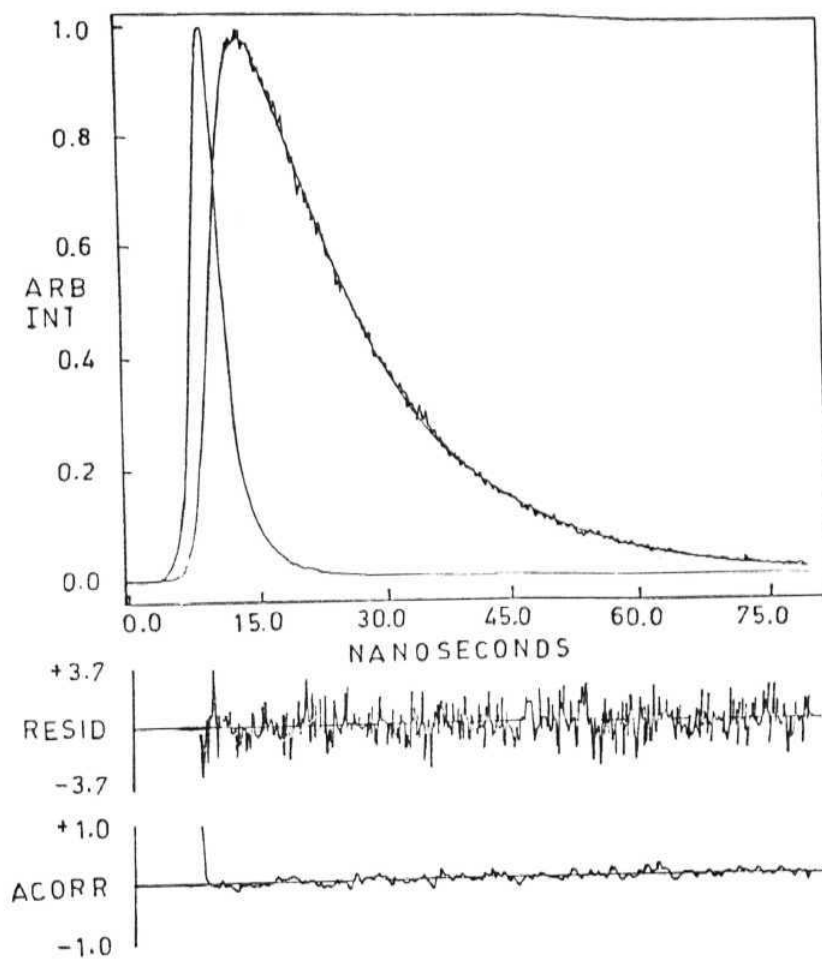


Fig.5.12. The exciting lamp profile, fluorescence decay curve and the fitted curve of DAP in dioxane, λ_{exc} = 370 nm.

Table 5.3. The fluorescence quantum yields and lifetimes of AP and DAP in selected solvents.

Compound	Solvent	ϕ_f	$\tau_f^{\text{exp}} \text{ (ns)}$
AP	1,4-Dioxane	0.73	15.6
	THF	0.70	14.0
	Acetonitrile	0.63	12.4
	Methanol	0.10	8.0
	Water	0.01	≈ 1.0
DAP	1,4-Dioxane	0.62	15.0
	THF	0.52	13.8
	Acetonitrile	0.12	3.4
	Methanol	0.005	≈ 0.4
	Water	0.001	≈ 0.5

In order to find out the influence of solvent polarity on the radiative and nonradiative rates, we have calculated the radiative rate constants (k_R^{calc}) from Strickler-Berg formula.²⁷ The calculated k_R^{calc} values of the two compounds are presented in Table 5.4. The radiative rate constants (k_R), independently estimated from the ratio (ϕ_f / τ), are also shown in the same Table. It can be seen that although there is minor variation in the radiative rate constants calculated by the two methods, the rate constants remain more or less similar for both the compounds in media of different polarities. The nonradiative rate constants (k_{nr}), estimated from $(1 - \phi_f) / T$, are also presented in the same Table. As seen from the Table, although the k_{nr} values for AP remain constant in various solvents (in the range $1.8 - 2.6 \times 10^7 \text{ s}^{-1}$), they increase by an order of

magnitude in the case of DAP on changing the solvent from dioxane to acetonitrile.

Table 5.4. The radiative (k_R^{SB} or k_R) and nonradiative rate constants (k_{nr}) of AP and DAP in selected solvents.

Compound	Solvent	k_R^{SB} / 10^7 s^{-1}	k_R / 10^7 s^{-1}	k_{nr} / 10^7 s^{-1}
AP	1,4-Dioxane	3.9	4.9	1.8
	THF	4.8	5.6	2.4
	Acetone	4.6	4.4	2.1
	Acetonitrile	2.7	4.5	2.6
DAP	1,4-Dioxane	6.4	4.2	2.5
	THF	7.3	3.8	3.5
	Acetone	4.6	3.1	6.0
	Acetonitrile	2.7	4.5	22.6

5.1.4. Theoretical calculations

In order to rationalise the difference in the Photophysical behaviour of two structurally similar systems, AP and DAP, we have carried out theoretical calculations based on AM1 method, the predictive ability of which is demonstrated in Chapter I and elsewhere.²⁸ Although it is possible to obtain a reasonably good estimate of a number of ground and excited state properties of the molecules such as geometries, dipole moments, transition energies, etc. from the calculation, one should take note of some of the limitations of the method. It may not be possible to obtain a precise estimate of the barrier height of the

intramolecular relaxation process from this calculation in which only the lowest excited state is considered. Thus, the calculated barrier heights may not represent the actual barriers involved in the process, but only indicate the trend. The second limitation of the method is associated with the validity of the solvation model in which the solvent is taken as a continuous dielectric. Further, an incorrect choice of the Onsager radius could lead to **overestimation** or underestimation of solvation energies. We had the following objectives while carrying out the calculations: 1) optimised geometries of the ground and excited states, 2) electronic effect of the substitution of the amino hydrogens by methyl groups, 3) the effect of twisting of the amino or dimethylamino group on the energetics of ground and excited states, 4) charge distribution in the ground and excited states (to obtain theoretical estimates of μ_g and μ_e), 5) solvent effect on the state ordering and the barrier height.

5. / 4.1. *Ground state properties*

A summary of the geometrical parameters such as bond angles (θ) and bond lengths (r) obtained from complete optimisation of the ground state of the two molecules at twist angle of zero, and ninety degrees are collected in Table 5.5. The ground state properties namely, heats of formation (ΔH_f) and dipole moment (D) values obtained from complete optimisation of each molecule at various twist angles are summarised in Table 5.6 and the charge densities are shown in fig. 5.13.

Table 5.5. AM1 calculated geometrical parameters for the planar (0°) and perpendicular (90°) conformers of AP and DAP in the ground state.^a

AP			DAP		
Geometrical parameters	0°	90°	Geometrical parameters	0°	90°
r (1-2)	1.3727	1.3967	r(1-2)	1.3872	1.4108
r(2-3)	1.4160	1.4068	r (2-3)	1.4169	1.4054
r(3-5)	1.4368	1.4273	r (2-4)	1.4358	1.4277
r(4-7)	1.3763	1.3732	r(3-5)	1.3991	1.4058
r(5-6)	1.3942	1.3755	r (4-7)	1.3700	1.3738
r(6-10)	1.4929	1.4977	r(5-6)	1.3782	1.3760
r(7-8)	1.5027	1.4999	r (6-10)	1.4900	1.4977
r(8-9)	1.4202	1.4171	r(7-8)	1.5025	1.5000
r(9-10)	1.4266	1.4170	r(8-9)	1.4139	1.4167
r (10-12)	1.2303	1.2328	r (9-10)	1.4213	1.4173
r (8-11)	1.2306	1.2327	r (10-12)	1.2333	1.2328
r(9-13)	0.9978	0.9877	r (8-11)	1.2340	1.2327
θ (1-2-3)	120.86	120.85	r(9-13)	0.9873	0.9877
θ (2-3-5)	121.50	121.54	r (1-14)	1.4335	1.4254
θ (2-4-7)	117.93	118.34	r(1-15)	1.4331	1.4254
θ (3-5-6)	118.68	118.63	θ (1-2-3)	121.15	120.77
θ (5-6-7)	120.35	120.41	θ (2-3-5)	121.85	121.71
θ(6-10-9)	106.50	106.43	θ (2-4-7)	118.30	118.14
θ (7-8-9)	106.47	106.51	θ (3-5-6)	118.83	118.22
θ(9-10-12)	123.89	124.45	θ (5-6-7)	120.05	120.73
θ (9-8-11)	124.68	124.36	θ (6-10-9)	106.46	106.48
			θ (7-8-9)	106.48	106.49
			θ (9-10-12)	123.89	124.37
			θ (9-8-11)	124.64	124.42

^a atom numbering as per Chart 5.1. Bond lengths (r) and bond angles (θ) are expressed in Å and degrees respectively.

Table 5.6. The ground state properties of AP and DAP as a function of twist angle.

TWIST ANGLE (Deg)	AP		DAP	
	AHf (kcal mol ⁻¹)	(Debye)	AHf (kcal mol ⁻¹)	(Debye)
0	-28.43	5.29	-18.26	5.65
10	-28.16	5.25	-17.94	5.62
20	-27.39	5.14	-17.89	5.42
30	-26.19	4.96	-17.21	5.15
40	-24.76	4.75	-16.15	4.81
50	-23.22	4.50	-14.93	4.45
60	-21.78	4.27	-13.69	4.16
70	-20.59	4.08	-12.59	3.91
80	19.83	3.94	-11.85	3.74
90	-19.56	3.89	-11.36	3.99

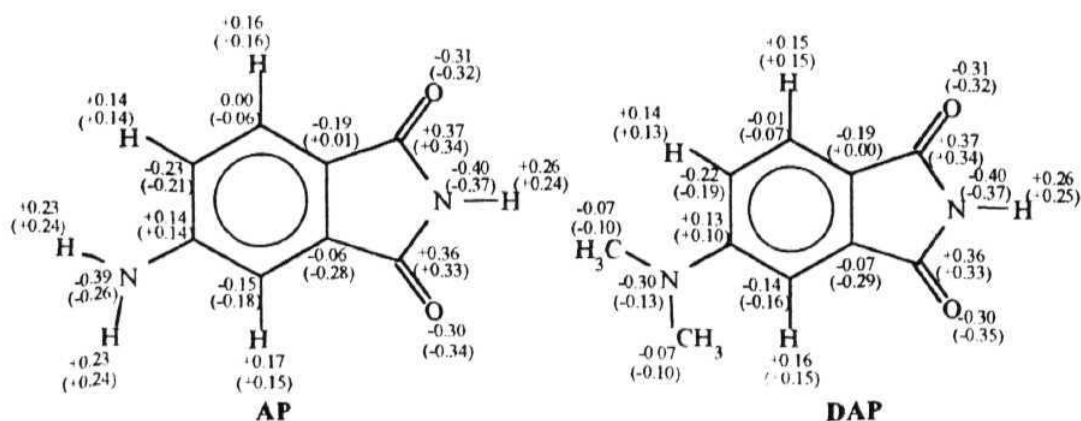


Fig 5.13. AM1 calculated electronic charge densities at ground and excited states for AP and DAP. The charge densities for the excited state are given within parentheses.

The variation of the ground state energy as a function of the twist angle of the amino or dimethylamino group is depicted in figs. 5.14 and 5.15 respectively. The calculations suggest planar conformation of both the molecules in the ground state. With increase in twist angle, the total energy of the system is increased. The energy difference between the twisted form (90 deg) and the planar form (0 deg) is found to be 0.38 eV for AP and 0.30 eV for DAP in the gas phase. The calculated energy profiles in dioxane, tetrahydrofuran and acetonitrile are also shown in the above figures. Since the dipole moments decrease with increase in twist angle (fig. 5.16), the solvent stabilisation of the planar form is more than that of the twisted form. Consequently, for both compounds the energy difference between the twisted and planar form is further increased on solvation. The calculated barrier to twisting is too large both in the gas phase and in solution (0.57 eV and 0.56 eV for AP and DAP respectively, in acetonitrile) to expect the twisted form to be present in the ground state in any significant amount.

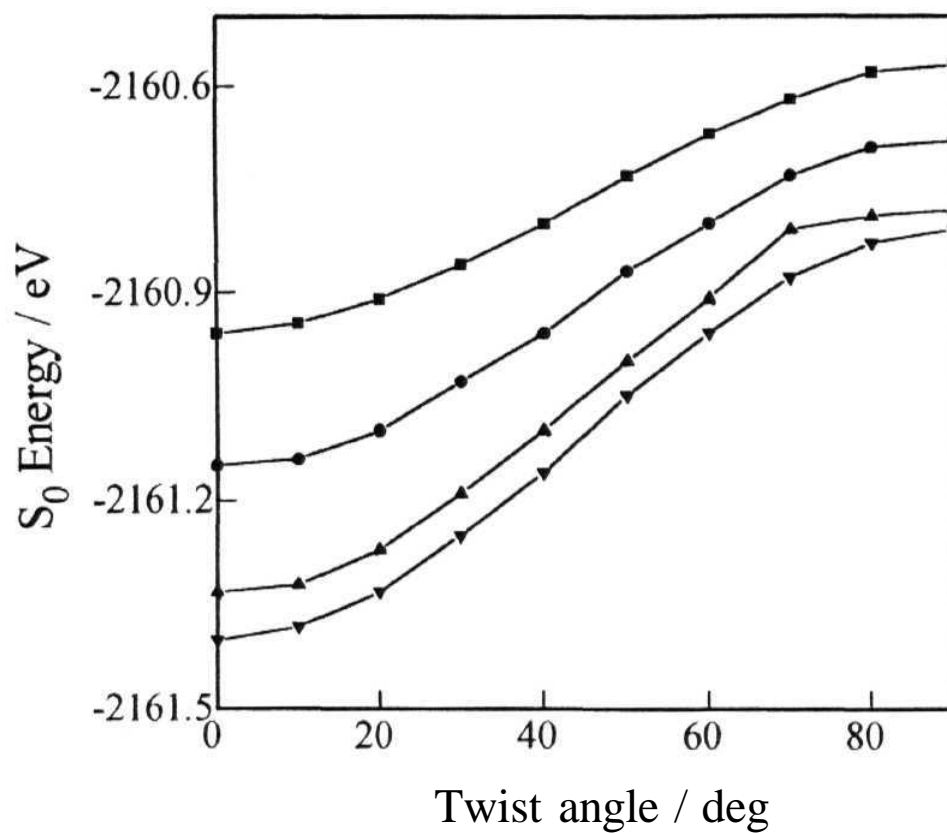


Fig.5.14. Variation of the ground state energy of AP as a function of the twist angle in the gas phase (•), dioxane (◊), THF (▲), and acetonitrile (▼).

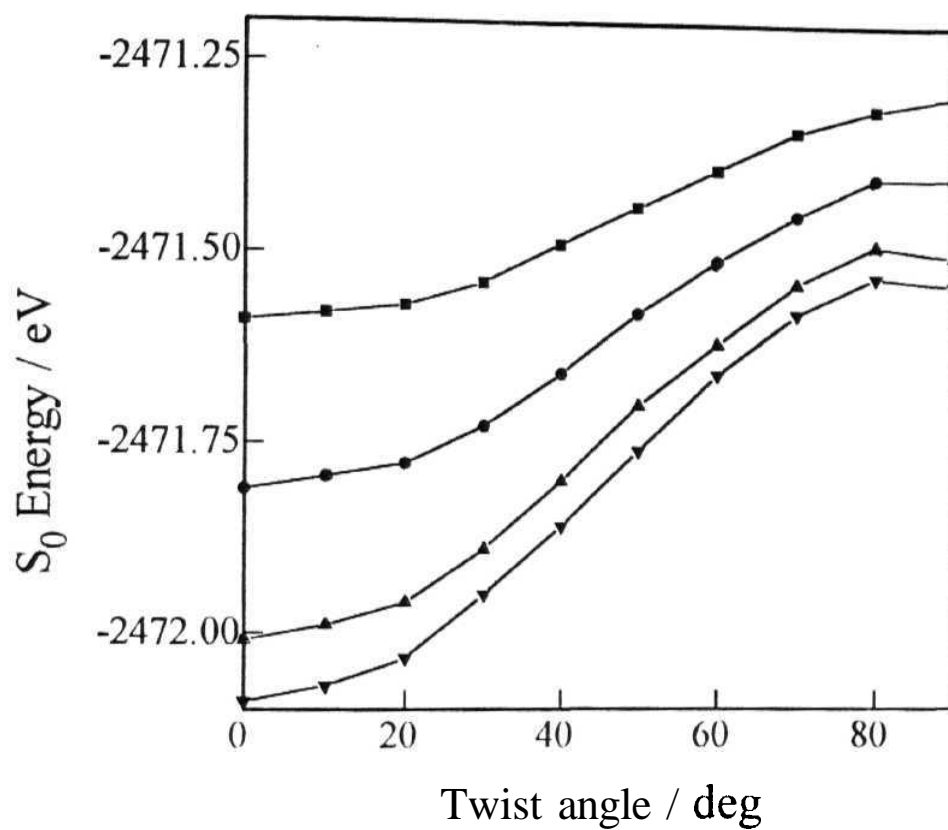


Fig.5.15. Variation of the ground state energy of DAP as a function of the twist angle in gas phase (○), dioxane (◻), THF (▲), and acetonitrile (▼).

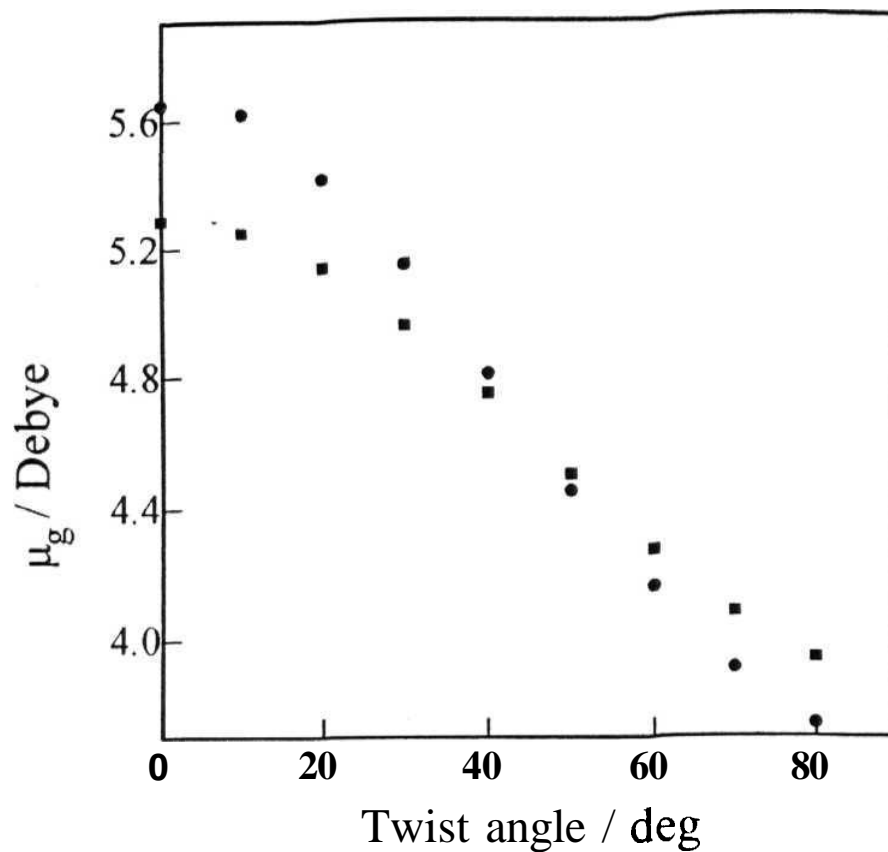


Fig.5.16. Variation of the ground state dipole moment as a function of the twist angle for AP (●) and DAP (◻)

5./4.2. Excited state properties

The excited state heats of formation and dipole moments of the lowest excited singlet state of AP and DAP for various twist angles are presented in Table 5.7. While the ground state dipole moments steadily decrease with

increase in the twist angle, the variation of the dipole moments in the excited state is quite different. The observed trend of the variation of the excited state dipole moment, shown in fig. 5.17, can be explained in terms of a **change** in the nature of the electronic state at around 40-50 degs. Similar changes have also been observed for DMABN (Chapter IV). The variation of the lowest excited state energy of AP and DAP as a function of the twist angle is depicted in figs. 5.18 and 5.19 respectively. It can be seen that the gas phase energy of AP increases continuously with increase in the torsion angle. For DAP, the trend is slightly different and the energy maximum is observed for an intermediate angle. However, on solvation the energy passes through a maximum for both the systems which is a consequence of the observed variation of the dipole moments of the systems. In acetonitrile, the TICT states of AP and DAP are found stable than the respective locally excited state by 0.27 eV and 1.59 eV respectively. The calculated barriers to twisting in the excited state are estimated as 0.55 eV and 0.06 eV for AP and DAP respectively, in acetonitrile.

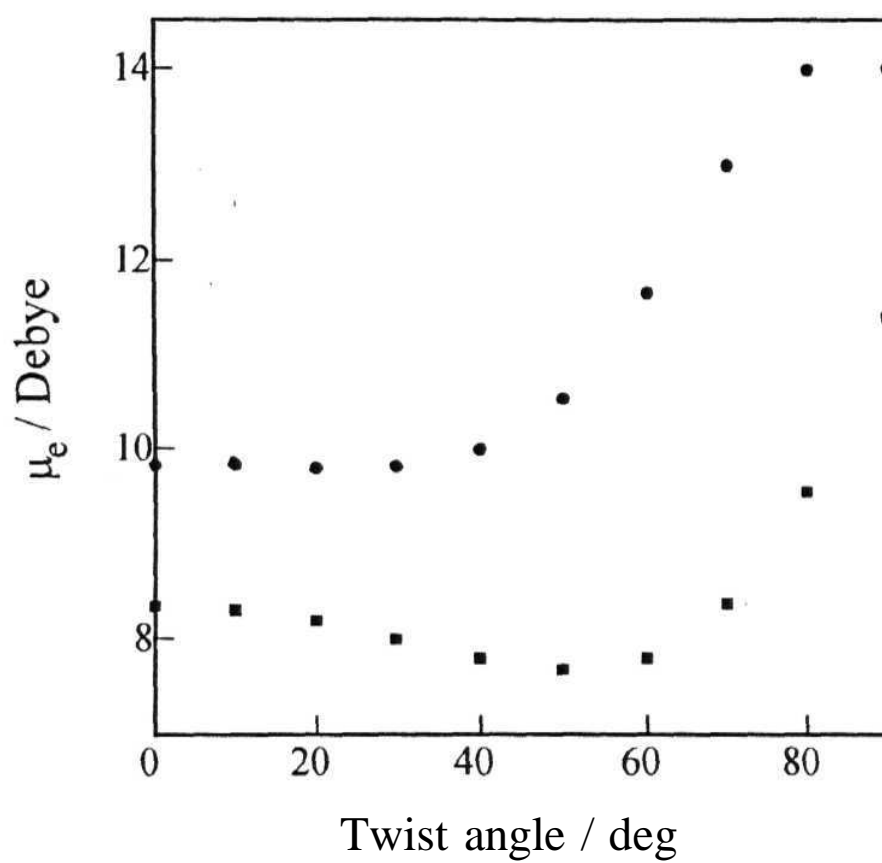


Fig.5.17. Variation of the excited state dipole moments of AP (●) and DAP (○) as a function of twist angle

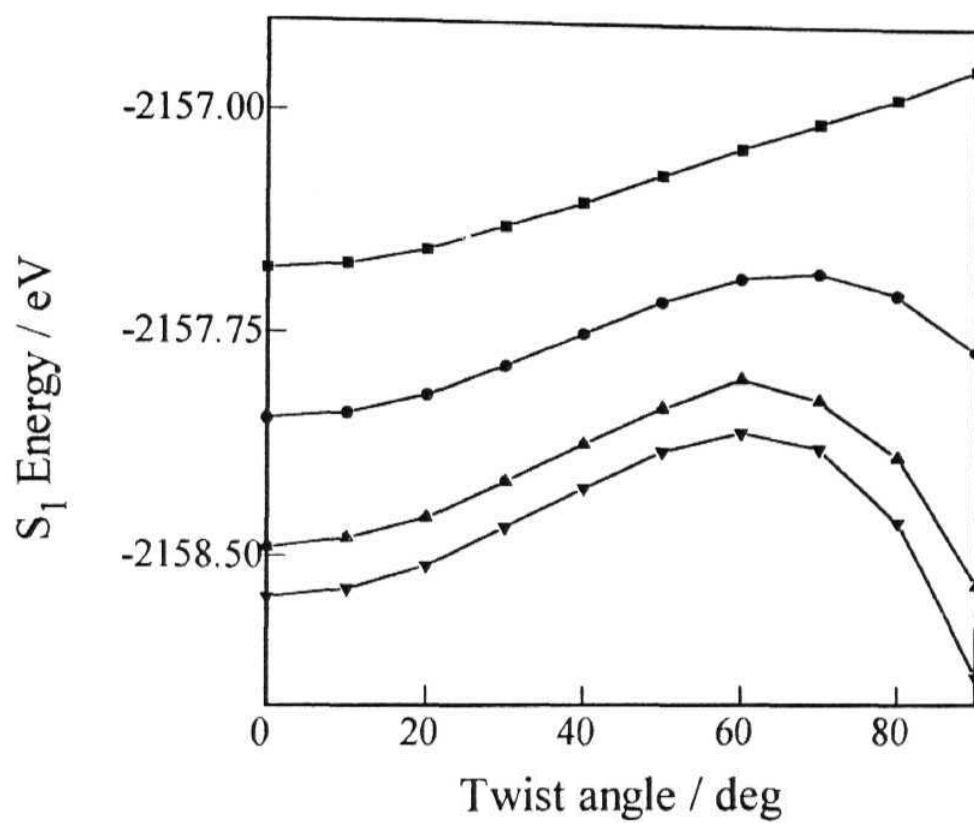


Fig.5.18. Variation of the first excited state energy of AP as a function of the twist angle in the gas phase (•), dioxane (◻), THF (▲) and acetonitrile (▼).

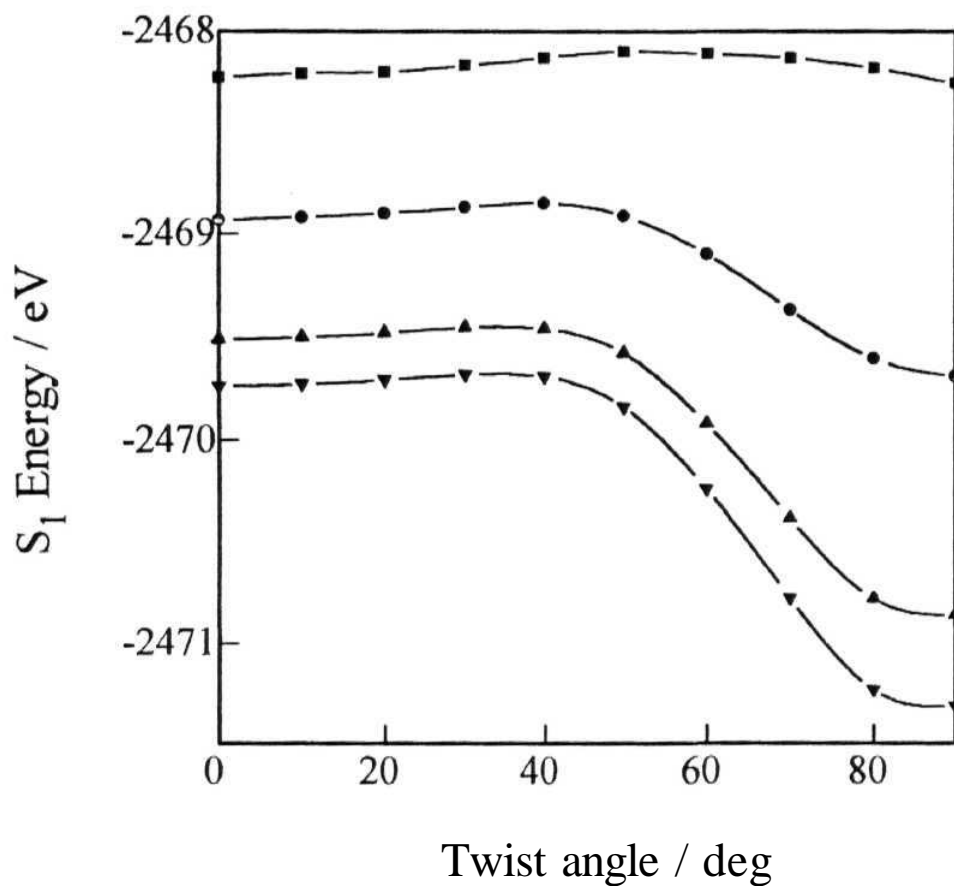


Fig.5.19. Variation of the first excited state energy of DAP as a function of the twist angle in the gas phase (■), dioxane (●), THF (▲) and acetonitrile (▼).

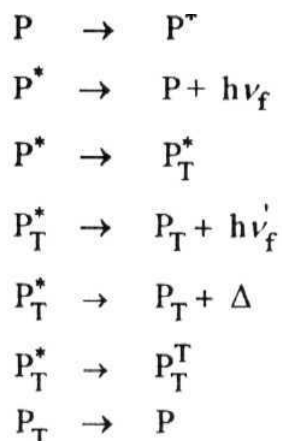
Table 5.7. Theoretically calculated excited state properties of AP and DAP as a function of the twist angle.

TWIST ANGLE (Deg)	AP		DAP	
	AHf kcal mol ⁻¹	μ _e (Debye)	AHf kcal mol ⁻¹	M _e (Debye)
0	50.46	8.33	59.18	9.82
10	50.85	8.29	59.15	9.83
20	51.96	8.18	59.72	9.79
30	53.86	7.99	60.45	9.81
40	55.77	7.79	61.45	9.99
50	57.97	7.67	62.12	10.53
60	60.16	7.79	61.96	11.66
70	62.16	8.36	61.34	12.99
80	64.18	9.54	60.38	13.99
90	66.47	11.40	58.60	14.00

5.1.5. An interpretation of the Photophysical properties in terms of TICT mechanism

The most interesting observation that has been made here is that the variation of the nonradiative decay rates with polarity is quite different for **the** two compounds in spite of their structural similarity. The enhanced nonradiative rate constant of DAP in polar media can not be explained simply in terms of a more polar excited state of the molecule as the difference in the excited state dipole moment values of the two compounds in the planar conformation is too small (shown in Table 5.7). Obviously, some other polarity dependent nonradiative decay mechanism is operational in the case of DAP.

We attempt to explain the difference in Photophysical properties of the two compounds in terms of the TICT mechanism¹⁴ for which we propose the following scheme



involving one species in the ground state (P) and two species (P^{\star} and P_T^{\star}) in the excited singlet state. The single light absorbing species (P) corresponds to the planar form of the compounds and this assumption is supported by theoretical results. P^{\star} , P_T and P_T^{T} represent the molecule in the locally excited state, perpendicular twisted state and triplet state of the twisted form respectively. One of the two singlet species proposed in the scheme must be nonfluorescent as dual emission required by the scheme is not observed experimentally. We analyse the dipole moments of the fluorescent state of the two molecules to determine whether the emission originates from P^{\star} , representing the molecule in the LE state or from P_T^{\star} , the twisted conformation. The dipole moments of AP and DAP calculated by AM1 and solvatochromic method are summarised in Table 5.8.

Table 5.8. Ground and excited state dipole moments of AP and DAP as calculated by **AM1** and solvatochromic methods.

Compound	μ_g			μ_e	
	AM1	AM1	Lippert	AM1 ^a	Lippert ^b
AP	5.29	3.04	3.6	8.33	8.89
DAP	5.65	4.17	4.10	9.82	9.75

^a assuming that emission occurs from the **planar conformation**. ^b Calculated on the basis of experimentally determined $\Delta\mu$ and theoretically estimated μ_g values.

As seen from the Table, the changes in the dipole moment ($|\Delta\mu|$), calculated by the Lippert Mataga equation (3.8 D for AP and 4.1 D for DAP) agree very well with the same obtained by AM1 calculations for the planar conformers. This indicates that the emission in both the compounds originates from the LE state and not from the TICT state. Since the theoretically calculated dipole moments for the twisted states of AP and DAP are respectively 11.4 and 14.0 D, the dipole moment changes of 6.1 and 8.4 D would have been observed if the emission originated from the TICT state.

The nature of the emitting state can also be ascertained from a comparison of the experimental and theoretical transition energies. The emission maxima of AP and DAP are observed at 2.70 eV and 2.52 eV with the onset of spectra at 3.10 eV and 2.91 eV respectively in acetonitrile. Thus the 0-0 transition is expected to lie between 2.70 eV and 3.10 eV for AP and 2.52 eV and 2.91 eV for DAP. Theoretically calculated emission energies for the locally

excited states of AP and DAP, 2.79 eV and 2.76 eV respectively in acetonitrile, correspond very well with the experimentally observed transition energies. Based on this supporting data we conclude that the fluorescence in both dyes result from the LE state.

We now attempt to rationalise the observed variation of fluorescence quantum yields, lifetimes and nonradiative constants of the two compounds with the solvent polarity. It is evident from the excited state energy profiles of AP shown in fig. 5.18 that the TICT state is higher in energy than the ICT state by 0.7 eV in the gas phase. In polar solvents such in acetonitrile the situation is reversed where the TICT state is stable by 0.27 eV in acetonitrile. However, the twisting process still involves a barrier of 0.56 eV. Since the available thermal energy at room temperature is much lower than the barrier associated with the twisting process, one does not expect the TICT state to play any role in the Photophysical properties of AP. Mere, we would like to emphasise that the consideration of state energies of ICT and TICT states alone does not preclude $P^* \rightarrow P_T^*$ transformation, it is the barrier height that should be considered before any conclusion regarding the feasibility of a process can be drawn. It is interesting to observe that despite the semiempirical nature, the calculation provides a realistic picture of the twisting process. A similar analysis of the excited state energy profiles of DAP shows that 1) in the gas phase, the TICT state is stable than the ICT state by 0.02 eV and the barrier associated with twisting is 0.13 eV, 2) in acetonitrile, the TICT state is stable by as large as 1.58 eV and barrier involved in twisting is only 0.06 eV. Thus in acetonitrile, both these conditions are highly favourable for twisting. Therefore, eventhough the TICT state in AP can not have any influence on the LE fluorescence, the same

in DAP is expected to act as a nonradiative decay route. This accounts for the contrasting behaviour of two structurally similar compounds.

The polarity dependent decrease of fluorescence lifetime and quantum yield or increase in the nonradiative rate constant of DAP actually results from the polarity dependence of $P^* \rightarrow P_T^*$ process. It has been shown by Eisenthal and co-workers²⁹ that the barrier height of the ICT \rightarrow TICT process is polarity dependent due to the polar nature of the activated complex. With increase in the polarity of the medium, the barrier height is reduced which enhances the rate of the above process and consequently the radiative efficiency and lifetime of the LE state is decreased.

One question which deserves attention is why the TICT state is nonfluorescent. One possible explanation could be that the energy gap between the TICT state and the corresponding ground state is very low. The calculated solvated energy profiles suggests that this gap is as low as 0.22 eV in acetonitrile. Although the actual energy gap, determined by the extent of solvation of the initial and the final states based on the actual lifetime of the TICT state, could be different from the one predicted above assuming complete solvation, it is apparent, however that the internal conversion to the ground state will be a major nonradiative decay channel that possibly would account for the nonfluorescent nature of the TICT state.

Secondly, we find that in polar solvents, where the TICT state of DAP will be sufficiently populated, a triplet state is almost isoenergetic (gap of 0.05

eV) with the TICT state (Table 5.9). This may favour intersystem crossing to the triplet in polar media. The nonfluorescent nature of the TICT state of DAP could also be due to the overlap forbidden character of the transition.

Table 5.9. Singlet and triplet state energies of DAP in twisted conformation in acetonitrile.

Nature of the state	Acetonitrile (eV)
(TICT)	-2471.3220
T ₁	-2471.2720
T ₂	-2469.0787
T ₃	-2468.5072

5.1.6. Effect of viscosity

In order to corroborate our conclusion on the nature of the emitting state of the systems and the involvement of a nonfluorescent TICT state in the case of DAP, we have carried out one final experiment in which the fluorescence yields of the two compounds in glycerol have been measured relative to their respective yields in methanol. The fluorescence spectra of the optically matched solutions of AP and DAP in two solvents are shown in fig. 5.20. In case of AP, slight decrease in quantum yield is observed on change of solvent from methanol to glycerol. On the other hand, an enhancement by a factor (of ≈ 2.0) is observed for the same change of solvent in the case of DAP. This contrasting behaviour again can be rationalised in terms of a nonfluorescent TICT state of DAP. Since the microscopic polarities of the two solvents, as measured by their

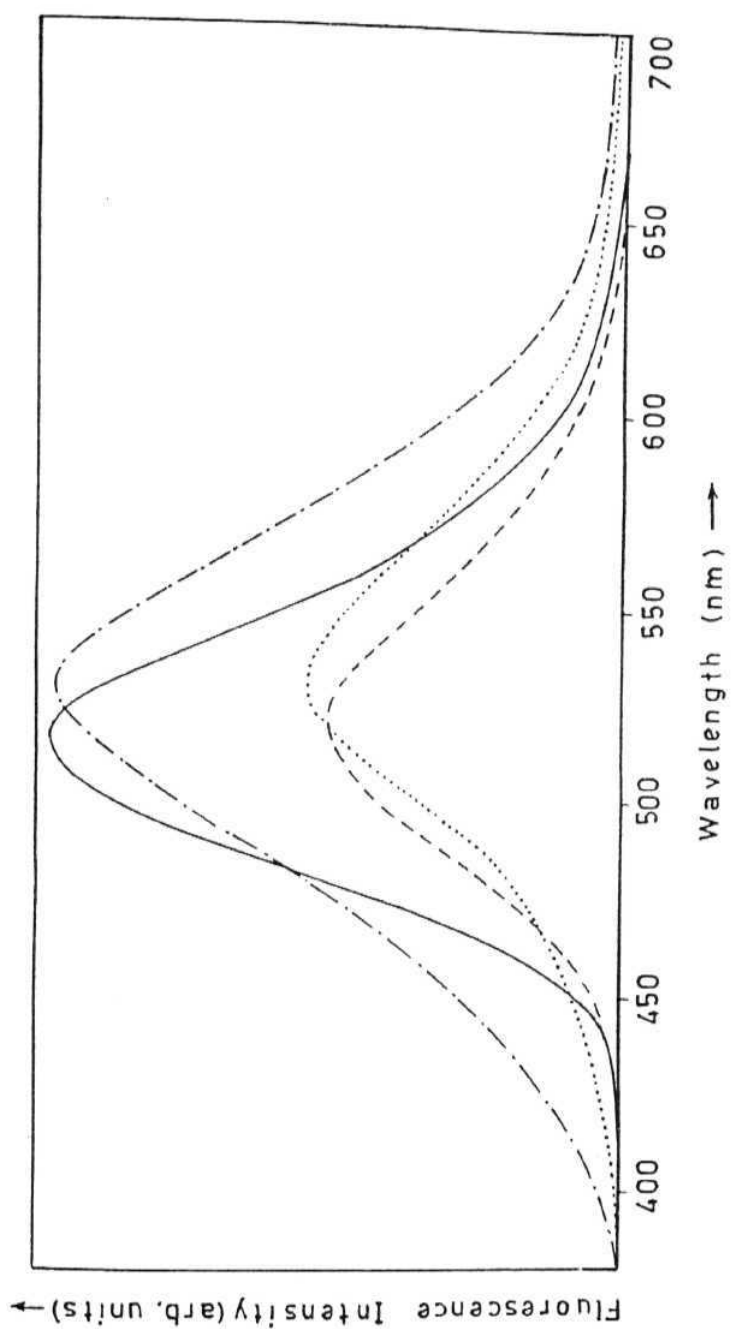


Fig.5.20. Fluorescence spectra of AP in methanol (—), glycerol (.....), and of DAP in methanol (---) and glycerol (-.-.-). For each compound, the solutions are optically matched at the exciting wavelength.

$E_T(30)$ values (55.9 and 57.2 respectively for methanol and glycerol respectively), are fairly close and the viscosities of the two media are widely different (0.544 cP for methanol and 934 cP for glycerol),³⁰ the difference in fluorescence quantum yield of any compound in these media reflects predominantly the influence of viscosity. A drastic reduction of the TICT formation yield and consequent enhancement of the fluorescence yield of the LE state in highly viscous media such as glycerol is expected when TICT state is coupled to the emitting LE state. This accounts for the fluorescence enhancement of DAP in glycerol. In case of AP, since the TICT state is much higher in energy, hindrance of the twisting motion is not expected to affect in any way the fluorescence from the LE state. However, since glycerol is marginally higher in polarity in compared to methanol, a small decrease in fluorescence yield is observed. We have examined a large number of systems that exhibit single emission so as to test whether a simple experiment like this can be used to find out the nature of the emitting state and to make prediction on the involvement of nonfluorescent TICT state. We have found that the above guideline generally holds for a number of coumarin derivatives C1, **C120**, **C152**, **C153** and the changes observed here are not due to the difference of the rotating volume of the amino and dimethylamino groups.

5.2. Photophysical studies in microheterogeneous environments

It is shown in the previous section that the fluorescence properties of AP and DAP are remarkably sensitive to the environments. A shift of the fluorescence maximum by 130-145 nm and 80-100 fold decrease of the fluorescence yield on changing the solvent from hexane to water clearly point to the application of these systems as reporter molecules for the microenvironments in organised media. Therefore, the following work, in which the fluorescence properties of the two compounds are studied to follow the guest-host interaction in cyclodextrins is undertaken.

The realisation of the overall importance of the cyclodextrin-guest interaction as a model for enzyme active sites has resulted in a large number of studies in recent years with cyclodextrins (CD) as hosts for a wide variety of guest molecules.¹⁻¹³ CDs are cyclic oligosaccharides containing six, seven and eight glucose units called α -CD, β -CD and γ -CD respectively. The most remarkable property of CDs is their ability to form inclusion complexes. The complexation process, driven mainly through hydrophobic interaction, requires a good match of size of the host and the guest molecules. Thus for benzene derivatives the ideal host is α -CD, for naphthalene derivatives β -CD is preferred and γ -CD usually accommodates larger molecules or more than one smaller molecules. The reduced polarity and restricted space inside the CD cavity often modify the Photophysical and photochemical processes of the encapsulated molecules.^{21,31-36} The emission properties of the electron donor-acceptor molecules have been used to estimate the polarity of the interior and rims of the CD cavities.¹

Eventhough a large number of systems form inclusion complexes with CD, the changes in the Photophysical properties on encapsulation in many cases, are too small to provide any meaningful and reliable information on the microheterogeneity of the CD structure or on the location of the probe. This necessitates further studies of the complexation processes involving probes whose Photophysical properties are sensitive to even a small change in environment. Having observed that the spectral properties of AP and DAP are extremely sensitive to the environment, we got interested to examine the potentials of these two systems as probes for microheterogeneous media. Secondly, we wanted to find out whether the reduced polarity and space restrictions of CD cavity can inhibit the twisting motion of the dimethylamino group in DAP.

5.2. / Absorption spectra

The changes in the absorption spectra on addition of various amounts of α -, β -, and γ -cyclodextrins to an aqueous solution of AP are shown in figs 5.21-5.23. Since the change in the absorption spectrum of AP is very small in all three cases, only the spectra at few concentrations of CDs are displayed in the figures for the sake of clarity. No shift of the spectral maximum is observed.

The existence of isosbestic point in figs. 5.21 and 5.22 at around 270 nm and 275 nm respectively is indicative of formation of 1:1 complex of AP with α - and β -CD. However, with γ -CD no such isosbestic point could be seen and this is presumably due to the formation of complexes with more than one stoichiometry which is frequently observed in γ -CD owing to its large cavity

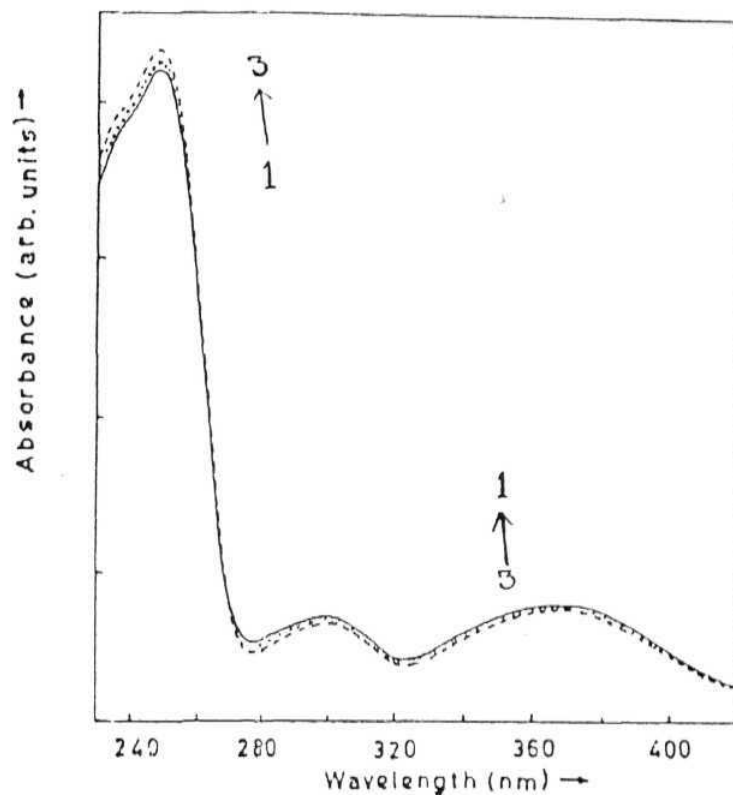


Fig.5.21. Absorption spectra of AP in aqueous solution with various amounts of α - CD. The CD concentrations are (1) 0 mM (solid line), (2) 5 mM (dotted line) and (3) 10 mM (dashed line). The spectra recorded at intermediate concentrations of CD are not displayed for the sake of clarity.

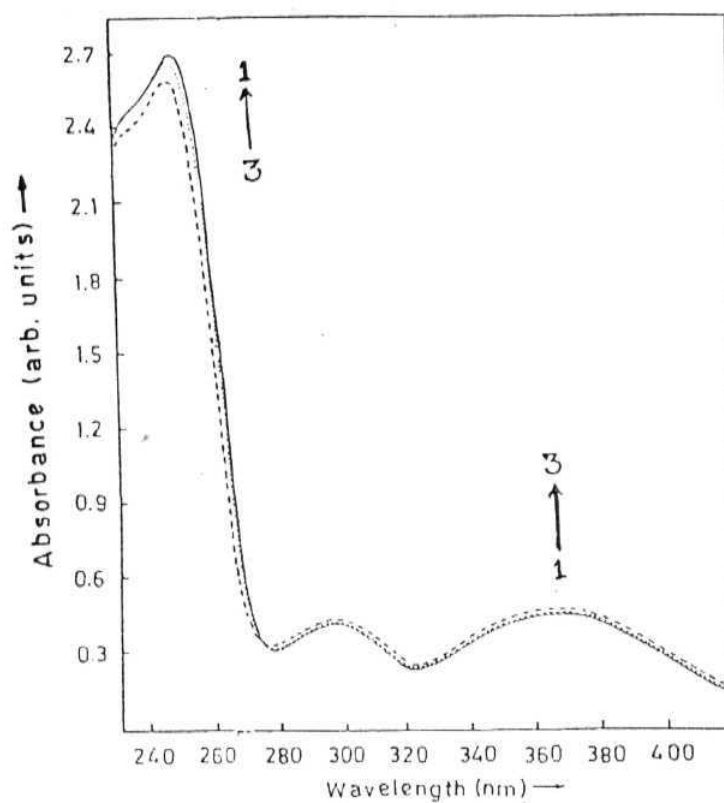


Fig.5.22. Absorption spectra of AP in aqueous solution with different amounts of P- CD. The CD concentrations are (1) 0 mM, (solid line) (2) 0.2 mM (dotted line) and (3) 1 mM (dashed line). The spectra of intermediate concentrations are not displayed for the sake of clarity.

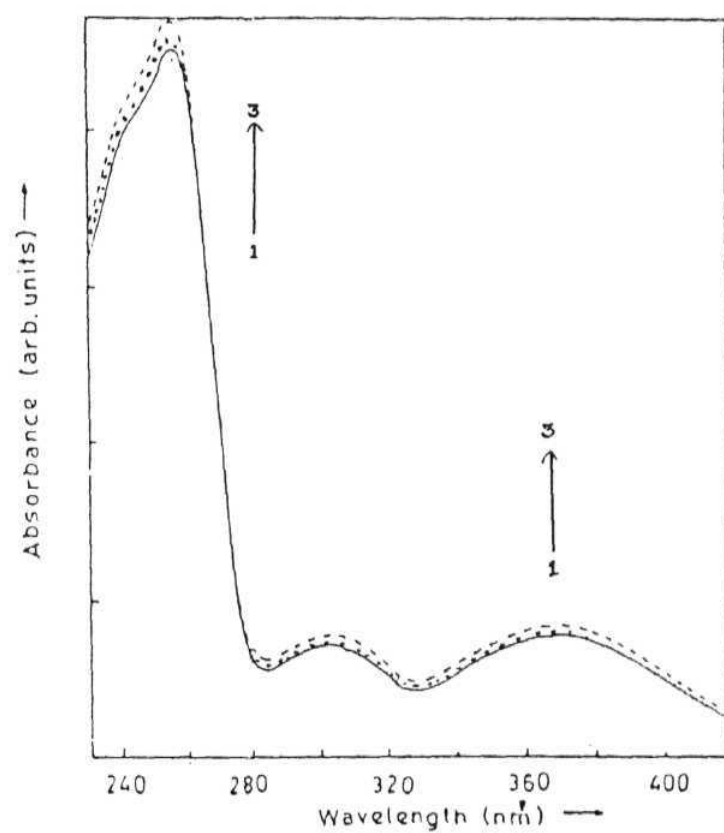


Fig 5 23. Absorption spectra of AP in aqueous solution with different amounts of T- CD The CD concentrations are (1) 0 mM, (2) 5 mM and (3) 10 mM. The spectra recorded at intermediate concentrations of CD are not shown for the sake of clarity.

size.³⁶ Interestingly, for DAP, no isosbestic point is observed in any cyclodextrin. This indicates that the binding of the two **fluorophores** with **cyclodextrins** is quite different. The absence of isosbestic point in the spectra of CD added solutions of DAP suggest the formation of complexes such as 1:2 complex (DAP:CD) in addition to 1:1 complexes in α - and β -CDs. In γ -CD, formation of 2:1 complex is also possible.

5.2.2. *Fluorescence spectra and enhancement*

Even though the change in the absorption spectrum is on addition of CDs, the fluorescence spectra of AP and DAP changes considerably on addition of small quantity of CDs. The fluorescence spectra of AP at various concentrations of α -, β -, and γ -CD are shown in **figs.** 5.24-5.26 and those of DAP are shown in **figs.** 5.27-5.29. Also shown, as insert in the **figs.** 5.24 and 5.25 is the variation of the relative fluorescence yield as a function of the concentration of CD. It is seen from these figures, that addition of CDs is associated with blue shift of the spectra and enhancement of the fluorescence intensity. Both are clear indication of the passage of the probe molecules from aqueous solution to the nonpolar cavity of CD. As seen from **fig.** 5.26, neither the shift nor the enhancement is significant for AP in presence of γ -CD. Since the absorption data point to formation of complexes of more than one **stoichiometry** and fluorescence spectral changes are also small, no further quantitative analysis could be carried out with the data obtained in γ -CD added solution. The absence of a plateau region in the inserts of the figures suggests that even at the highest concentration of CDs, a majority of the molecules are in the free form.

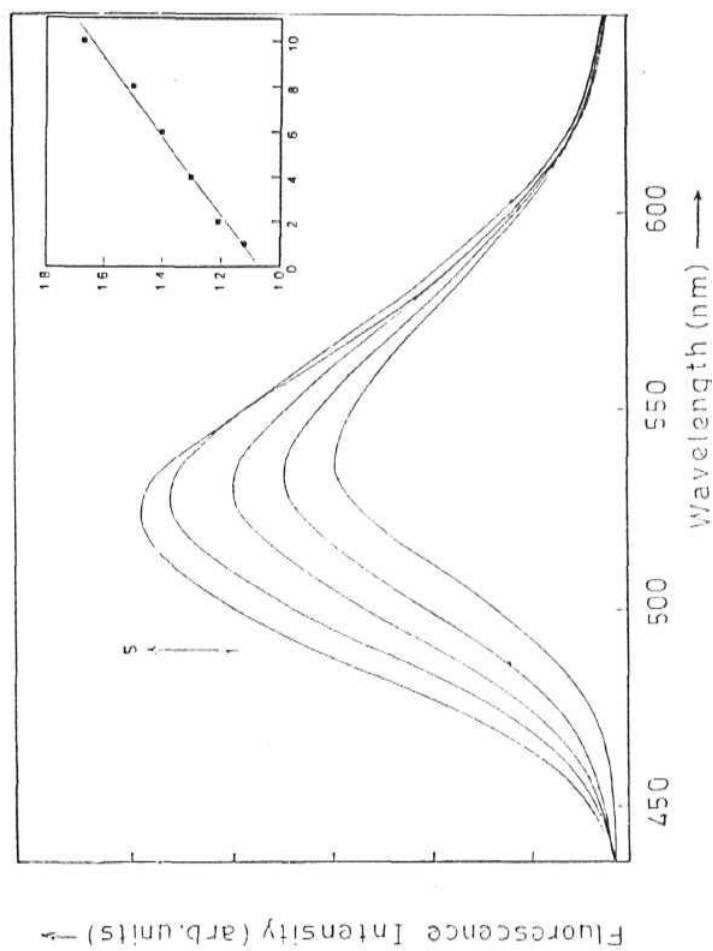


Fig.5.24. Fluorescence spectra of AP in aqueous solution with different amounts of α -CD. (1) 0 mM, (2) 2 mM, (3) 4 mM, (4) 6 mM and (5) 10 mM. $\lambda_{\text{exc}} = 360$ nm. The insert shows the variation of I/I_0 with CD concentrations.

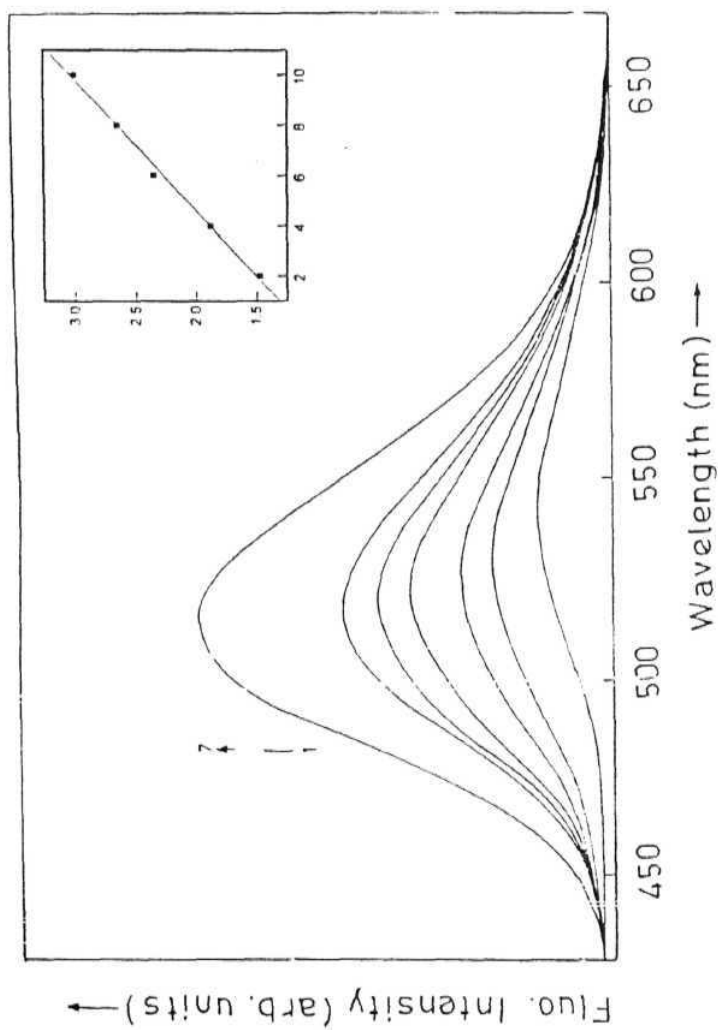


Fig.5.25. Fluorescence spectra of AP in aqueous solution with different amounts of β -CD. (1) 0 mM, (2) 0.2 mM, (3) 0.4 mM, (4) 0.6 mM, (5) 0.8 mM and (6) 1 mM (7) 2 mM. $\lambda_{\text{exc}} = 360$ nm. The insert shows the variation of I/I_0 with CD concentrations.

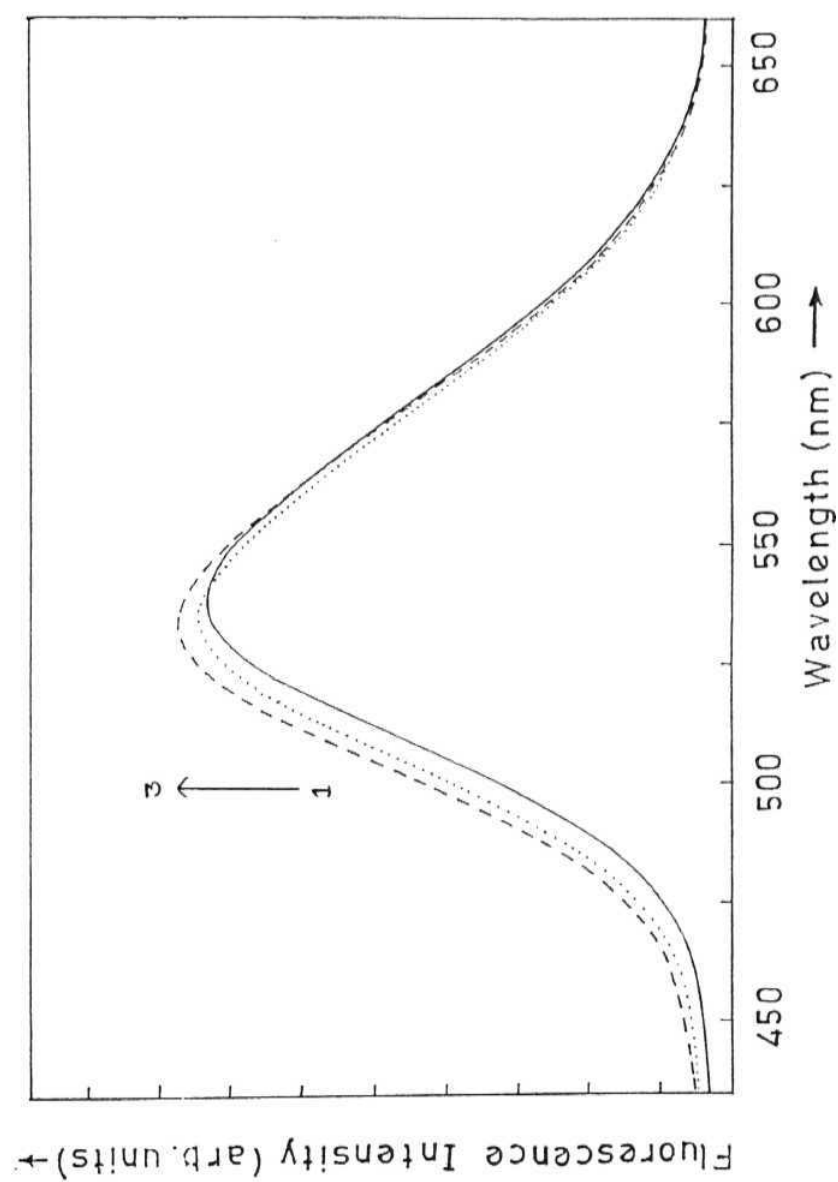


Fig.5.26. Fluorescence spectra of AP in aqueous solution with different amounts of γ -CD. (1) 2 mM, (2) 6 mM and (3) 10 mM. $\lambda_{\text{exc}} = 360$ nm.

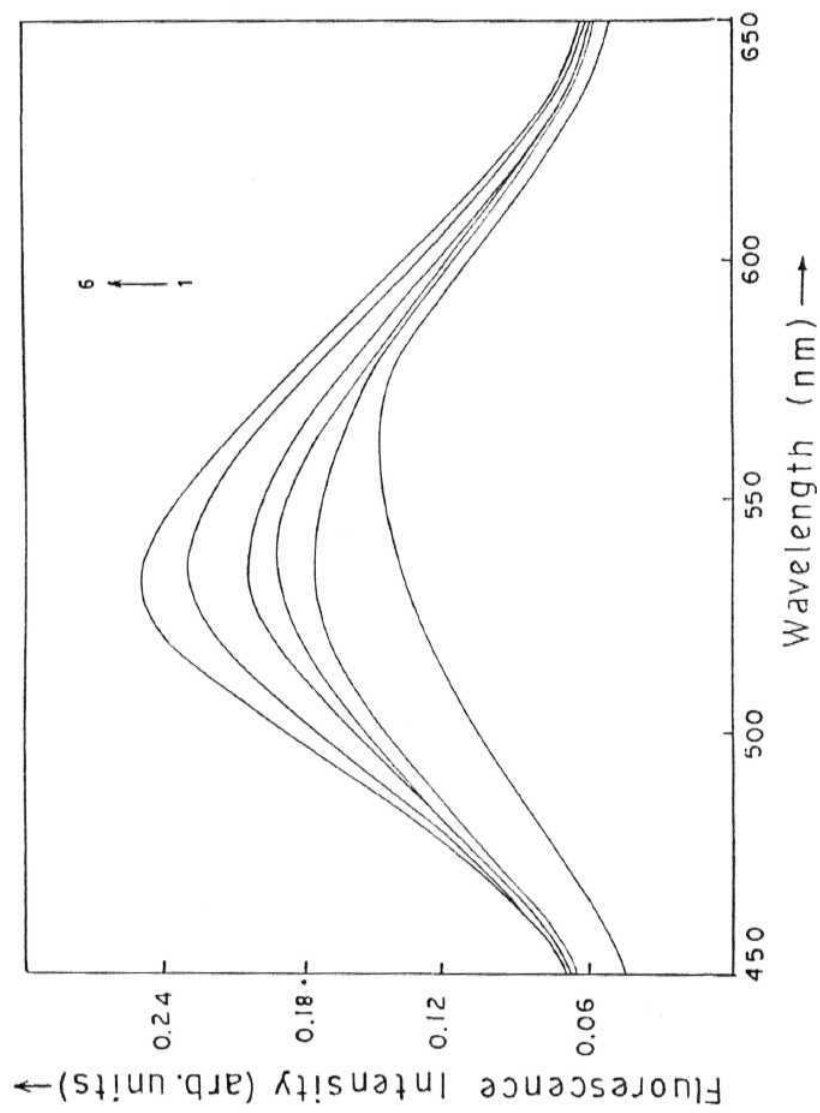


Fig.5.27. Fluorescence spectra of DAP in aqueous solution with different amounts of α -CD. (1) 0 mM, (2) 2 mM, (3) 4 mM, (4) 6 mM, (5) 8 mM and (6) 10 mM. $\lambda_{\text{exc}} = 370$ nm.

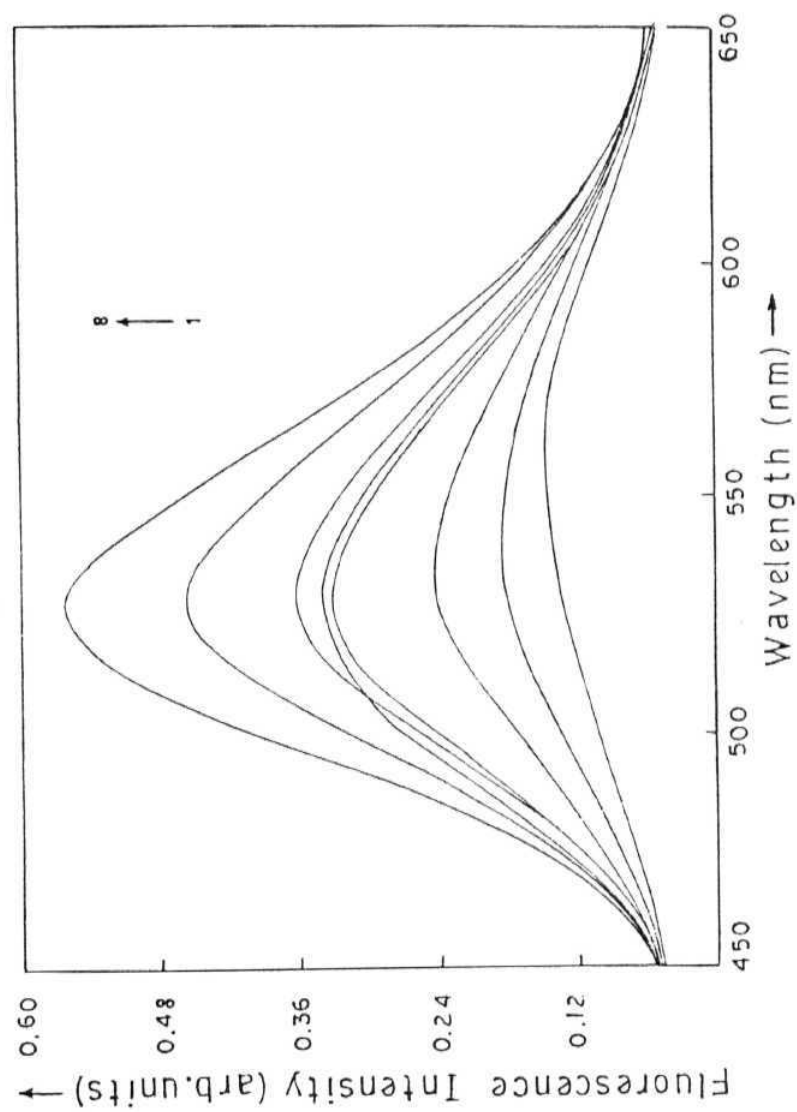


Fig.5.28. Fluorescence spectra of DAP in aqueous solution with different amounts of β -CD. (1) 0 mM, (2) 0.2 mM, (3) 0.4 mM, (4) 0.6 mM, (5) 0.8 mM, (6) 1 mM, (7) 2 mM and (8) 4 mM. $\lambda_{exc} = 370\text{nm}$.

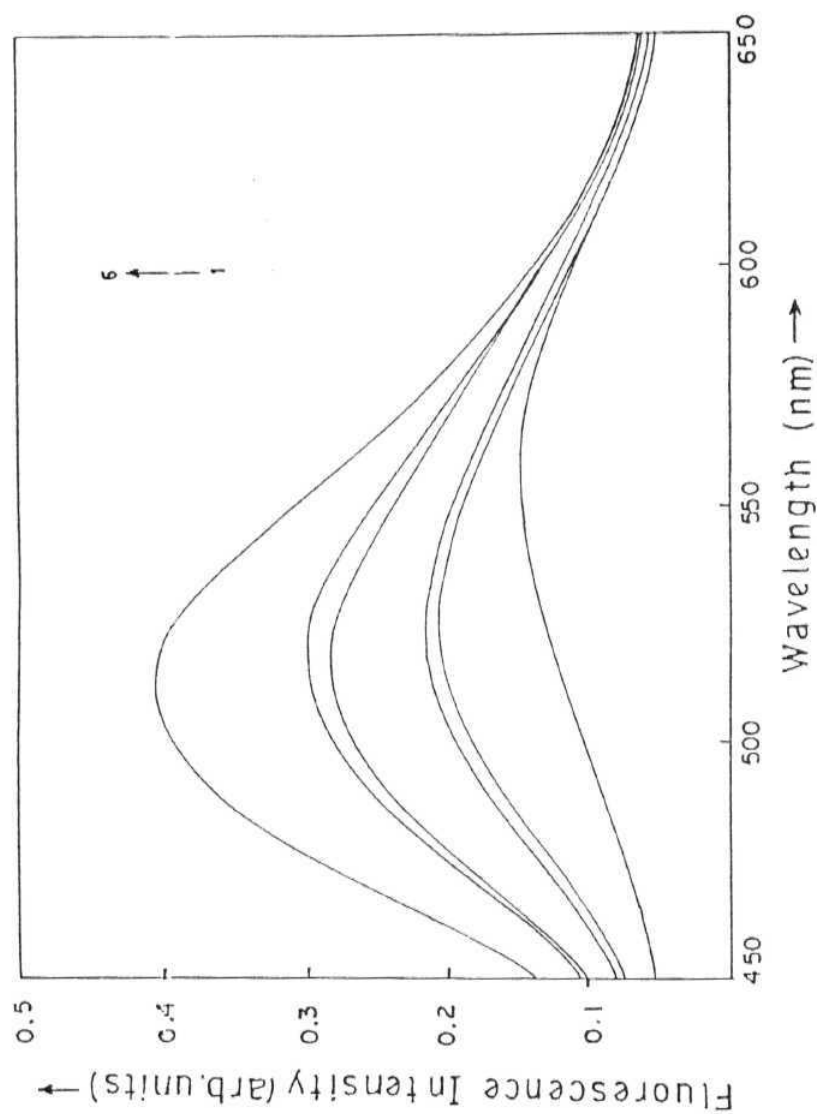


Fig.5.29. Fluorescence spectra of DAP in aqueous solution with various concentrations of γ -CD (1) 0 mM, (2) 2 mM, (3) 4 mM, (4) 6 mM, (5) 8 mM and (6) 10 mM. $\lambda_{\text{exc}} = 370$ nm.

A summary of the fluorescence spectral shift and intensity data is presented in Table 5.10 for AP and in Table 5.11 for DAP.

Table 5.10. Fluorescence spectral and intensity data of AP in α - and cyclodextrins added solutions.

α -CD			[β]-CD		
Conc. (mM)	λ_{max} (nm)	I_f/I_0	Conc. ^a (mM)	λ_{max} (nm)	I_f/I_0
0	540	-	0	540	-
0.5	537	1.11	0.2	530	1.50
2.0	535	1.21	0.4	515	1.90
4.0	530	1.30	0.6	520	2.40
6.0	528	1.40	0.8	517	2.70
8.0	526	1.51	1.0	520	2.95
10.0	523	1.67	2.0	513	4.10

^a because of limited solubility of β -CD,¹ experiment at higher concentrations could not be carried out.

Table 5.11. The fluorescence spectral and intensity' data of DAP in α - , P- and γ -cyclodextrin added solutions.

α			β			γ		
Conc. (mM)	λ_{max} (nm)	If/I ₀	Conc. (mM)	λ_{max} (nm)	If/I ₀	Conc. (mM)	λ_{max} (nm)	If/I ₀
0	568	–	0	568	–	0	568	–
2	556	1.41	0.2	538	1.27	2	532	1.56
4	544	1.47	0.4	534	1.71	4	524	1.64
6	534	1.48	0.6	530	2.12	6	520	2.19
8	533	1.65	0.8	529	2.22	8	519	2.40
10	532	1.87	1.0	529	2.32	10	506	3.14
–	–	–	2.0	528	2.81	–	–	–

It can be seen from Table 5.10 that for the same concentration of α - and β -CD (2 mM), the blue shift and enhancement of intensity for AP are much higher in β -CD. This is indicative of relatively stronger binding in this case. The data presented in Table 5.11 for α - and β -CD added solutions led us to draw similar conclusion for DAP. However, the most interesting observation in this case is perhaps significant fluorescence enhancement and blue shift in γ -CD added solutions. This behaviour is quite different from what has been observed for AP. Since multiple complexes are indicated by the absorption spectral data, it is difficult to arrive at any definite conclusion to account for the data. However, data presented in Table 5.11 can possibly be analysed in the following lines. First, for the same concentration of α -CD, both the enhancement and shift are larger for DAP than with AP. This could result from encapsulation of DAP by two CDs from two sides in 1:2 complex. Second, in β -CD added solution of

DAP, even though the shift is more, the intensity enhancement is less compared to that for AP. One generally expects steeper increase of intensity and larger spectral shift for small change in the microenvironments in the case of DAP based on the Photophysical data of the compound in the homogeneous media. If the twisting motion of DAP was affected on encapsulation, then one would have observed greater enhancement of intensity of the LE emission than that expected from the spectral shift alone. Since for the same concentration of β -CD (2 mM) the enhancement is comparatively less for DAP, we come to conclusion that whatever be the nature of the complex in this case, no enhancement due to rotational restriction is observed. Third, while the data for AP in γ -CD suggests formation of loose complex because of larger cavity size, in the case of DAP larger shift and enhancement most likely to result from better shielding of the fluorophore from the water molecules by two CDs. This is very similar to what we have proposed to account for the data in α -CD. The only difference in the two cases is the extent of coverage provided by the CDs.

The fluorescence enhancement observed with these dyes is similar in magnitude to that found for other fluorescence probes such as DMABN and diethylaminobenzonitrile (DEABN).²¹ The fluorescence is enhanced by factors of 3.5 and 4.2 in CD solutions of DMABN and DEABN respectively. However, one should be careful in making such comparison to find out the effectiveness of a fluorescence probe as the degree of enhancement depends on the cyclodextrin concentrations.

5.2.3. The binding constants

On the basis of the 1:1 association between AP and α - or p-CD, we can write



The binding constant, K for such a complex is given by

$$K = \frac{C_c}{C_a C_{CD}} \quad 5.2$$

where C_c represents the concentration of the complex; C_a , the concentration of AP and C_{CD} , the concentration of CD.

Assuming that C_c is much less than C_{CD}^0 , the initial concentration of CD, C_{CD} can be replaced by C_{CD}^0 . One can then write

$$K = \frac{C_c}{C_a C_{CD}^0} \quad 5.3$$

Since the fluorescence from a CD added solution results from both free AP and the complex, the fluorescence quantum yield of a solution of AP containing CD can be written as

$$\phi = \frac{(\phi_a I_a + \phi_c I_c)}{(I_a + I_c)} \quad 5.4$$

where I_a and I_c represent the fluorescence intensities of free AP in aqueous solution and complexed AP.

However, since

$$\frac{I_a}{I_c} = \frac{\epsilon_a C_a}{\epsilon_c C_c} \quad 5.5$$

we arrive at using equations 5.3 - 5.5

$$\{(\phi - \phi_a) / \phi_a\}^{-1} = (\phi_c / \phi_a - 1)^{-1} + (\phi_c / \phi_a - 1)^{-1} \epsilon_a / K \epsilon_c C_b^0 \quad 5.6$$

Thus according to the above formulation a plot of $\{(\phi - \phi_a) / \phi_a\}^{-1}$ vs $1 / C_{CD}^0$ would yield a straight line. The plots $\{(\phi - \phi_a) / \phi_a\}^{-1}$ vs $1 / C_{CD}^0$ for AP in α and β -CD are shown in figs. 5.30 and 5.31 respectively.

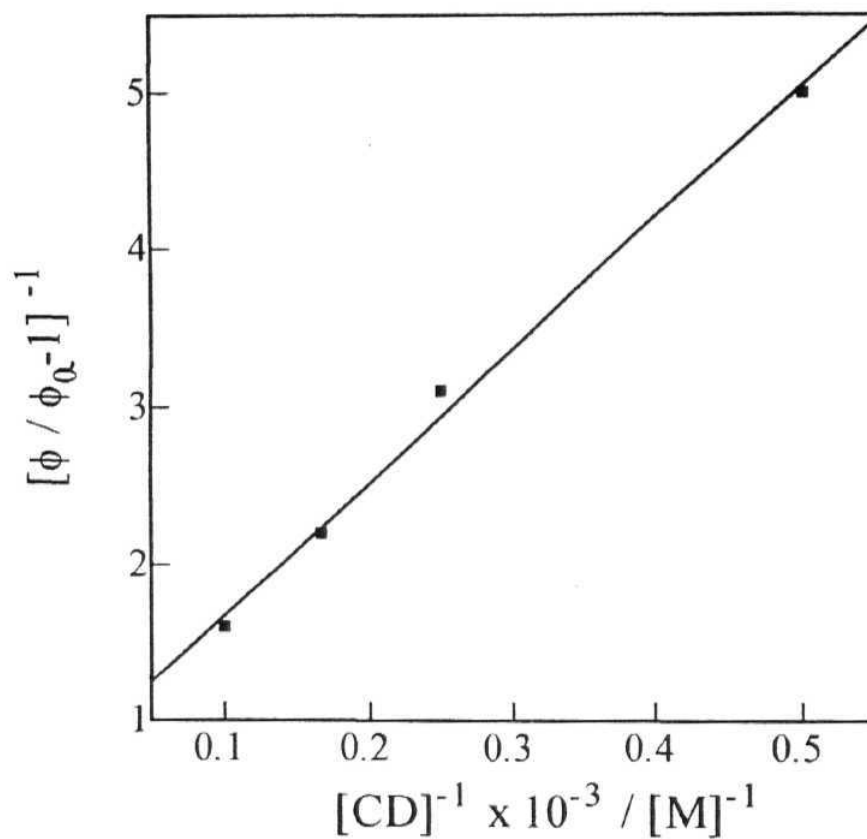


Fig. 5.30 Plot of $\{(\phi - \phi_a) / \phi_a\}^{-1}$ against reciprocal concentration of α -CD for AP.

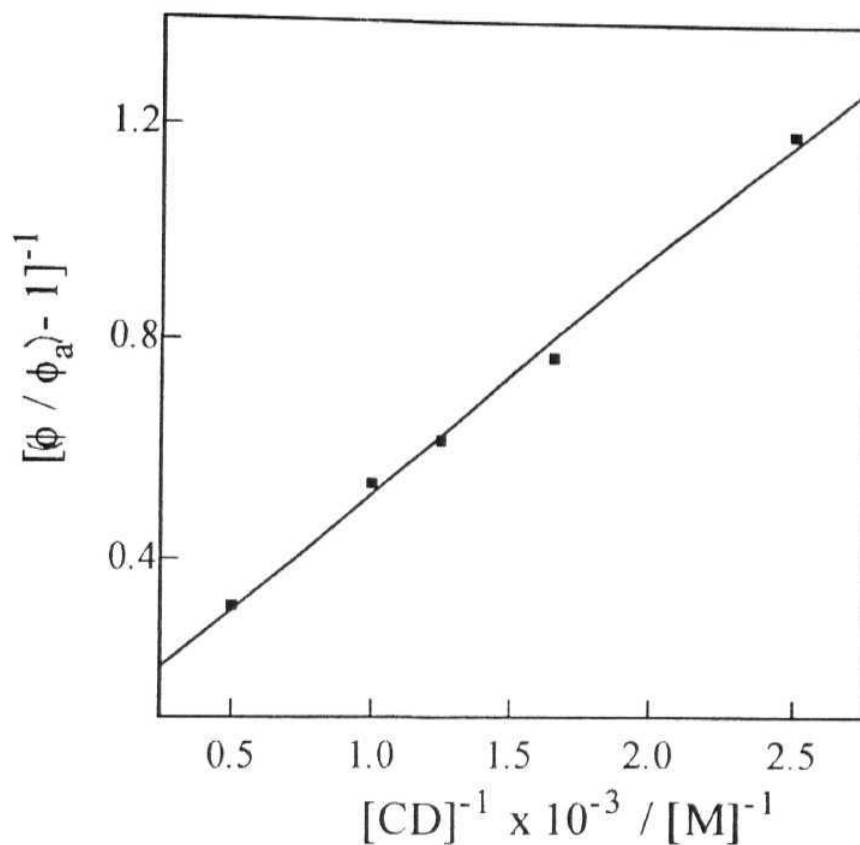


Fig. 5.31. Plot of $\{(\phi - \phi_a) / \phi_a\}$ against reciprocal concentration of β -CD for AP.

With the assumption of $\epsilon_a \approx \epsilon_c$ (this is justified by small changes in absorption spectra on addition on CD), K is obtained from the intercept and the slope. The estimated binding constants with α - and β -CD are 92 M^{-1} and 208 M^{-1}

respectively. Thus, the measured binding constants of the two complexes suggest that P-CD provides a better fit for the probe.

With DAP similar estimation of binding constant is not attempted in view of complications resulting from complexes with more than one stoichiometry.

5.2.4. Fluorescence decay curves

In order to substantiate the inclusion process we have measured the fluorescence decay curves of AP in the absence of CD and in presence of a- and p-CDs and the results are presented in figs. 5.32 - 5.34 respectively. The fluorescence decay curve of AP in water can be fitted to a single exponential decay with a lifetime of approximately 1 ns. However, in a- and p-CD added aqueous solutions, the decay curves can be best fitted to biexponential decay of the form,

$$F(t) = A_1 \exp (-t / \tau_1) + A_2 \exp (-t / \tau_2) \quad 5.7$$

The pre-exponential factors, A_1 and A_2 obtained from the analysis of the decay curves in P-CD added solution are 0.665 and 0.335 and the respective lifetimes of the two components are 1 ns and 8.9 ns; the A_1 and A_2 values for a-CD added solutions are 0.86, 0.14 and the lifetimes are 1 ns and 7.98 ns respectively.

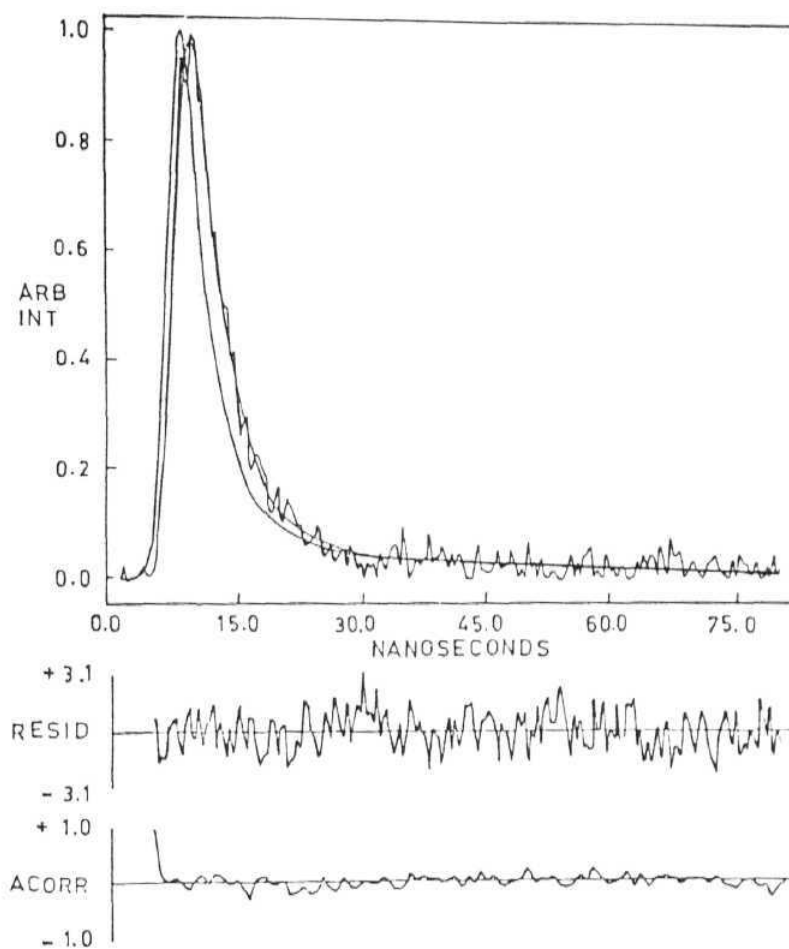


Fig.5.32. Exciting lamp profile, fluorescence decay curve along with the fit to the decay curve of AP in aqueous solution with no CD. $\lambda_{\text{exc}} = 360 \text{ nm}$.

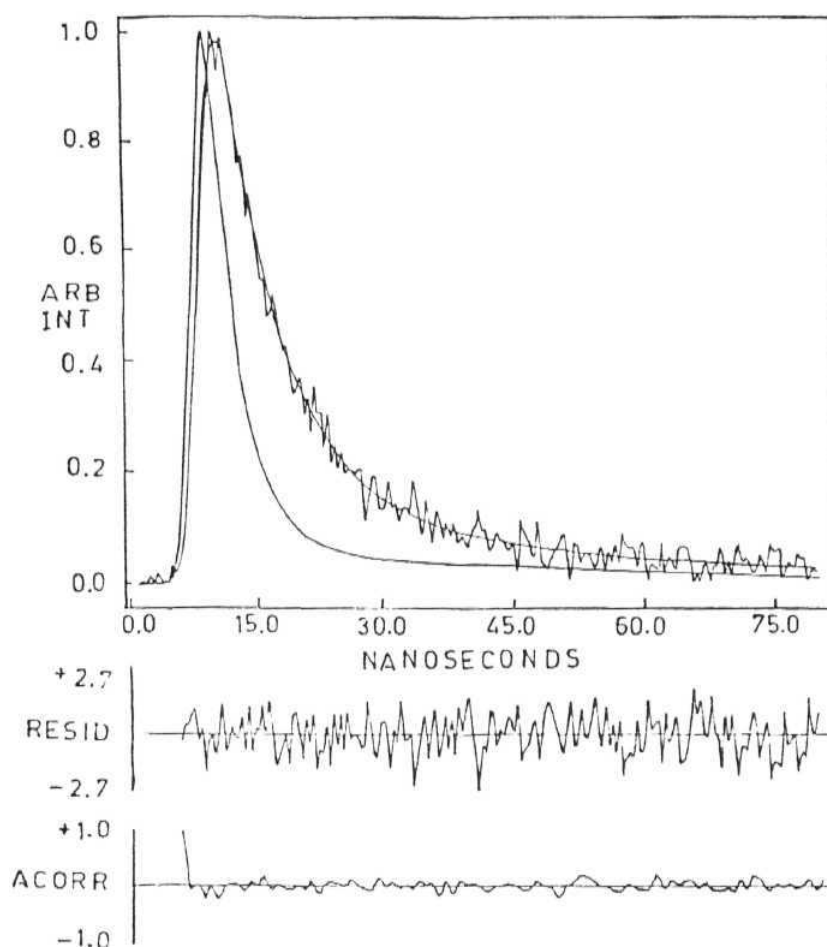


Fig.5.33. Exciting lamp profile, fluorescence decay curve along with the fit to the decay curve of AP in aqueous solution in presence of 10 mM α -CD. $\lambda_{\text{exc}} = 360$ nm.

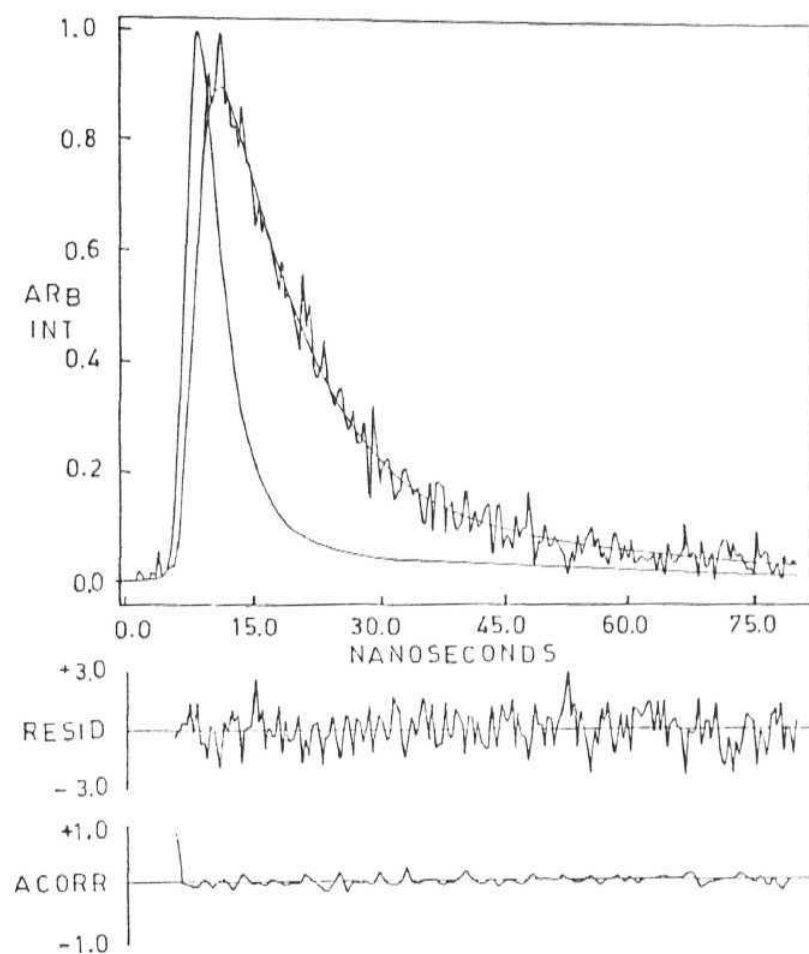


Fig.5.34. Exciting lamp profile, fluorescence decay curve along with the fit to the decay curve of AP in aqueous solution in presence of 2 mM β - CD. $\lambda_{\text{exc}} = 360$ nm.

The component with a lifetime of 1 ns corresponds to **the** lifetime of free AP molecules in aqueous solution, the latter values therefore represent the fluorescence lifetime of the complex. The significant changes in lifetime on inclusion clearly indicate that AP in the complex is in a relatively nonpolar environment. In γ -CD, the fluorescence decay curve of AP when fitted to bi-exponential decay yielded lifetimes of ≈ 1 ns and 3.1 ns.

As it is possible to clearly resolve the two components through temporal resolution of fluorescence in both α -CD, β -CD solutions, we have made an attempt to estimate the guest-host interaction from the lifetime data too. In a two-component system, the pre-exponential factors, A_a and A_c contributing to the signal at zero time are indicative of the relative contributions of the free and complex forms of the fluorophore respectively. In a multi-component system, the pre-exponential factors A_1 and A_2 can be written as

$$A_i \propto C_i \epsilon_i \phi_i \tau_i^{-1} \quad 5.8$$

provided that all components are irradiated with a light source of the same intensity and the fluorescence is collected for the same amount of time. As both the conditions are met in our experiment conditions, we can write

$$\frac{C_a}{C_c} = \frac{A_a \tau_a \epsilon_c \phi_c}{A_c \tau_c \epsilon_a \phi_a} \quad 5.9$$

Using the experimentally obtained values of A and T and assuming $\epsilon_a \approx \epsilon_c$, C_a/C_c is found to be 0.367 at a P-CD concentration of 2 mM and 0.528 at α -CD concentration of 10 mM. The estimated values of ϕ_c , as obtained from the intercepts of figs. 5.24 and 5.25, are 0.02 (a-CD complex) and 0.1 (P-CD complex). The binding constants thus obtained for P-CD and a-CD complex are respectively 185 M and 53 M⁻¹. The agreement of the K values as determined by the steady state and time-resolved methods in the case of p-CD complex is excellent. For the a-CD complex, even though the binding constant obtained from lifetime data is different from the steady state results, the value is of the right order of magnitude indicating that this method of temporal analysis can be used for estimation of binding constants when significant change in the lifetime value is observed on complexation. The better agreement of the K value in the case of p-CD complex must be due to a larger change in lifetime on complexation. Thus both steady state and time-resolved experiments on CD added solutions of AP indicate that P-CD provides a better fit for AP.

5.2.5. Nature of the complexes

A knowledge of the possible arrangement of the probe molecule inside the CD cavity is necessary in order to rationalise its Photophysical properties in CD cavity quantitatively. In order to find out the nature of the complex we have utilised the structural data of AP obtained from theoretical calculations.

The distance between atoms numbered 13-14 (Chart 5.1) represents the long axis of the molecule which is equal to 7.69 Å. The reported cavity depth of

both α - and P-CDs is 7.9 Å.⁶ Therefore, the entire molecule can go inside the cavity of CD, provided it gets inside. The distance between atoms **16** and **18** is 5.06 Å, whereas that between atom **11** and **12** is 4.64 Å. Since the cavity diameter of α -CD is 4.9 Å, which is less than the atoms **16-18** distance, a portion of the molecule has to lie outside the cavity. The situation is, however, different for P-CD, which has a cavity diameter of 6.2 Å. Thus we see that the molecular dimensions of AP and the cavity size of p-CD are such that AP can completely reside inside the cavity. It is however left to be seen whether AP is completely encapsulated or not. In the case of the α -CD complex, the question to be answered is which side of the probe molecule is enclosed (amino group or imino group).

It is shown earlier that the absorption maximum of AP shifts nearly by 15 nm on passage from aprotic to protic solvents. Therefore, if AP binds to the interior hydrophobic environment of the CD cavity, a blue shift of the absorption maximum by this magnitude is expected. We notice, however, that on complexation, the absorption maxima do not change their position. Further, the excitation spectra of the aqueous solutions of AP (with or without CD) remain the same, pointing to the fact that the probe in the complex is still hydrogen bonded to the water molecules or to the secondary hydroxyl groups of CDs which constitute the top of the doughnut shaped molecules. This information can be used to determine the configuration of AP in the CD cavity. There are three centres (amino, imino and carbonyl) which can participate in hydrogen bond formation with the solvents. Amino and imino groups, have hydrogen bond donating ability and are expected to form a hydrogen bonded complex with hydrogen bond accepting solvents such as dimethylsulfoxide,

ethyl acetate, etc. and the carbonyl groups to participate in hydrogen bonding with solvents which have hydrogen donating capability. Experimentally, hydrogen bonding is observed only in hydrogen bond donating solvents such as water, ethanol, etc. Thus, we are led to conclude that $>\text{C}=\text{O}$ groups are responsible for hydrogen bond formation in protic media. As hydrogen bonding is evident in CD complexes of both α - and β -CD, $>\text{C}=\text{O}$ groups must be exposed to water or secondary hydroxyl groups of CD. It is interesting to find that though AP can completely go inside the cavity of β -CD, it chooses to leave a portion of it outside the cavity. This might be due to the hydrophobic character of the compound which is evident from the dipole moment value of AP (5.3 D). The same line of arguments can be used to determine the possible geometry of the AP- α -CD complex. Since hydrogen bonding is also evident in this case, the inclusion of the probe takes place from the side of the amino group of the molecule. As the distance between atoms 16 and 18 is larger than the cavity opening of α -CD (4.9 Å), the AP- α -CD complex is a loose one with very small portion of the probe inside the cavity. The proposed structures of the complexes of AP are shown in fig. 5.35.

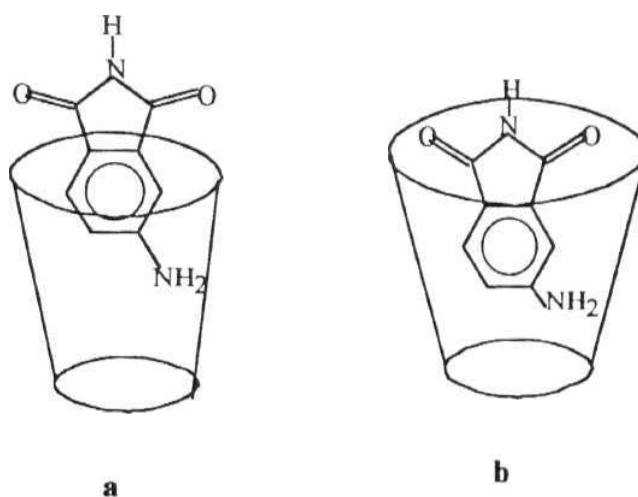


Fig. 5.35. Proposed structures of the complexes of AP in (a) α -CD and (b) β -CD

We now show from the fluorescence enhancement data that in spite of the availability of the space, AP does not enter fully into the cavity of β -CD. It is shown earlier that the fluorescence quantum yield of AP changes from 0.01 (in water) to 0.7 (in dioxane). Therefore, if AP is completely transferred from aqueous solution to hydrophobic cavity of CD, the fluorescence enhancement is expected to be nearly 70-fold. However, as the binding constant is approximately 200 M^{-1} , the ratio, $[\text{complex}] / [\text{AP}]$ at β -CD concentration of 2 mM is 0.4. Under this condition, a completely included molecule is expected to show an enhancement by a factor of 28. As observed enhancement is far less than this estimated value, the probe molecule in the complex must be partially exposed to water. Further, 4-fold enhancement (as observed here) suggests that ϕ_f of the complex is 0.1. As this quantum yield value is the same as that of AP in methanol, the overall polarity experienced by the probe in the particular arrangement shown in fig. 5.35 is equivalent to that in methanol. In order to substantiate this point further we have constructed the fluorescence spectrum of complex alone by the following procedures.

An aqueous solution of known concentration of AP was prepared, and a known amount of CD was added to it. The fluorescence spectrum of the resulting solution was recorded. Using the relation $K = [\text{complex}] / ([\text{AP}]_{\text{free}} [\text{CD}])$ and $[\text{AP}]_{\text{total}} = [\text{AP}]_{\text{free}} + [\text{complex}]$, $[\text{AP}]_{\text{free}}$ was determined. Another solution of AP with concentration $[\text{AP}]_{\text{free}}$ was prepared in water, and the

fluorescence spectrum was recorded. Subtraction of the later spectrum from the former one yielded the spectrum due to complex alone.

The spectrum of the p-CD-AP complex, shown in fig.5.36, resembles closely that of AP in methanol which once again confirms that the effective polarity experienced by the fluorophore in the complex is equivalent to that in methanol. The application of the same procedure to α -CD-AP complex indicated a slightly more polar environment experienced by the probe.

5.2.6. Aminophthalimides in micellar environment

That aminophthalimides can act as reporter molecules for the microenvironments of other organised media as well, is illustrated by the following study in micellar environment. The aim of this preliminary investigation is just to highlight the potentials of these derivatives in sensing and reporting heterogeneity of the organised systems in general.

Micelles are aggregates formed by the interaction of surfactant molecules.^{1-3,4} Usually the hydrophobic part of the surfactant molecule is a long chain hydrocarbon (eight or more), while the hydrophilic portion of the molecule may be a group of ethylene oxide units, as in the Triton series of surfactants, or an anionic group, as in SDS or a cationic group as in CTAB. Above certain concentration, called critical micelle concentration (CMC), the surfactant molecules group together forming micelles. The most important property of the micelles' is their ability to solubilise hydrophobic molecules in aqueous solution.³⁸ Because of structural similarities, micelles provide convenient models for both enzymes and bilayer membranes. We have selected

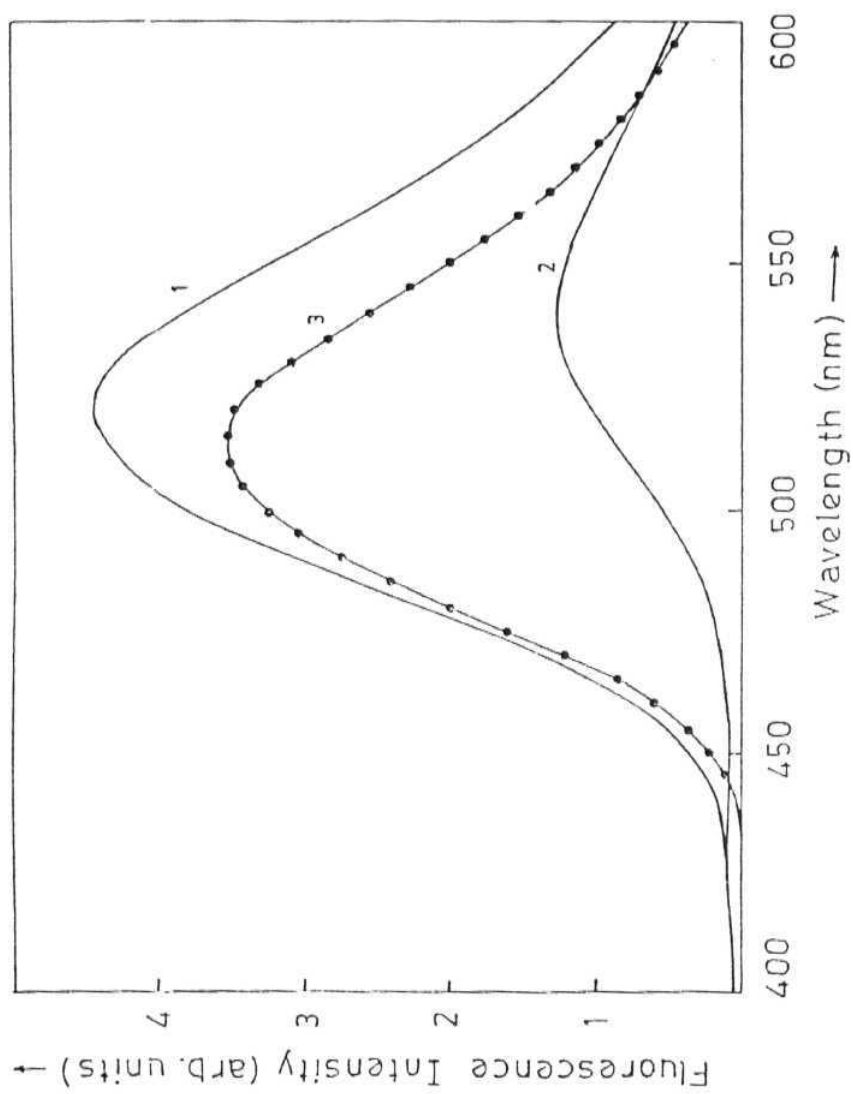


Fig.5.36. The fluorescence spectrum (3) of the AP- β -CD complex obtained by subtraction of spectrum (2) from spectrum (1). See text for details.

three most commonly used cationic, anionic and neutral surfactants namely, ClAB, SDS and Triton-X respectively to examine whether micellar aggregation can be followed by aminophthalimide fluorophores.

As with CDs, the change in the absorption spectra on addition of the surfactants to aqueous solutions of AP and DAP was found very small. The emission spectra displayed blue shift and enhancement of fluorescence intensity in surfactant added solutions is observed. These changes were prominent only beyond a certain concentration of surfactant in micelles which corresponded very well with the CMC values of the micelles. This is illustrated in fig 5.37 in which the variation of the relative intensity of DAP is plotted against the concentration of ClAB. The CMCs were determined from the intersection of the two straight lines shown in the figure. We could not observe enhancement of more than 3 - 4 in micellar environment. This is again suggestive of the fact that the probe molecules are located at the micelle-water interface which is believed to be due to strong hydrogen bonding interaction of the carbonyl groups with the water molecules.

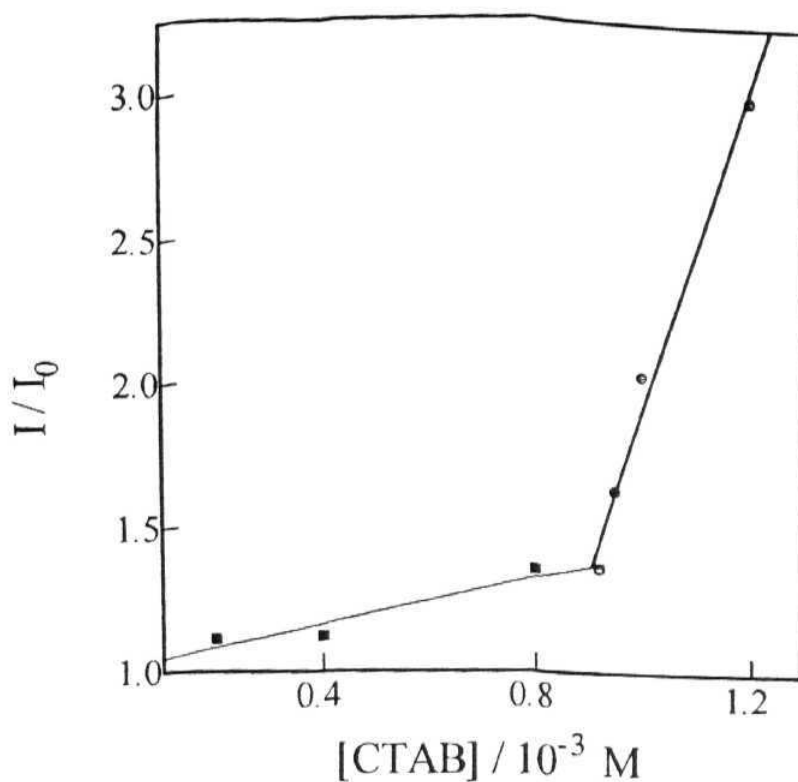


Fig.5.37. Plot of I/I_0 against CTAB concentration for DAP in aqueous solution

5.3. References

- 1 K. Kalyanasundaram, *Photochemistry in Microheterogeneous Systems*, Academic Press: New York, **1987**.
- 2 *Organic Phototransformations in Microheterogeneous systems*, M.A. Fox, ed American Chemical Society: Washington, D C , **1982**.

- 3 *Micellisation, Solubilisation and Microemulsions*, K.L. Mittal, ed Vol. 1, 2, **Plenum: New York, 1991.**
- 4 *Photochemistry in Organised and Constrained Media*, V. Ramamurthy, ed. VCH: New York, **1991.**
- 5 K. Bhattacharyya, M. Chowdhury. *Chem. Rev.*, 93, 507, **1993.**
- 6 *Inclusion compounds*, J.L. Atwood, J.E.D. Davis, D.D. Mac Nicol, eds. Vol. 1-3, Academic Press: London, **1984.**
- 7 M.L. Bender M. Komiyama. *Cyclodextrin Chemistry, React. Struct. Concepts Org. Chem.*, Vol. 16. Springer: New York, **1978.**
- 8 F. Cramer, W. Saenger, H. Spatz, *J. Am. Chem. Soc.*, **14**, 89, **1967.**
- 9 W. Saenger, *Angew. Chem Int. Ed Engl.*, **19**, 344, 1980.
- 10 I. Tabushi, *Acc. Chem Res.*, **15**, 66, **1982.**
- 11 R. Breslow, *Science*, **218**, 532, **1982.**
- 12 V.T. D'Souza, M.L. Bender, *Acc. Chem. Res.*, 20, 146, **1987.**
- 13 R. Breslow, *Acc. Chem. Res.*, 28, 146, **1995**
- 14 Z.R. Grabowski, K. Rotkiewicz, A. Siemiarz, D.I. Cowley, W. Baumann, *Nouv. J. Chim.*, 3, 443, **1979.**
- 15 a) G. Jones II, W.R. Jackson, A.M. Halpern, *Chem. Phys. Lett.*, 72, 391, **1980**; b) M. Vogel, W. Rettig, U. Fiedeldei, H. Baumgaertel, *Chem. Phys. Lett.*, 148, 347, **1988.**
- 16 a) N.G. Bakhshiev, *Opt. Spektrosk.*, **12**, 1557, **1962**; **12**, 350, **1962**, b) W.R. Ware, S.K. Lee, G.J. Brant, P.P. Chow, *J. Chem. Phys.*, 54, 4729, **1971**, c) Y.T. Mazurenko, *Opt. Spectrosk.*, 36, 283, **1974**, d) S.W. Yeh, L.A. Philips, S.P. Webb, L.F. Buhse, J.H. Clark, In *Ultrafast Phenomena, II*, D.A. Auston, K.B. Eisenthal, eds Springer: Berlin, p 359, **1987**; e) H. Langhals, *Anal Lett.*, **23**, 2243, **1991.**

- 17 P. Suppan,/. *Chem.Soc. Faraday Trans. /.*, 83, 495, **1987**.
- 18 T. Hagan, D. Pilloud, P. Suppan, *Chem. Phys. Lett.*, 139, 499, **1987**.
- 19 V. Nagarajan, A.M. Brearly, T.J. Kang, P.F. Barbara, *J. Chcm. Phys.*, 86, 3183,1987.
- 20 C. Reichardt, *Solvents and Solvent Effects in Organic Chemistry*, VCH: Weinheim, **1988**.
- 21 a) G.3. Cox, P.J. Hauptman, NJ. Turro, *Photochem. Photobiol.*, 39, 597, **1984**
- 22 a) E. Lippert, W. Luder, H. Boos, *Adv. Mol. Spectr.*, 6, 125, **1956**; b) N. Mataga, Y. Kaifu, M. Koizumi, *Bull. Chem. Soc. Jpn.*, 28, 690, **1955**, c) N. Mataga, Y. Torihashi, *Bull. Chem. Soc. Jpn.*, 36, 356, **1963**.
- 23 a) K.A. Zachariasse, TV. Haar, A. Hebecker, U. Leinhos, W. Kuhnle, *Pure Appl. Chcm.*, 65, 1705, 1993; b) W Baumann, H. Bischof, J.C. Frohling, C. Brittinger, W. Rettig, K. Rotkiewicz, *J. Photochem. Photobiol. A: Chem.*, 64, 49, **1992**; c) J.C. Tseng, L. A. Singer,/. *Phys. Chem.*, 93, 7092, **1989**.
- 24 S. Wang, J. Cai, R. Sadygov, E. C. Lim, *J. Phys. Chem.*, 99, 7416, **1995**.
- 25 C.J. Seliskar, L. Brand,/. *Am. Chem. Soc*, 93, 5414, **1971**.
- 26 J.B. Birks, *Phofophysics of Aromatic Molecules*, Wiley London, 1969.
- 27 S.J. Strickler, R.A. Berg, *J. Chem. Phys.*, 37, 874, **1962**.
- 28 a) P.K. McCarthy, .G.J. Blanchard, /. *Phys. Chem.*, 97, 12205, **1993**; b) MA. Awad, P.K. McCarthy, G.J. Blanchard, /. *phys. Chem.*, 98, 1454, **1994**
- 29 a) J.M. Hicks, M.T. Vandersall, E.V. Sitzmann, K.B. Eisenthal, *Chem. Phys. Letts.*, 135, 413, **1987**; b) J.M. Hicks, M.T. Vandersall, Z. Babarogic, KB. Eisenthal, *Chem. Phys. Letts.*, 116, 18, **1985**.

- 30 *Handbook of Chemistry and Physics 7th edition*, DR. Lide, ed. CRC Press: London, **1992**.
- 31 a) A Nag, R. Dutta, N. Chattopadhyay, K. Bhattacharyya, *Chem. Phys. Lett.*, **83**, 157, **1989**; b) A. Nag, K. Bhattacharyya, *J. Chem. Soc. Faraday Trans I*, **86**, 53, **1990**, c) A Nag, T. Chakraborty, K. Bhattacharyya, *J. Phys. Chem.*, **94**, 4203, **1990**.
- 32 a) M. Hoshino, M. Imamura, K. Ikahara, Y. Hama, *J. Phys. Chem.*, **85**, 1820, **1981**; b) M. El. Baraka, R. Garcia, E. Quinones, *J. Photochem Photobiol. A: Chem.*, **79**, 181, **1994**, c) N.J. Turro, J.D. Bolt, Y. Kuroda I. Tabushi, *Photochem. Photobiol.*, **35**, 69, **1982**; d) N.J. Turro, T. Okubo C.J. Chung, *J. Am. Chem. Soc.*, **104**, 1789, **1982**; e) N.J. Turro, G.S. Cox and X. Li, *Photochem. Photobiol.*, **37**, 149, 1983., f) S. Hamai, *J. Am. Chem Soc.*, **111**, 3959, **1989**, g) S. Scypinski C.J. Cline Love, *Anal. Chem.*, **56**, 331, **1984**.
- 33 a) I. Tabushi, K. Fujita, L.C. Yuan, *Tetrahedron Lett.*, **29**, 2503, **1977**, b) H. Murai, Y. Mizunuma, K. Ashikawa, Y. Yamamoto, Y. Iihaya, *Chem. Phys. Lett.*, **144**, 417, **1988**.
- 34 a) N.J. Turro, T. Okubo, G.C. Weed, *Photochem. Photobiol.*, **35**, 325, **1982**, b) R. A. Yellin, D.F. Eaton, *J. Phys. Chem.*, **87**, 5051, **1983**, c) A. Ueno, K. Takahashi, T. Oka, *J. Chem. Soc. Chem. Commun.*, 921, **1980**, d) T. Yoroze, H. Hoshino, M. Imamura, *J. Phys. Chem.*, **86**, 4426, **1982**, e) G.S. Cox, N.J. Turro, *J. Am. Chem. Soc.*, **106**, 422, **1984**.
- 35 a) R. Chenevert, N. Voyer, *Tetrahedron. Lett.*, **25**, 5007, **1984**, b) R. Chenevert, R. Plante, *Can. J. Chem.*, **61**, 1092, **1983**.
- 36 a) N. Sarkar, K. Das, D. Nath, K. Bhattacharya, *Chem. Phys. Lett.*, **196**, 491, **1992**; b) K. Das, N. Sarkar, D. Nath, K. Bhattacharya, *Spectrochim. Acta.*, **48A**, 1701, 1992.

- 37 K. Kano, I. Iakenoshita, T. Ogawa, *Chcm. Phys. Lett.*, **321**, **1982**; b) T. Yorozu, M. Hoshino, M. Immamura, *J. Phys. Chem.*, **86**, 4426, **1982**.
- 38 a) J.K. Thomas, *Chcm. Rev.*, 80, 283, **1980**. and references therein; b) F.W.J. Teale, *Nature.*, **181**, 415, 1958, c) H.C. Chiang, A. Lukton, *J. Phys. Chem.*, 79, 1935, **1975**.

EXCITED STATE DIPOLE MOMENTS FROM SOLVATOCHROMIC DATA

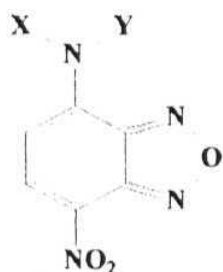
This Chapter is organised in two sections. The first section is devoted to studies on some 7-nitrobenz-2-oxa-1,3-diazol-4-yl (NBD) derivatives in which we first attempt to find out the correct Onsager cavity radii required for the analysis of solvatochromic data to measure the change in the dipole moment on excitation using the Lippert-Mataga equation. Then we focus on two other model compounds containing the NBD chromophore to determine the nature of the emitting state and possible role of rotary decay mechanism using AMI calculations. The second section of the Chapter is concerned with estimation of the excited state dipole moments of a set of coumarin derivatives using a recently developed modified Lippert Mataga equation in which the Stokes **shift** between the absorption and fluorescence wavenumbers is conelated with the microscopic solvent polarity parameter, E_T^1 .¹

6.1. Studies on NBD derivatives

6.1.1. Selection of Onsager cavity radius

Even though a number of direct methods such as fluorescence polarisation,² electric dichroism,³ stark splitting of rotational levels⁴ and microwave conductivity or absorption⁵ are available and considered to be fairly accurate for the estimation of the excited state dipole moment, the most common ones are based on the analysis of the solvatochromism of the absorption and fluorescence maxima.^{6,7} In the method suggested by Lippert and

Mataga, the Stokes shift **between the** absorption and fluorescence **maxima** is related to the dipole moment change on excitation **and** solvent polarity function involving the dielectric constant and refractive index (equn. 3.3).^{6,7} The main difficulty associated with quantitative measurement of the change in dipole moment on excitation using the above method is the choice of the Onsager cavity radius. In fact, it has been reported that the values obtained for $\Delta\mu$ of a fluorophore from the above equation may differ from the actual values by as much as 50% depending on the choice of the cavity radius.⁸ In the absence of any clear guidelines for the selection of the cavity radius of a particular system, the choice is often arbitrary ⁸⁻¹¹ and hence the determined Aji values are far from **accurate**. We address to this Onsager radius problem by considering some NBD derivatives in which the length of the molecules is varied keeping the basic chromophore unchanged (Chart 6.1).

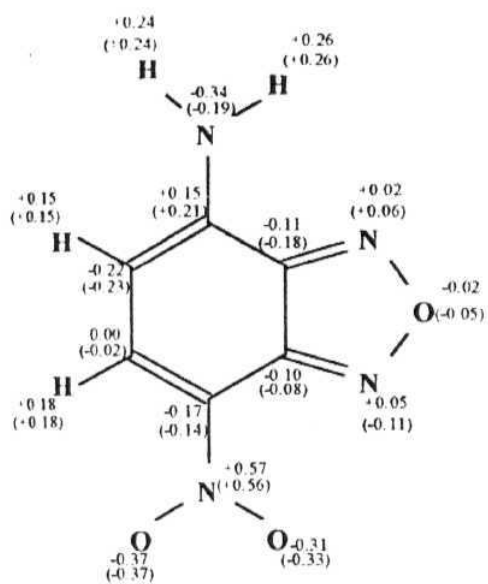


1. X and Y = H
2. X =CH₃ and Y = H
3. X = CH₂-CH₃ and Y = H
4. X =CH₂-(CH₂)₄-COOH and Y = H
5. X =CH₂CH₂CH₃ and Y =H
6. X and Y =CH₂CH₃
7. X and Y = CH₃

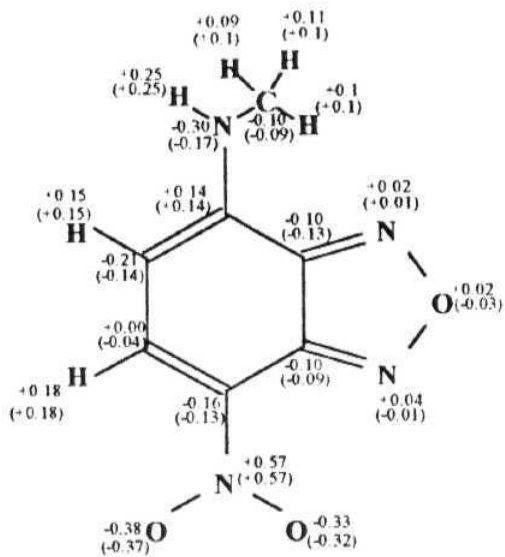
CHART 6.1

NBD molecules are extensively used as fluorescence probes to follow a variety of processes such as membrane fusion, lipid motion, organisation of lipids and proteins in membranes etc.¹²⁻¹⁶ The fluorescence properties of NBD derivatives are quite similar to those of aminophthalimides discussed earlier. The fluorescence quantum yield of the NBD derivatives is reasonably high in aprotic solvents (≈ 0.5) and extremely low in water ($\approx 10^{-2}$). This property is ideally suited for its application as fluorescence probe. Labelling biological compounds with the NBD chromophore is fairly easy to achieve as the NBD halides react readily with thiols and amino groups. Amino NBD derivatives also find application in non linear optics.¹⁴ The applications of NBD derivatives have been reviewed recently.¹⁵

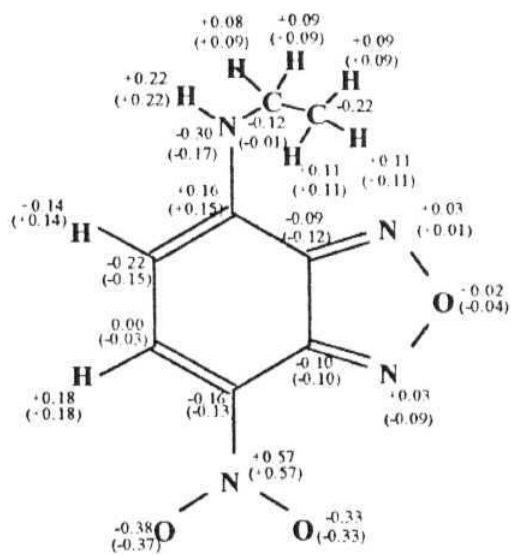
We have estimated theoretically the charge densities at different atoms (Chart 6.2) of the fully optimised structures of 1-3 and then calculated their dipole moments in the ground and excited state. It can be seen from the data presented in Table 6.1 that for 1 the difference between the ground and excited state dipole moment amounts to 3.5 D. When one of the hydrogens is replaced by a methyl group to form 2, both the ground and excited state dipole moments increase by 0.5 D (so that the change in the dipole moment remains constant). This behaviour is consistent with the inductive effect of the alkyl group which favours increased charge separation. On replacement of the methyl group by an ethyl group as in 3, the dipole moment remains more or less constant. It is interesting to observe that although the longest molecular axis in NBD derivatives 1-3 vary significantly, it does not have any effect on the calculated value of $\Delta\mu$.



1



2



3

CHART 6.2

The invariance of the $\Delta\mu$ values on the length of the alkyl chain suggests that for even longer derivatives such as 4, which is actually used in fluorescence applications, one should not consider, for the purpose of the selection of the Onsager radius, the length of the long axis of the molecule; instead, the cavity radius should be measured from the maximum distance across which the charge separation takes place. If it were not so, $\Delta\mu$ for the compound 3, based on its longest molecular axis (as calculated theoretically) and solvatochromic data for 4 (as solvatochromism of the absorption and fluorescence bands of these compounds do not differ significantly) would have been 5.5 D which is nearly 55% more than the estimated value of 3.5 D. The theoretically calculated distance between the average coordinates of the oxygen atoms in the nitro group and the nitrogen atom of the amino group (which remains practically the same in all these derivatives), where charge separation could occur is 6.38 Å. Half of this, i.e. 3.19 Å when used for the analysis of the solvatochromic data of 4, $\Delta\mu$ value is obtained as 3.9 D which is in line with the $\Delta\mu$ values for the other compounds.

Table 6.1. Dipole Moments (in D) of NBD Derivatives.

Compound		μ_e	$\Delta\mu$	Method used
1	9.1	12.6	3.5	AM1
2	9.6	13.2	3.6	AM1
3	9.5	13.2	3.5	AM1
4^a	-	-	3.9	Spectral shift

^a assuming an Onsager cavity radius of 3.19 Å

*6.1.2. Nature of the emitting state and the **role** of rotary decay mechanism: A theoretical analysis*

Recently, nonfluorescent TICT state has been proposed for one of the two NBD derivatives, 5 and 6 (Chart 6.1) to account for the polarity dependence of the fluorescence **properties**.¹⁷ In order to get insight into the Photophysical behaviour of NBD derivatives we have carried out calculations, similar to those performed on DMABN and aminophthalimides, on two simpler compounds, 1 and 7 whose application encompasses large areas of **interest**.¹²⁻¹⁶ We highlight only the salient features of the results which are relevant to the rotary decay process.

6.1.2.1. Ground state properties

The ground state profiles of the two molecules in the gas phase, shown as a function of the twist angles in figs 6.1 and 6.2, are quite similar to those obtained for other compounds reported in the thesis. The planar conformation is the most stable form (energy minimum observed for dihedral angle of 0-10 deg). The planar form is significantly stabilised with respect to the twisted form on solvation. The twisted forms are high enough in energy compared with the respective planar forms so as not to expect any twisting in the ground state either in the gas phase or in presence of any solvent. The ground state dipole moments at the planar conformation are 9.1 and 9.76 D for 1 and 7 **respectively**

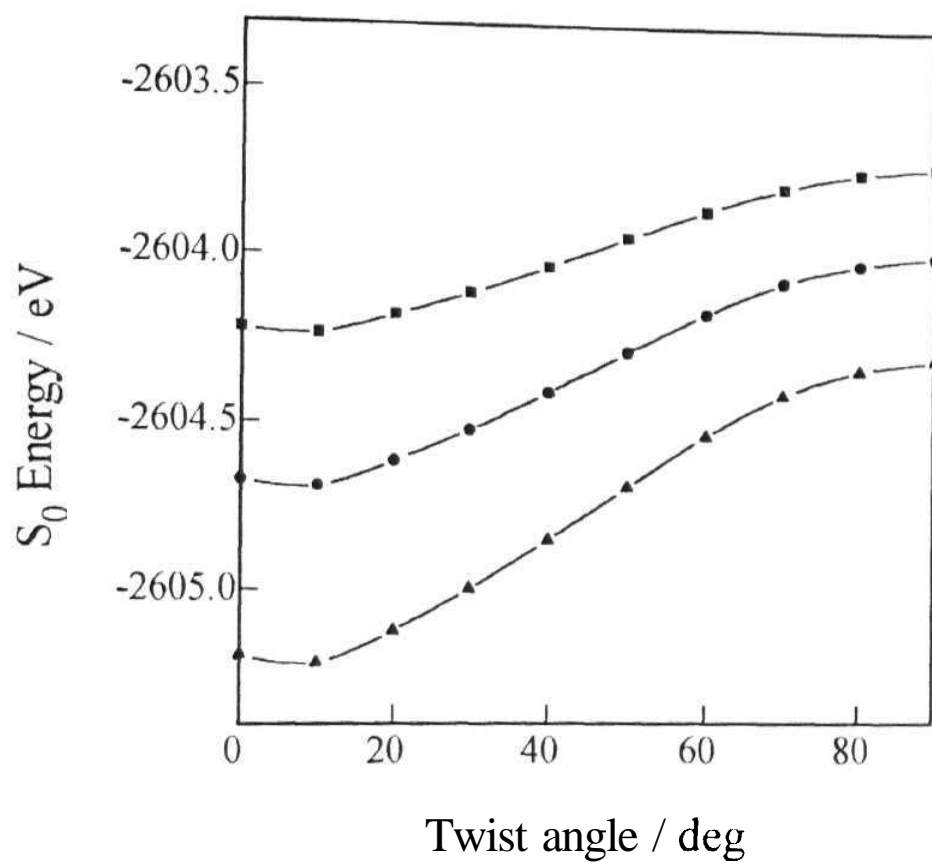


Fig.6.1. Variation of the ground state energy of 1 as a function of the twist angle in the gas phase (■), dioxane (●), and Acetonitrile (▲)

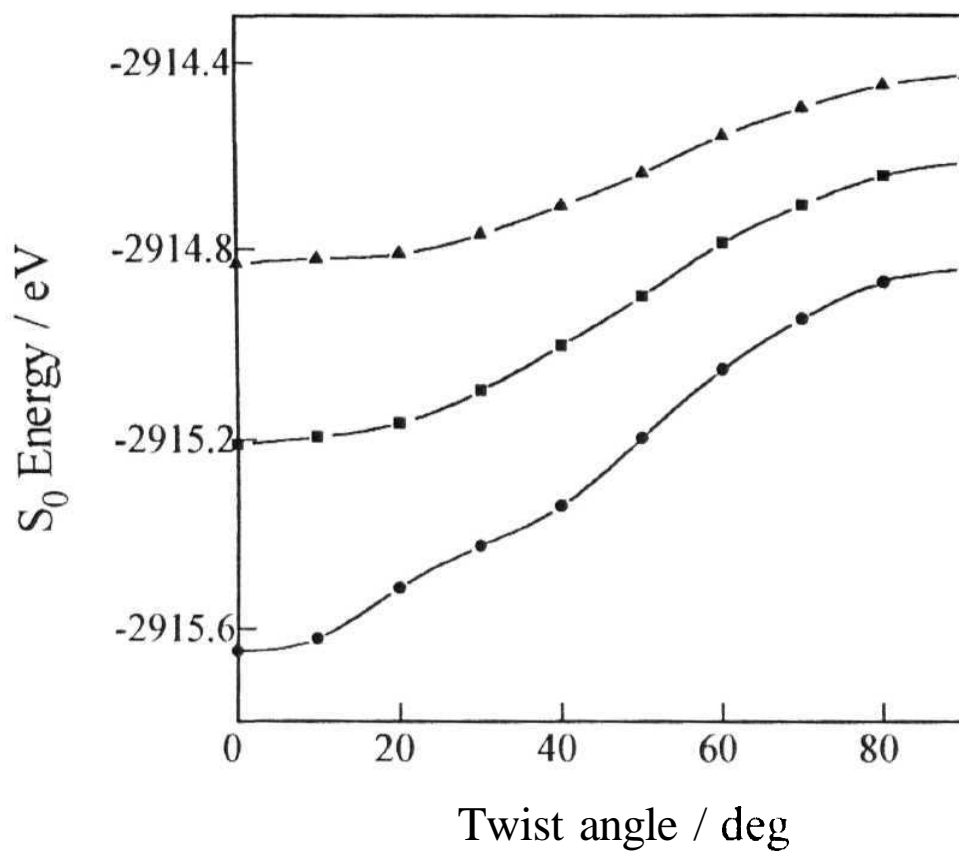


Fig.6.2. Variation of the ground state energy of 7 as a function of the twist angle in the gas phase (▲), dioxane (●), and Acetonitrile (◻)

6.1.2.2. *Excited state properties*

The variation of the lowest excited singlet state energy as a function of the twist angle of the amino group in the gas phase as well as in two solvents is shown in fig. 6.3 for **1**. The calculated energy profiles in dioxane and acetonitrile suggest that for **1** twisting is not possible because of high barrier involved (0.41 eV in acetonitrile). Therefore, the emitting state of **1** can only be an LE state whose dipole moment is estimated as 12.6 D. For **7**, the energy profiles are shown in fig. 6.4. It can be seen that LZ \rightarrow TICT process is almost barrier-less in polar media such as in acetonitrile. Therefore, one expects the TICT state to be populated for this compound. However, it is interesting to note that in this particular case the solvent stabilisation of the excited TICT state leads to lowering of its energy below the ground state in this particular conformation. In other words, crossing of the zeroth order ground and excited states results in a situation such that on excitation, **7** is expected to slide down the surface to a twisted conformation without emission of photons. Thus the TICT state in N-alkylated derivatives of NBD should be nonfluorescent.

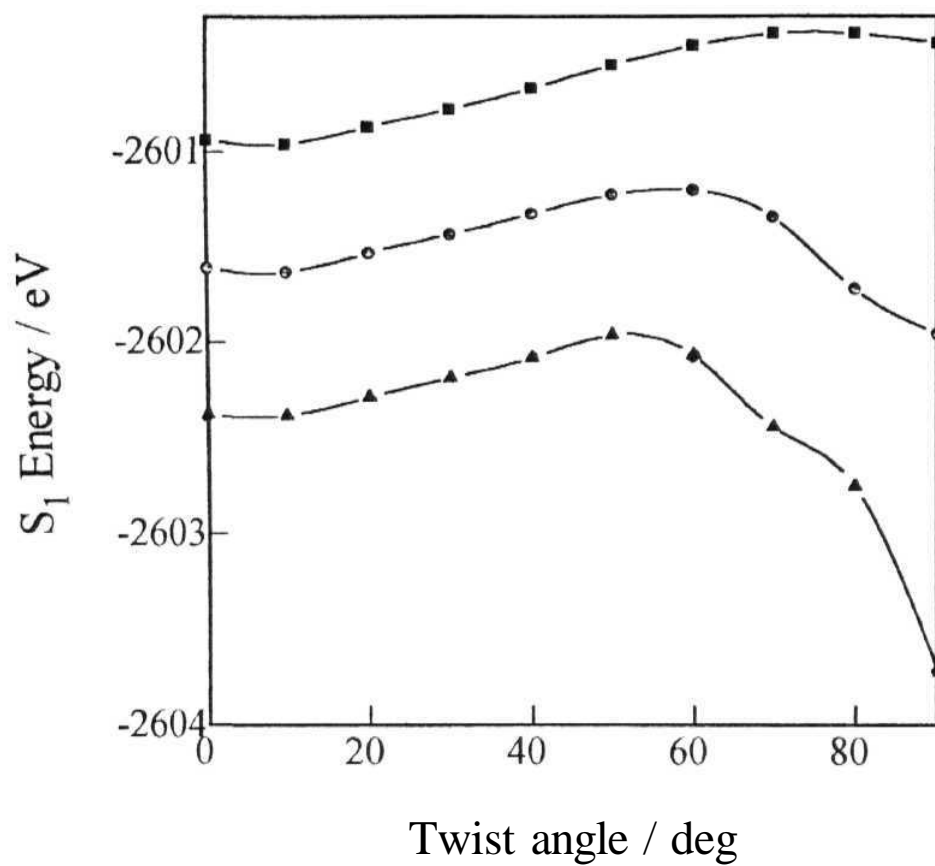


Fig.6.3. Variation of the first excited state energy of 1 as a function of the twist angle in the gas phase (○), dioxane (●), and Acetonitrile (▲).

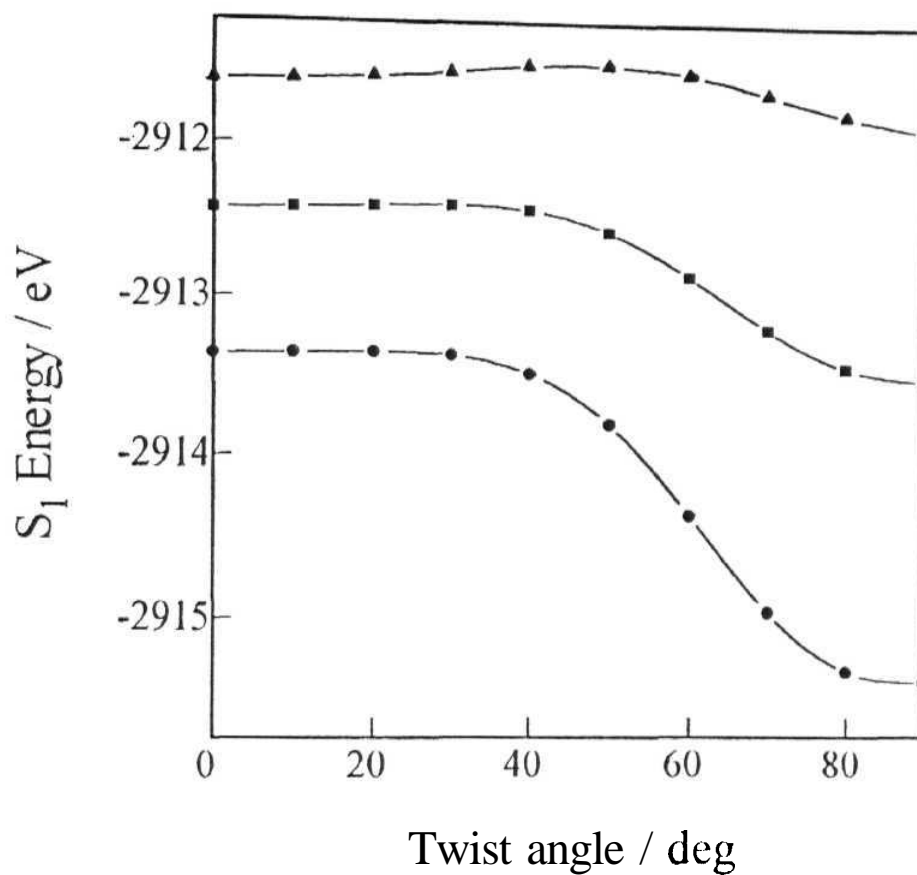


Fig.6.4. **Variation** of the first excited state energy of 7 as a function of the twist angle in the gas phase (▲), dioxane (◻), and Acetonitrile (●).

6.2. Studies on coumarin derivatives

It is well documented in the literature that solvatochromic shifts of dipolar species correlate much better with the microscopic solvent polarity parameters such as $E_T(30)$ or E_T^N ¹⁸ than with traditionally used bulk solvent polarity functions, f (as defined in Chapter III) or $F_2(D,n)$ ⁷ (as defined below) involving dielectric constant (D) and refractive index (n).¹⁹

$$F_2(D,n) = \left[\left\{ \frac{(D-1)}{(D+2)} \right\} - \left\{ \frac{(n^2-1)}{(n^2+1)} \right\} \right] \left[\frac{2n^2+1}{(n^2+2)} \right] \quad 6.1$$

This has also been demonstrated by us in Chapter V using the solvatochromic data for AP and DAP. The theoretical basis for the correlation of the Stokes shift with E_T^N has been published recently¹ (discussed in detail in Chapter III). According to this formulation

$$\Delta \bar{\nu} = 11307.6 \left\{ \left(\frac{A_{\parallel}}{A_{\perp}} - \frac{A_{\parallel}}{A_{\perp D}} \right)^2 \left(\frac{a}{a_D} \right)^3 \right\} E_T^N \text{constant.} \quad 6.2$$

$\Delta \mu$ can be determined from the slope of the plot of the Stokes shift vs E_T^N using the reported $\Delta \mu_D$ of 9 D of the betaine dye and its Onsager radius, a_D of 6.2 Å.¹³

In view of better correlation observed in plots of $\Delta \bar{\nu}$ against E_T^N , the slope from which the $\Delta \mu$ values are evaluated is expected to be more accurate. In addition, the above equn. provides a number of practical advantages. First, the formulation used in this method provides a partial cancellation of the problems associated with Onsager radius in the original Lippert-Mataga equation⁶, because ratios of two Onsager radii are involved. Second, the method

provides definite advantage for studies with binary solvent mixtures. Since the use of a mixture of just two solvents, one polar and the other nonpolar, provides systematic variation of the polarity with any desired number of data points and the polarity of various compositions are experimentally determined simply by measuring E_T^N , the experimental procedure is simplified and statistical analysis is more reliable than that using different solvents. In view of this we apply the method to determine the excited state dipole moments of a set of coumarin dyes (Chart 6.3) extensively used in laser applications.²⁰

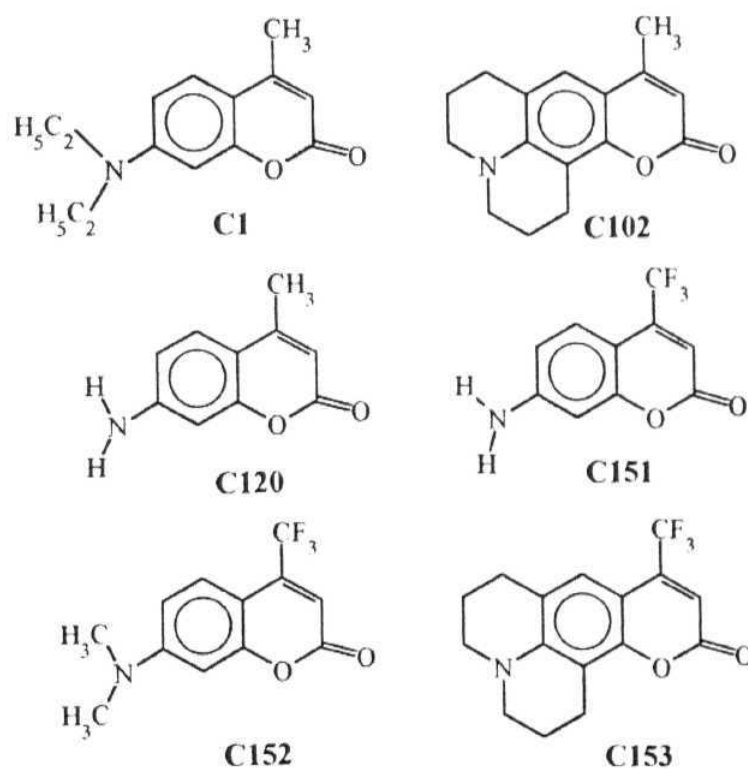


CHART 6.3

The excited state dipole moments of these molecules control the tunability range of their emission energy as a function of the solvent polarity. Further, since some of these systems may possess low-lying TICT state,²¹ the fluorescence can originate from either an LE state or a TICT state. Since it is possible to differentiate these two states on the basis of their dipole moments, our measurements should provide insight to the nature of the emitting state.

The absorption and emission maxima of the dyes in various solvents are compiled in Table 6.2. The solvents where strong specific interactions (e.g. H-bonding) with the dyes are possible were excluded. As can be seen from the Table, the shift of emission peaks with solvent polarity changes is more pronounced than the same for the absorption peaks. This indicates that $\Delta\mu$ ($\mu_e - \mu_g$) is positive. The correlation coefficients of the Stokes shifts of the six dyes with the solvent polarity functions $F_2(D, n)$, recommended by Koutek on the basis of a detailed statistical analysis⁷ as well as E_T^N , are presented in Table 6.3. As seen from the Table, the correlation of experimental Stokes shifts of the coumarins with E_T^N is far superior to that with the $F_2(D, n)$ function. Fig. 6.5 and 6.6 show typical plots of Stokes shifts versus $F_2(D, n)$ and E_T^N respectively for **C102** as an illustrative example.

Table 6.2. Wave numbers (cm⁻¹) of the absorption and emission (within parenthesis) maxima of the six coumarin dyes in the different solvents.

Compound	CCl ₄	Toluene	1,4-Dioxane	THF	Ethyl acetate	Acetone	Acetonitrile
C1	28011 (24863)	27855 (24449)	27777 (24271)	27624 (24178)	27739 (24026)	27247 (23618)	27137 (23694)
C102	27027 (24260)	26882 (23923)	23667 (23641)	26525 (23343)	26738 (23063)	26247 (22624)	26110 (22302)
C120	30030 (25893)	29762 (25562)	29498 (25240)	29070 (24975)	29498 (24950)	29070 (24643)	29325 (24486)
C151	28490 (24108)	27933 (23288)	27624 (22748)	26810 (22371)	27472 (22492)	27027 (21949)	27322 (21844)
C152	26596 (22810)	26042 (22212)	26110 (21720)	25840 (21249)	25740 (21258)	25510 (20483)	25381 (20317)
C153	25000 (22371)	24630 (21386)	24510 (29790)	24331 (20492)	24450 (20358)	24038 (19717)	23923 (19470)

Table 6.3. Correlation coefficients for the fit of the Stokes shifts of the coumarin dyes against the solvent polarity functions E_T^N and F_2 (D,n).

Molecule	Using polarity functions		Using E_T^N of binary mixture ^a
	F_2 (D,n)	E_T^N	
C1	0.780	0.945	0.963
C102	0.899	0.968	0.989
C120	0.693	0.887	0.910
C151	0.676	0.892	0.949
C152	0.924	0.948	0.957
C153	0.863	0.931	0.958

^aacetonitrile:benzene mixture; 9 compositions used in the correlation.

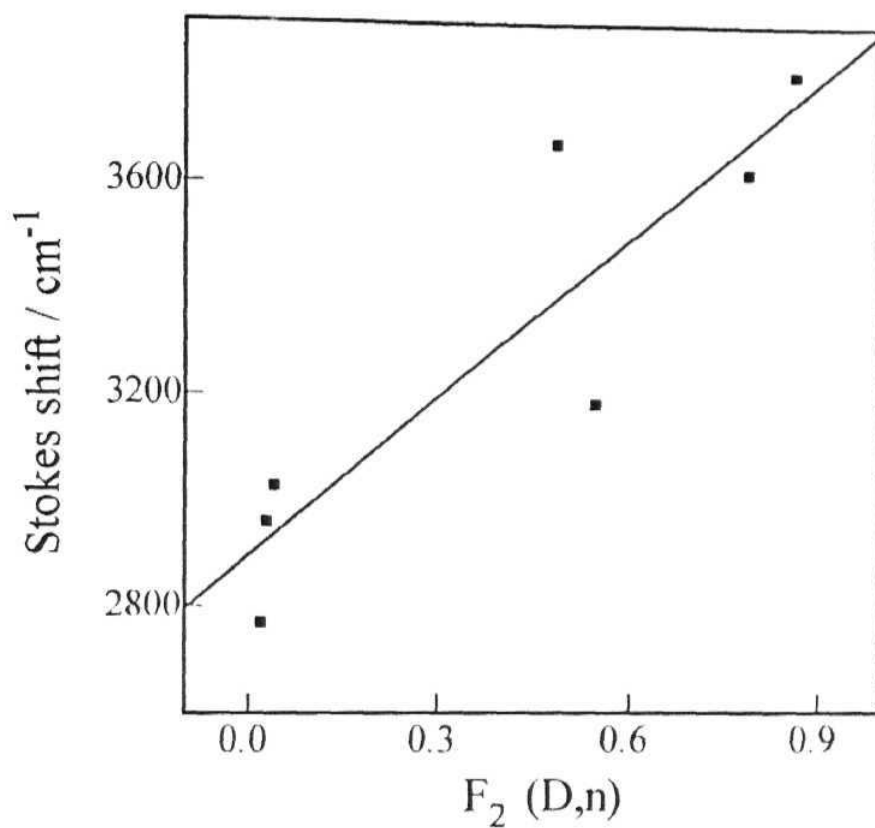


Fig.6.5. Plot of Stokes shifts of C102 versus the solvent polarity function, $F_2(D,n)$ of the seven solvents shown in Table 6.2.

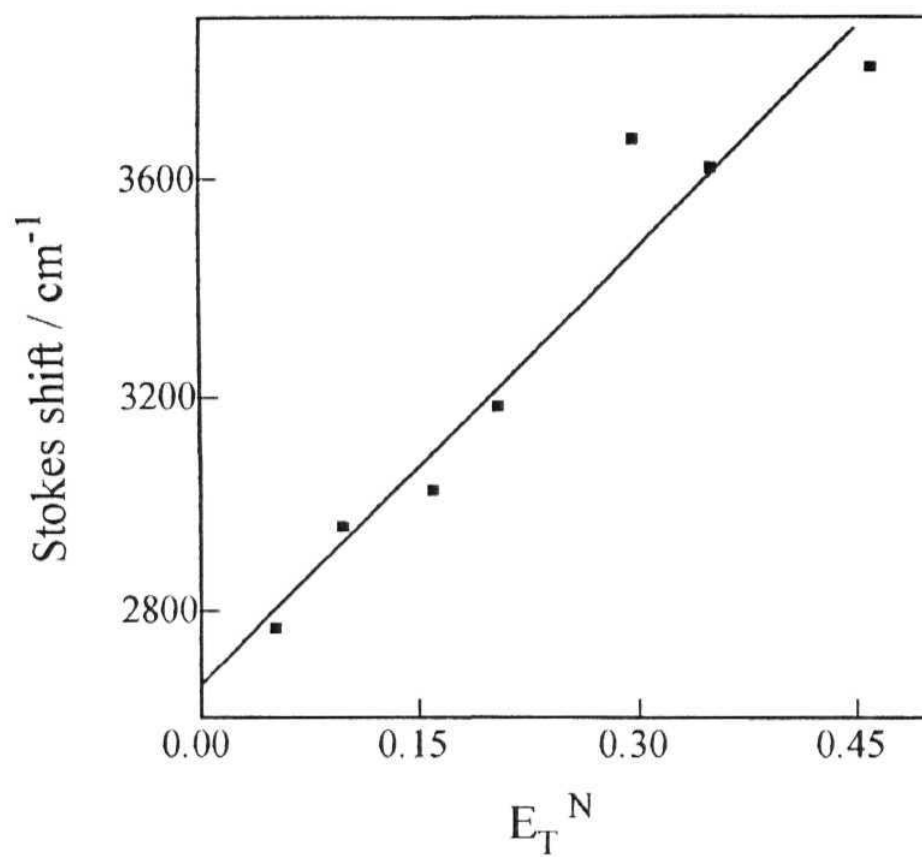


Fig.6.6. **Plot of Stokes shifts of C102 versus the solvent polarity function, E_T^N of the seven solvents shown in Table 6.2.**

Table 6.3 also provides the correlation coefficients for the plot of the Stokes shift versus the E_T^N obtained in a separate experiment employing the binary solvent mixtures of benzene and acetonitrile. Nine compositions ranging from 20% to 100% acetonitrile were used and the E_T^N values experimentally determined. We have examined the reproducibility of these experimentally determined E_T^N values using the empirical equation for E_T^N suggested by Langhals.²² The agreement between the theoretical and experimental E_T^N values of the mixtures is excellent at the compositions used. As seen in Table 6.3, the correlation of Stokes shifts of the six dyes is at its best with E_T^N values of the solvent mixtures. Since the number of data points used here are more, the statistical relevance of this fit is also enhanced over that using the different solvents. The plot of Stokes shifts versus the E_T^N parameter employing the acetonitrile-benzene binary mixture, for **C102** is shown in fig 6.7. Though the E_T^N values and the Stokes shifts span a slightly smaller range here, the number of data points is larger and the superiority of the fit is clearly seen.

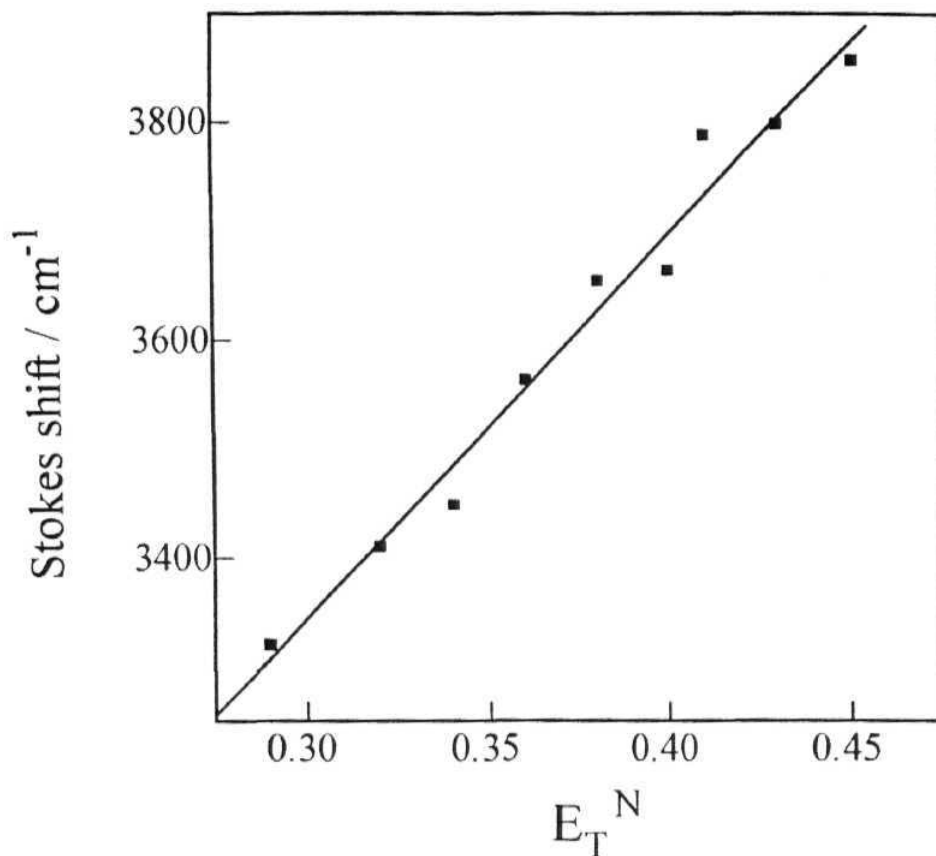


Fig. 6.7. Plot of Stokes shifts of the molecule C102 versus E_T^N values of the acetonitrile-benzene mixture of nine different compositions.

The Onsager radius, the ground and excited state dipole moments and $\Delta\mu$ values of six dyes are given in Table 6.4. The ground state dipole moments of the dyes **C1**, **C102** and **C120** are those evaluated using the AM1 procedure of McCarthy and Blanchard.²³ The last three compounds (**C151**, **C152** and **C153**) contain fluorine atoms for which the AM1 parametrisation is known to be

inadequate, especially for the computation of the heats of formation and geometry. Therefore, we have carried out the geometry optimisation for these molecules using the PM3 parametrisation.²⁴ Using these geometries, the μ_g and μ_e were calculated using the AM1 procedure. It is seen that between every pair of dyes related by a $\text{CH}_3 / \text{CF}_3$ substitution, the latter has a slightly lower dipole moment. Examination of the atomic charges on the amino group, carbonyl oxygen, CH_3 and CF_3 groups provides an insight into the reason for this. The decrease in μ_g is caused by the fact that the $\text{CH}_3 \rightarrow \text{O}$ dipole component that adds to the principal $\text{N} \rightarrow \text{O}$ vectors in the methyl-substituted compound is replaced by the much smaller $\text{CF}_3 \rightarrow \text{O}$ component in the trifluoromethyl-substituted molecules. The experimental $\Delta\mu$ values obtained (using eqn 6.2) from the slopes of the plots against E_T^N values of the different solvents as well as of the binary mixtures are found to be similar, except for some variation in the case of C1. However, it appears from the Table that $\Delta\mu$ values for the dyes as determined by this method are slightly lower than the reported values.^{23,25} This suggests that there is a need for the Onsager radius used for the betaine dye to be scaled to slightly larger value. However, it would be probably appropriate that scaling of Onsager radius, if necessary, be undertaken only when the excited state dipole moment of the compounds are available from one of the direct methods such as microwave absorption or conductivity measurements which produces more accurate values and does not depend on the Onsager cavity radius. The last column of Table 6.4 provides the μ_e calculated using theoretical μ_g and the $\Delta\mu$ determined experimentally using the binary mixture.

Table 6.4. Comparison of $\Delta\mu$ values obtained from the present analysis in various solvents and binary mixture with the computed values.

Molecule	a (Å)	(theory)	$\Delta\mu/D$			μ_e/D^b
			Various solvents	Binary mixture	Theoretical ^a	
C1	3.48	6.35	1.45	2.25	3.46	8.60
C102	3.46	6.43	1.84	2.11	3.66	8.54
C120	3.46	6.03	1.43	1.44	2.16	7.47
C151	3.46	4.49	1.72	1.58	2.60	6.07
C152	3.45	5.96	1.92	2.16	4.03	8.12
C153	3.46	5.36	2.27	2.22	4.46	7.58

^a the values for C1, C102 and C120 are from ref 23. The values for C151, C152 and **C153** are those calculated in the present study using PM3 optimised geometries.

Calculated using the experimental μ_g and the theoretical μ_g values.

As seen from Table 6.4, the change of dipole moment on electronic excitation is rather small for all the molecules studied. This suggests that the emission of these dyes originate from a state, which although more polar than the ground state, is probably an LE state. Further, it may be noted that the compounds **C102** and **C153** are fairly rigid and incapable of showing a twist around the C-N bond. The close similarity of the μ_e of these molecules with their respective counterparts capable of twisting, implies that the emitting states of all these systems are ICT in nature. ICT states if present, appear to be non-emissive.

6.3. References

- 1 M. Ravi, A. Samanta, T.P. Radliakrishnan, *J. Phys. Chem* 98, 9133, **1994**.
- 2 J. Czekalla, *Z. Electron.*, 64, 1221, **1960**, b) ty. Liptay, *Z. Naturforsch*, **18a**, 705, **1963**.
- 3 a) W. Liptay, J. Czekalla, *Z. Naturforsch*, **15a**, 1072, **1960**; b) J. Czekalla, W. Liptay, K.O. Meyer, *Ber. Bunsenges. Phys. Chem.*, **67**, 465, **1963**, c) W. Liptay, *Angew. Chem.*, 81, 195, **1969**, d) W. Liptay, In *Excited States*, E.C. Lim, ed. Academic Press New York, Vol 1, p 129, **1974**.
- 4 a) D.E. Freeman, W. Klemperer, *J. Chem. Phys*, 45, 52, **1966**, b) DE. Freeman, J.R. Lombardi, W. Klemperer, *J. Chem. Phys.*, 45, 58, **1966**
- 5 a) R.J. Visser, P.C.M. Weisenborn, C.A.G.O. Vanna, M.P. dellaas, J.M. Warman, *Chem. Phys Lett.*, **104**, 38, 1984; b) S.A. Jonker, J.M. Wannan, *Chem. Phys. Lett.*, **185**, 36, **1991**; c) RW. Fessenden, P.M. Carton, H. Paul, H. Shimamori, *J. Phys. Chem.*, **83**, 1676, **1979**.
- 6 a) E.Z. Lippert, *Z. Naturforsch*, 10A, 541, **1955**, *Z. Electrochem.*, 61, 962, **1957**; b) E. Lippert, W. Luder, H. Boos, *Adv. Mol. Spectros.*, **6**, 125, **1956**, c) N. Mataga, Y. Kaifu, M. Koizumi, *Bull. Chem. Soc. Jpn.*, 28, 690, **1955**, d) N. Mataga, Y. Torihashi, *Bull. Chem. Soc. Jpn.*, 36, 356, **1963**; e) N. Mataga, *Bull. Chem. Soc. Jpn.*, 36, 620, 654, **1963**.
- 7 B. Koutek, *Collect. Czech Commun.*, 43, 2368, **1978**.
- 8 a) C.J. Seliskar, I. Brand, *J. Am. Chem. Soc* 93, 5414, **1971**; b) J. C. Werner, R.M. Hoffman, *J. Phys. Chem.* 77, 1611, **1973**.

- 9 a) K.A. Zachariasse, T.V. Haar, A. Hebecker, U. Leinhos, W. Kuhnle, *Pure Appl. Chem.*, 65, 1705, **1993**, b) W. Baumann, H. Bischof, J.C. Frohling, C. Brittinger, W. Rettig, K. Rotkiewicz, *J. Photochem. Photobiol. A: Chem.*, 64* 49, **1992**; c) J.C. Tseng and L. A. Singer *J. Phys. Chem.*, 93, 7092, **1989**.
- 10 S. Wang, J. Cai, R. Sadygov and E. C. Lim *J. Phys. Chem.*, 99, 7416, **1995**.
- 11 a) T. Hagan, D. Pilloud, P. Suppan, *Chem. Phys. Lett.*, 139, 499, **1987**; b) P. Suppan, *J. Chem. Soc. Faraday Trans. 1*, 83, 495, **1987**.
- 12 P.B. Ghosh, M.W. Whitehouse, *Biochem. J.*, 108, 155, **1968**.
- 13 K.W. Street, S.A. Krause, *Anal. Lett.*, **19**, 735, **1986**.
- 14 J. Mori, T. Kaino, *Phys. Lett. A*, 127, 259, **1988**.
- 15 A. Chattopadhyay, *Chem. Phys. Lipids.*, 1, 53, **1990**.
- 16 A. Chattopadhyay, *J. Biophys.* 59, **191**, **1991**.
- 17 S.F. Forgues, J. Fayet, A. Lopez, *J. Photochem. Photobiol. A: Chem.*, 70, 229, **1993**.
- 18 C. Reichardt, *Solvents and Solvent Effects in Organic Chemistry*, Chapter 7, VCH; Weinheim, **1988**
- 19 a) G.S. Cox, P.J. Hauptman, N.J. Turro, *J. Photochem. Photobiol.*, 39, 597, **1984**; b) V. Nagarajan, A.M. Brearly, T. Rang, P.F. Barbara, *J. Chem. Phys.* 86, 3183, **1987**.
- 20 a) K.H. Drexhage, In *Topics in Applied Physics, Dye Lasers*, Vol. 1, F.P. Schafer, ed. Springer: Berlin, **1973**; b) A.N. Fletcher, *Appl. Phys.*, **14**, 295, **1977**.
- 21 a) G. Jones II, W.R. Jackson, A.M. Halpern, *Chem. Phys. Lett.*, 72, 391, **1980**, b) G. Jones II, W.R. Jackson, C. Choi, W.R. Bergmark, *J. Phys. Chem.*, **89**, 294, **1985**.

- 22 H. Langhals, *Angew. Chcm. Int. Ed. Engl.*, 21, 724, **1982**
- 23 P.K. McCarthy, GJ. Blanchard, *J. Phys. Chcm.* 97, 12205, **1993**.
- 24 J.J.P. Stewart, *J. Comput. Chcm.*, 10, 209, **1989**.
- 25 K. Rechthaler, G. Kohler, *Chcm. Phys.*, 189, 99, **1994**.

SUMMARY

A summary of the results presented in the thesis along with the scope of further work is outlined in this Chapter.

7.1. The results

The work embodied in this thesis deals with some aspects of the photophysics of donor-acceptor systems. First, we have explored the potentials of a **semi-empirical** quantum chemical method (AM1) in predicting the ground and excited state properties of donor-acceptor molecules. The calculations have been performed on DMABN as it is one of the thoroughly investigated systems for which there is a wealth of experimental as well as theoretical data available for comparison to test the merits of the calculations. We noted in this context the difference in luminescence properties of DMABN and structurally very similar molecule, ABN which possesses an amino group instead of a dimethylamino group. According to the literature report, the difference in the Photophysical properties of the two compounds results from weak electron donating ability and less steric interaction of the amino group with the *pen* hydrogens in the ring. We thought it appropriate to carry out the investigation on ABN as well to examine whether the method can account for the different behaviour of the two compounds.

The results of the excited state calculations in which we have taken into account 128 singly excited microstates (8 HOMO and 8 LUMO) for configuration interactions are shown to be in good agreement with the experimental results despite some of the limitations of the method. According to our calculation, in which the gas phase ground and the lowest excited state potential energy surfaces of the molecules are calculated as a function of the twist angle followed by the calculation of solvation energy for each angle in different solvents, the absence of the anomalous fluorescence band in ABN results from a comparatively higher barrier to $LE \rightarrow TICT$ process. We have also shown the superiority of the AM1 method over some other semi-empirical methods. However, we are unable to account for the polarity dependence of the barrier by this calculation. Other semi-empirical methods also fail to reproduce this behaviour. We think that the barrier height obtained from one-dimensional quantum chemical calculations may not represent the actual barrier. Instead, the transition state may receive considerable stabilisation from solvent shell reorganisation thus making the barrier height dependence on the polarity of the media.

We have studied the Photophysical behaviour of two donor-acceptor aminophthalimide dyes, AP and DAP in homogeneous media with a view to find out whether the rotary motion of the amino or dimethylamino group play any role in dictating the fluorescence yield of these systems. While the spectral features (both UV-vis absorption and fluorescence) of the two systems are found very similar, the polarity dependence of the fluorescence yields and lifetimes is quite different. In aprotic environment, the rate

constant for the nonradiative deactivation of the emitting state is seen to increase with increase in polarity for DAP even though it remains constant for the structurally similar molecule AP. The effect of viscosity on the emission yield is also found to be widely different for the two compounds. In order to rationalise this difference in fluorescence properties we have invoked a scheme with two close-lying excited states. While one of these two states is the LE state, the other one represents the TICT state of the molecule. We have shown from the measurement of the dipole moments of the emitting state that the fluorescence originates from the LE state in both systems and therefore the TICT state proposed in the scheme is either nonfluorescent or not populated due to unfavourable energetics. AM1 calculation of the energy profiles as a function of the twist angle shows that while LE \rightarrow TICT transition in DAP is an energetically favourable process in polar environment, the same for AP is not feasible as the barrier is much higher than the available thermal energy at room temperature. Having obtained this supporting data in favour of the rotary decay process in DAP, we interpret the polarity dependence of the nonradiative rate constants due to polarity dependent barrier height of LE \rightarrow TICT process. The nonfluorescent nature of the TICT state of DAP could be due to efficient internal conversion to the ground state (because of low energy gap), intersystem crossing to the triplet (one of the triplet state isoenergetic with the TICT singlet) and forbidden nature of the transition. We believe that a combined experimental and theoretical approach as used here could be followed for the identification of nonfluorescent TICT states in many other donor-acceptor systems.

Since donor-acceptor fluorescent systems are excellent candidates as probes or reporter molecules for the microheterogeneous or organised systems, we decided to study the potentials of the aminophthalimides as sensors of micro environments. For this purpose, a detailed investigation of the Photophysical behaviour of these molecules has been carried out in cyclodextrin added solutions. A preliminary study of the micellar environment employing AP has also been carried out to show that these systems can be used to follow other microheterogeneous environments as well. Inclusion of the probe molecules into the non polar hydrophobic cavities of cyclodextrins is associated with enhancement of fluorescence intensity and lifetime, and shift of the fluorescence spectra. For AP, the changes were found most significant in presence of β -CD which presumably results from good match of the size of the cavity and the guest molecule. Since formation of 1:1 complex with α - and β -CD is evident from the UV-vis absorption spectra, quantitative analysis of the steady state fluorescence data has been made for the estimation of the formation constant of the complexes. As the change in fluorescence lifetime on encapsulation is found quite significant, we have also estimated the binding constants from the lifetime data although this is not a commonly used practice. A fairly good agreement of the binding constants obtained by the two methods is observed. Further, we have shown that it is possible to predict with reasonable accuracy the arrangement of the guest molecules inside the cyclodextrin host cavities. Since formation of multiple complexes is apparent from the spectral behaviour, it was not possible to make definite conclusion on the data obtained for AP in γ -CD and for DAP in all the cyclodextrins.

Excited state dipole moment is an extremely useful quantity that help determination of the nature of the emitting state in donor-acceptor molecules where TICT state plays a significant role. As mentioned earlier, Lippert-Mataga equation is the most commonly used expression that permits measurement of the change of excited state dipole moment from the solvatochromic absorption and fluorescence data. Because of critical dependence of $\Delta\mu$ on the Onsager cavity radius it is necessary to select the correct value of this quantity. No clear prescription for the selection of the cavity radius can be found in the literature. To address to this problem we have theoretically estimated the ground and excited state dipole moments of a number of NBD derivatives (which are also known to be excellent reporter molecules for biological membranes) of different non interacting alkyl chain length. The results of the calculation indicate that despite a difference in the size of the molecules, the change in dipole moment on excitation is almost constant. This suggests that actual NBD derivatives used for biological applications, even though much longer, have very similar $\Delta\mu$ values. We have shown that when the maximum distance between the principal positive and the negative centres across which the charge separation takes place is considered as the cavity radius, the expected dipole moment is obtained for longer molecules. The possibility of the rotary decay mechanism in two simple NBD derivatives is also investigated theoretically.

Recently, a method for the determination of the change of dipole moment is reported in which the Stokes shifts are related to the microscopic solvent polarity parameters, E_T^N . We have analysed the

solvatochromic spectral data of six coumarin dyes using this equation. Even though the correlation of the Stokes shift data with E_T^N is excellent and the estimated dipole moment changes are in agreement with theoretically predicted numbers, the measured values appear to be on the lower side. In all these systems, the emitting state is determined to be *LE* in character.

7.2. Scope of further work

We believe that there are a number of aspects in the Thesis on which further work can be carried out either for the improvement of the results or extension into new areas.

AMI method is found to be quite satisfactory in interpretation of the Photophysical data of the donor-acceptor molecules studied in the Thesis. In fact, in a recent article it is commented that the AMI results are as good as 6-31 G* *ab initio* results⁺. Our experience tells us that, with limited computational resources, AMI is an appropriate method for the calculation of both the ground and excited state properties of large molecules. However, our results point out the requirement of a better model for the calculation of solvation energy. The apparently more sophisticated recent method of solvation[†] does not produce any better results. Further, the

+ A. D. Corse, M. Pesquer, *J. Phys. Chem.* 99, 4039, 1995

barriers obtained from these calculations, even though qualitatively explains the main features of different systems, fails to interpret the experimental data quantitatively. Thus further work is necessary to improve upon this prediction.

The fact that nonfluorescent, TICT state plays a crucial role in the photophysics of the aminophthalimides suggests that substitution of the amino hydrogens by alkyl groups even though extends the tunability range of these dyes, a reduction of the fluorescence yield of these dyes takes place in polar media. To improve upon the fluorescence efficiency of N-alkylated derivatives one needs prevent the rotary decay motion by rigidisation of the amino group. Secondly, it would be quite appropriate perhaps to study a series of compounds with different alkyl groups to examine the influence of the steric and electronic factors on the nonradiative rate constants.

The results obtained in studies on microheterogeneous environments clearly indicate that aminophthalimides could be used to probe more complex organised systems such as membranes, proteins, etc. Since the molecules contain a hydrophilic carbonyl groups prone to hydrogen bonding with protic solvents in addition to a hydrophobic portion, deeper penetration into the non polar hydrophobic cavity of cyclodextrin is not observed. However, it may be possible to achieve this objective using appropriate dihydroxy derivatives of aminophthalimides in which the carbonyl groups are engaged in intramolecular hydrogen bond formation.

As far as the recently developed equation for the determination of the change of dipole moment on excitation is concerned, there appears to be a need of scaling of suggested Onsager cavity radius of the betaine dye. However, unless the method is applied to more systems for which reliable dipole moment data are available it would be inappropriate to find the factor by which the radius should be modified to produce better results.